Koninklijk Belgisch Instituut voor Natuurwetenschappen
OD NATUUR – BEHEERSEENHEID VAN HET MATHEMATISCH MODEL

MOnitoring en MOdellering van het cohesieve sedimenttransport en evaluatie van de effecten op het mariene ecosysteem ten gevolge van bagger- en stortoperatie (MOMO)

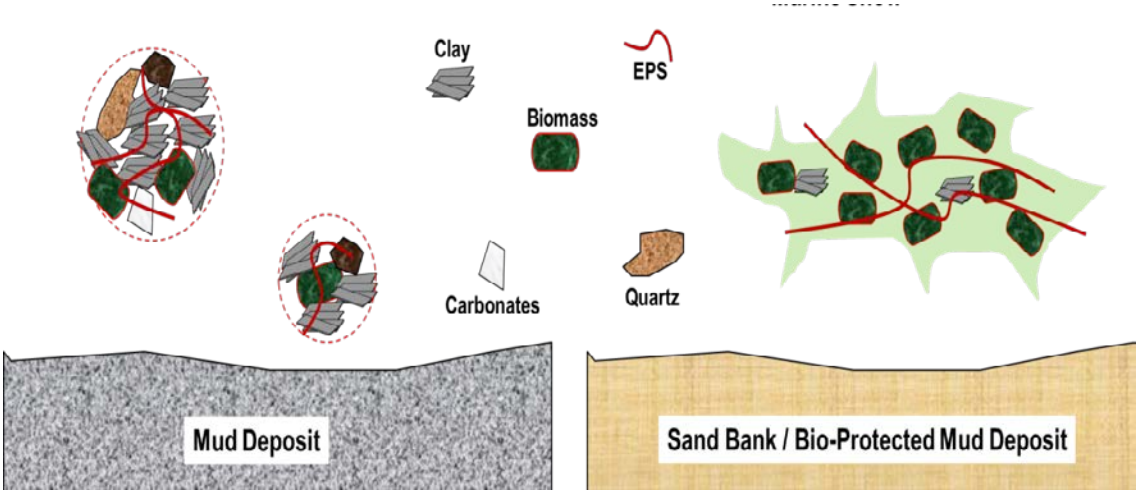

Activiteitsrapport (1 juli 2017 – 31 december 2017)

Michael Fettweis, Matthias Baeye, Frederic Francken, Dries Van den Eynde, Byung Joon Lee[1]

MOMO/8/MF/201801/NL/AR/2

museum
Operational Directorate Natural Environment
OD Nature I OD Natuur I DO Nature

KBIN-OD Natuur - BMM
Gulledelle 100
B–1200 Brussel
België

Inhoudstafel

[1] Department of Construction and Environmental Engineering, Kyungpook National University, 2559 Gyeongsang-daero, Sangju, Gyeongbuk 742-711, Korea

1. Inleiding

1.1. Voorwerp van deze opdracht

Het MOMO-project (monitoring en modellering van het cohesieve sedimenttransport en de evaluatie van de effecten op het mariene ecosysteem ten gevolge van bagger- en stortopera-tie) maakt deel uit van de algemene en permanente verplichtingen van monitoring en evaluatie van de effecten van alle menselijke activiteiten op het mariene ecosysteem waaraan België gebonden is in overeenstemming met het verdrag betreffende de bescherming van het mariene milieu van de noordoostelijke Atlantische Oceaan (1992, OSPAR-Verdrag). De OSPAR Commissie heeft de objectieven van haar Joint Assessment and Monitoring Programme (JAMP) gedefinieerd tot 2021 met de publicatie van een holistisch "quality status report" van de Noordzee en waarvoor de federale overheid en de gewesten technische en wetenschappelijke bijdragen moeten afleveren ten laste van hun eigen middelen.

De menselijke activiteit die hier in het bijzonder wordt beoogd, is het storten in zee van baggerspecie waarvoor OSPAR een uitzondering heeft gemaakt op de algemene regel "alle stortingen in zee zijn verboden" (zie OSPAR-Verdrag, Bijlage II over de voorkoming en uitschakeling van verontreiniging door storting of verbranding). Het algemene doel van de opdracht is het bestuderen van de cohesieve sedimenten op het Belgisch Continentaal Plat (BCP) en dit met behulp van zowel numerieke modellen als het uitvoeren van metingen. De combinatie van monitoring en modellering zal gegevens kunnen aanleveren over de transportprocessen van deze fijne fractie en is daarom fundamenteel bij het beantwoorden van vragen over de samenstelling, de oorsprong en het verblijf ervan op het BCP, de veranderingen in de karakteristieken van dit sediment ten gevolge van de bagger- en stortoperaties, de effecten van de natuurlijke variabiliteit, de impact op het mariene ecosysteem in het bijzonder door de wijziging van habitatten, de schatting van de netto input van gevaarlijke stoffen op het mariene milieu en de mogelijkheden om deze laatste twee te beperken.

Een samenvatting van de resultaten uit de voorbije vergunningsperiode kan gevonden worden in het Syntheserapporten over de effecten op het mariene milieu van baggerspeciestortingen (Lauwaert et al. 2016) dat gepubliceerd werd conform art. 10 van het K.B. van 12 maart 2000 ter definiëring van de procedure voor machtiging van het storten in de Noordzee van bepaalde stoffen en materialen.

1.2. Algemene doelstellingen

Het onderzoek heeft als doel om de effecten van baggerspeciestortingen op het mariene ecosysteem (fysische aspecten) te onderzoeken en kadert in de algemene doelstellingen om de baggerwerken op het BCP en in de kusthavens te verminderen en om een gedetailleerd inzicht te verwerven van de fysische processen die plaatsvinden in het mariene kader waarbinnen deze baggerwerken worden uitgevoerd. Dit impliceert enerzijds beleidsondersteunend onderzoek naar de vermindering van de sedimentatie op de baggerplaatsen en het evalueren van alternatieve stortmethoden. Anderzijds is vernieuwend onderzoek vereist om een beter inzicht te bereiken over de fysische processen van slibtransport en het inschatten van de effecten van het storten van baggerspecie. Dit is specifiek gericht op het dynamische gedrag van slib in de waterkolom en op de bodem en zal uitgevoerd worden met behulp van modellen, in situ metingen en remote sensing data.

<u>1) In situ en remote sensing metingen en data analyse</u>

De monitoring van effecten van baggerspeciestortingen gebeurd met behulp van een vast meetstation in de nabijheid van MOW1, en met meetcampagnes met de RV Belgica (een 4

tal meetcampagnes voor het verzamelen van traject informatie, profielen en de calibratie van sensoren; en een 10 tal campagnes voor het onderhoud van het meetstation te MOW1). De geplande monitoring is gericht op het begrijpen van processen, zodoende dat de waargenomen variabiliteit en de effecten van baggerspeciestortingen in een correct kader geplaatst kunnen worden. Een belangrijk deel is daarom gericht op zowel het uitvoeren van de in situ metingen, het garanderen van kwalitatief hoogwaardige data en het archiveren, rapporteren en interpreteren ervan. Remote sensing data afkomstig van onder andere satellieten worden gebruikt om een ruimtelijk beeld te bekomen.

2) Uitbouw en optimalisatie van het modelinstrumentarium

Het tijdens de voorbije jaren verbeterde en aangepaste slibtransportmodel zal verder worden ontwikkeld. Dit zal parallel gebeuren met de nieuwe inzichten die voorvloeien uit de metingen en de proces gerichte interpretatie van de metingen.

3) Ondersteunend wetenschappelijke onderzoek

Monitoring gebaseerd op wetenschappelijke kennis is essentieel om de effecten van menselijke activiteiten (hier het storten van baggerspecie) te kunnen schatten en beheren. Om te kunnen voldoen aan de door OSPAR opgelegde verplichtingen van monitoring en evaluatie van de effecten van menselijke activiteiten is het ontwikkelen van nieuwe monitorings- en modelleeractiviteiten nodig. Dit houdt in dat onderzoek dat de actuele stand van de wetenschappelijke kennis weerspiegelt wordt uitgevoerd en dat de hieruit voortvloeiende nieuwe ontwikkelingen geïntegreerd zullen worden in zowel de verbetering van het modelinstrumentarium als voor het beter begrijpen van het fysisch milieu.

1.3. Onderzoek Januari 2017 – December 2018

In het bijzonder is bij het opstellen van de hieronder vermelde taken rekening gehouden met de aanbevelingen voor de minister ter ondersteuning van de ontwikkeling van een versterkt milieubeleid zoals geformuleerd in het “Syntheserapport over de effecten op het mariene milieu van baggerspeciestortingen (2011)” dat uitgevoerd werd conform art. 10 van het K.B. van 12 maart 2000 ter definiëring van de procedure voor machtiging van het storten in de Noordzee van bepaalde stoffen en materialen. De specifieke acties in de periode 2017-2018 zullen uitgevoerd worden om de algemene doelstellingen in te vullen zijn de volgende:

Streven naar een efficiënter stortbeleid door:

- Optimalisatie van de stortlocaties. Bijkomende simulaties worden uitgevoerd voor het opzetten van een MER voor een alternatieve stortplaats (zie taak 2.2). Verder zullen de effecten van een efficiënter verplaatsen van het gebaggerde materiaal te Nieuwpoort en Blankenberge naar de stortzones (lozen i.p.v. storten) geëvalueerd worden (zie Taak 3.4);
- Onderzoek naar de mogelijkheden voor het opzetten van een operationeel stortmodel in overleg met aMT (Taak 2.3). Dit model zal geïntegreerd worden in de binnen BMM-OD Natuur beschikbare operationele modellen. Het model zal gebruikt worden om in functie van de voorspelde fysische (wind, stroming, golven, sedimenttransport, recirculatie), economische (afstand, grootte baggerschip) en ecologische aspecten op korte termijn een keuze te kunnen maken tussen de beschikbare stortlocaties. Hiervoor zal binnen de huidige periode het slibtransportmodel gevalideerd worden op de geografische variabiliteit van de turbiditeitszones en de flocculatie van het slib.

Continue monitoring van het fysisch-sedimentologische milieu waarbinnen de baggerwerken worden uitgevoerd (Taak 1) en aanpassing van de monitoring aan de nog op te stellen targets voor het bereiken van de goede milieutoestand (GES), zoals gedefinieerd

binnen MSFD;

Uitbouw en optimalisatie van het numerieke modelinstrumentarium, ter ondersteuning en verfijning van het onderzoek (Taak 2.1).

Taak 1: In situ en remote sensing metingen en data analyse

Taak 1.1 Langdurige metingen

Sinds eind 2009 worden er continue metingen uitgevoerd te MOW1 met behulp van een meetframe (tripode). Met dit frame worden stromingen, slibconcentratie, korrelgrootteverdeling van het suspensiemateriaal, saliniteit, temperatuur, waterdiepte en zeebodem altimetrie gemeten. Om een continue tijdreeks te hebben, wordt gebruik gemaakt van 2 tripodes. Na ongeveer 1 maand wordt de verankerde tripode voor onderhoud aan wal gebracht en wordt de tweede op de meetlocatie verankerd. Op de meetdata wordt een kwaliteitsanalyse uitgevoerd, zodat de goede data onderscheiden kunnen worden van slechte of niet betrouwbare data.

In 2013-2016 werden enkele langdurige metingen uitgevoerd met behulp van een OBS-5 sensor vastgemaakt aan de AW boei; deze metingen zullen verdergezet worden. De data geven informatie over de SPM concentratie aan het oppervlak en zijn aldus complementair aan de bodemnabije metingen met de tripode. De data zijn ook van belang voor het calibreren en valideren van de oppervlakte SPM concentraties uit satellietbeelden.

Taak 1.2 Calibratie van sensoren tijdens in situ metingen

Tijdens 4 meetcampagnes per jaar met de R/V Belgica zullen een voldoende aantal 13-uursmetingen uitgevoerd worden met als hoofddoel het calibreren van optische of akoestische sensoren en het verzamelen van verticale profielen. De metingen zullen plaatsvinden in het kustgebied van het BCP. De optische metingen (transmissometer, Optical Backscatter Sensor) zullen gecalibreerd worden met de opgemeten hoeveelheid materie in suspensie (gravimetrische bepalingen na filtratie) om te komen tot massa concentraties. Naast de totale hoeveelheid aan suspensiemateriaal (SPM) wordt ook de concentratie aan POC/PON, TEP, chlorofyl (Chl-a, Chl-b) en phaeofytine (a, b) bepaald. Stalen van suspensiemateriaal zullen genomen worden met de centrifuge om de samenstelling ervan te bepalen.

Taak 1.3 Kwaliteitscontrole van de data

In situ metingen zijn steeds onderhevig aan onzekerheden ten gevolge van random meetfouten (gebrek aan precisie), systematische fouten (onnauwkeurigheid), menselijke fouten, en de statistische variabiliteit van de parameter. De fouten hebben hun oorsprong in de onnauwkeurigheid en het gebrek aan precisie van het meetinstrument of de procedures (bv. waterstaalname en filtratie). Doel is om de fout op de verschillende onderdelen van de metingen (filtratie, calibratie, langdurige trends...) te schatten. Een procedure die de best practice beschrijft zal worden opgesteld.

Een belangrijk aandachtspunt bij deze langdurige datareeksen is het garanderen van een gelijke kwaliteit in de tijd van de verzamelde data. De vraag die zich bij onze SPM concentratiemetingen stelt is niet zozeer het opmeten van hogere of lagere waarden, mogelijks veroorzaakt door het toepassen van een andere stortstrategie, maar het garanderen dat deze waarden inderdaad veroorzaakt worden door menselijke activiteiten (bv storten) en niet het effect zijn van natuurlijke fluctuaties. Om kwaliteitsvolle data te kunnen leveren over een lange periode, die gebruikt kunnen worden om langdurige trends te identificeren, is het nodig om een rigoureuze kwaliteitscontrole uit te voeren. OBS alsook akoestische sensoren zijn gevoelig aan de samenstelling en korrelgrootte van het gesuspendeerde materiaal. Dit kan variëren in functie van de boven vermelde frequenties, maar hierom-

trent is er nog geen afdoende duidelijkheid wat de metingen te MOW1 betreft. De wetenschappelijke vragen die daarom moeten worden, hebben betrekking tot in situ en in lab calibratie van de OBS sensoren en van akoestische backscatter sensoren en de meetfouten.

Taak 1.4: Verwerking en interpretatie van de data

De metingen vergaard tijdens de 13-uursmetingen aan boord van de Belgica en met de tripode worden verwerkt en geïnterpreteerd. Hiervoor werden in het verleden al heel wat procedures (software) toegepast of ontwikkeld, zoals de berekening van de bodemschuifspanning uit turbulentiemetingen, entropieanalyse op partikelgrootteverdelingen, de opsplitsing van multimodale partikelgrootteverdeling in een som van lognormale verdelingen, het groeperen van de data volgens getij, meteorologie, klimatologie en seizoenen. Deze methodes zijn opgenomen in de standaardverwerking van de data. De aldus verwerkte data dienen als basis voor het verder gebruik binnenin wetenschappelijke vragen.

Taak 1.5: Sedimentologie van zeebodem

De sedimentologie van stortplaatsen en referentiezones zal, in samenwerking met het ILVO, worden bestudeerd met alternatieve meettechnieken, zoals de Sediment Profile Imaging (SPI).

Taak 1.6: TBT analysen

TBT analysen op stalen aangeleverd door het ILVO zullen door het chemisch labo van het KBIN (Ecochem) worden uitgevoerd. Het betreft de analyse van 6 stalen (2 replica's).

Taak 2: Uitbouw en optimalisatie van het modelinstrumentarium

Taak 2.1: Verdere ontwikkelingen en validatie van een slibtransportmodel voor het BCP gebaseerd op Coherens V2

Het tijdens de voorbije jaren verbeterde en aangepaste slibtransportmodel zal worden gevalideerd met behulp van de langdurige meetreeksen en de satellietbeelden. Hierbij zal dezelfde methode als in Baeye et al. (2011) en zoals in taak 1.4 worden gebruikt om de modelresultaten te groeperen en te klasseren volgens windrichting, weertype en getij. Het voordeel van deze werkwijze is dat niet zozeer gekeken wordt of de correlatie tussen meting en modelresultaat in één of meerder punt goed is, maar dat globaal nagegaan wordt of het model de SPM dynamica op het BCP goed kan reproduceren.
Verdere ontwikkelingen aan het model parallel met nieuwe inzichten die voorvloeien uit de metingen en de proces gerichte interpretatie van de metingen zullen worden geïmplementeerd in het model.

Taak 2.2: Ondersteuning bij de MER studie van een alternatieve stortlocatie

Op dit moment worden op het BCP vijf stortplaatsen gebruikt voor het gebaggerd materiaal afkomstig uit de vaargeulen op zee en de zeehavens: Zeebrugge Oost, S1, S2, B&W Oostende en Nieuwpoort. Door OD Natuur- BMM werd in het kader van het MOMO project onderzoek gedaan naar de efficiëntie van de stortplaatsen. Daaruit blijkt dat de recirculatie naar de baggerplaatsen het grootste is vanuit de stortplaats Zeebrugge Oost. Met behulp van numerieke modellen werden een aantal alternatieve locaties voor de stortplaats Zeebrugge Oost bestudeerd. In 2012-2013 werd een terreinproef uitgevoerd om de resultaten van de numerieke modellering op het terrein te valideren. Uit de resultaten van de terreinproef bleek dat er aanwijzingen zijn die de resultaten van de numerieke modellering bevestigen.

OD Natuur-BMM zal in deze studie instaan voor het uitvoeren van de nodige numerieke modelleringen in de eerste helft van 2017. Hiervoor zal gebruik gemaakt worden van het geüpdatete 3D stromingsmodel dat beschikbaar is bij OD Natuur-BMM. Het model is

opgebouwd in Coherens V2, inclusief sedimenttransportmodule en flocculatiemodel. Meer specifiek zal de OD Natuur-BMM betrokken zijn bij:

Fase 1 (long list van mogelijke locaties en exploitatiescenario's opgemaakt worden): berekening van de recirculatie voor maximaal 10 mogelijke locaties en/of stortscenario's. Voor iedere berekening zullen voor een aantal combinaties van hydro-meteo randvoorwaarden simulaties uitgevoerd worden. Deze randvoorwaarden zijn zo gekozen dat ze optimale aansluiting verzekeren met de al eerder uitgevoerde simulaties.

Fase 2 (opmaak Milieu Effect Rapport): Bij de opmaak van het MER zelf is geen specifieke modellering nodig voor de inschatting van de effecten. Indien uit overleg met de vergunningverlenende instanties blijkt dat simulaties moeten uitgevoerd worden ter onderbouwing van de gemaakte keuzes (recirculatie bij een bepaalde locatie/stortstrategie) kan dit uitgevoerd worden.

Taak 2.3: Operationeel stortmodel (vanaf 2018)

Overleg met aMT over het opstellen van een operationeel stortmodel om de noden en de mogelijkheden te definiëren. Het model zal later (vanaf 2018) kunnen opgesteld worden en kan dan geïntegreerd worden in de binnen BMM-OD Natuur beschikbare operationele modellen. Het model zal kunnen gebruikt worden om in functie van de voorspelde fysische (wind, stroming, golven, sedimenttransport, recirculatie), economische (afstand, grootte baggerschip) en ecologische aspecten op korte termijn een keuze te kunnen maken tussen de beschikbare stortlocaties.

Taak 3: Ondersteunend wetenschappelijk onderzoek

Monitoring gebaseerd op wetenschappelijke kennis is essentieel om de effecten van menselijke activiteiten (hier het storten van baggerspecie) te kunnen schatten en beheren. Om te kunnen voldoen aan de door OSPAR opgelegde verplichtingen van monitoring en evaluatie van de effecten van menselijke activiteiten is een verdere implementatie van huidige en het ontwikkelen van nieuwe monitoringsactiviteiten nodig. Meer specifiek gericht op de activiteit 'storten van baggerspecie' worden hier – wat het fysische milieu betreft - turbiditeit, samenstelling van de zeebodem, bathymetrie en hydrografische condities beoogd. Deze taak speelt hierop in door de ontwikkeling van nieuwe tools die de actuele stand van de wetenschappelijke kennis weerspiegelen teneinde de mathematische modellen te optimaliseren en verfijnen.

Taak 3.1: Sedimentuitwisseling tussen de zee en de haven van Zeebrugge

Slib stroomt de haven van Zeebrugge binnen rond HW, wanneer de stroming maximaal is. Gezien de grote turbulentie op dit moment op zee bestaat het SPM uit voornamelijk kleine vlokken met een lage valsnelheid. Eens het suspensiemateriaal de haven binnenkomt, neemt de turbulentie plots af, ontstaan er grotere vlokken en treed er een snelle bezinking op. Het verloop van de SPM concentratie in de haven zelf is goed gekend (zie onder andere de SPM concentratie metingen in de haven tijdens de terreinproef en de metingen van de topsliblaag), maar aan de havenmond zijn minder data beschikbaar om de sedimentuitwisseling in kaart te brengen en dit tijdens verschillende getij- en meteocondities. In deze taak zal de sedimentdynamica bestudeerd worden gebruikmakend van ADCP transects gemeten met de RV Belgica, van verticale profielen van SPM concentratie en vlokgrootte in en uit de haven, en van remote sensing beelden.

Taak 3.2: Microbiologische activiteit en de wisselwerking met sedimentdynamica

Een sleutelelement in het functioneren van kustnabije ecosystemen is de aanwezigheid van biotische en abiotische partikels. Verticale en dus ook horizontale fluxen van SPM worden bepaald door hun valsnelheid, die afhangt van de capaciteit van de deeltjes om te

flocculeren. Flocculatie beïnvloedt de grootte van de gesuspendeerde deeltjes en bepaald daardoor de depositie van het slib. Op zijn beurt wordt flocculatie gestuurd door turbulentie, de SPM concentratie, en de oppervlakteigenschappen van de deeltjes, die van elektrochemische of biologische oorsprong kunnen zijn. Wat dit laatste betreft heeft dit een wederzijdse invloed tot gevolg tussen het SPM en de primaire productie doordat stoffen zoals TEPs (transparent exopolymeric particles), die vrijkomen door het fytoplankton en de bacteriën, de vlokgrootte en dus ook de valsnelheid van het SPM beïnvloeden. Het belang van deze processen voor de slibdynamica in onze kustzone en dus ook voor de aanslibbing van havens en vaargeulen wordt gegeven door de uitzonderlijk hoge primaire productie in de Belgische kustzone ten gevolge van eutrofiëring (algenbloei). Dat er een effect is werd al aangetoond door de metingen te MOW1 die lieten zien dat het SPM zich anders gedraagt in de winter dan in de biologisch actieve zomerperiode. In de winter is het SPM beter gemengd in de waterkolom dan in de zomer en treden er dus hogere concentraties op in de waterkolom. In de zomer bevindt zich meer suspensiemateriaal dicht tegen de bodem en daalt de SPM concentratie in de waterkolom. Dit roept volgende vragen op, in het bijzonder 1) Hoe moet het modelinstrumentarium (flocculatiemodule) worden aangepast om deze seizoenaliteit te kunnen modelleren? 2) Wordt de seizoenaliteit in SPM concentratie en biologische activiteit veroorzaakt doordat de algen TEP produceren, dat aanleiding geeft tot de vorming van grotere vlokken en dus een hogere bezinking van het SPM als gevolg heeft, of daalt eerst de SPM concentratie ten gevolge van fysische processen (afname van de stormfrequentie in de lente) en start de algenbloei nadat het water minder troebel is geworden? 3) De troebelheid in de waterkolom is in de Belgische kustzone altijd hoog en de lichtindringing is ook in de zomer beperkt. Speelt troebelheid (en dus ook SPM concentratie) een belangrijke rol bij start van de algenbloei bepaald of is dit eerder een secundair proces?

Het onderzoek zal gericht zijn op het verzamelen van in situ meetdata van TEP, SPM en Chl concentratie te MOW1 en op andere plaatsen; het analyseren van de data in functie van boven aangehaalde vragen; het incorporeren van de biologische activiteit in een flocculatiemodel en het uitvoeren van modelberekeningen.

<u>Taak 3.3: Overgang kustzone – offshore: Waarom is het turbiditeitsgebied beperkt tot de kustzone?</u>

Turbulentie samen met de SPM concentratie bepalen de lichthoeveelheid in het water. De cross-shore stroming in vele kustgebieden is gekenmerkt door landinwaarts gerichte stroming dicht tegen de bodem en een zeewaarts gerichte aan het wateroppervlak (estuariene circulatie). Het is op dit moment niet duidelijk hoe het Schelde estuarium deze circulatie beïnvloed. Hierdoor wordt het SPM (en het fytoplankton) naar de kust getransporteerd in de bodemlaag nadat het eerst naar offshore werd getransporteerd in de oppervlaktelaag. Dit mechanisme is mogelijks verantwoordelijk voor de scherpe gradiënt in SPM concentratie langsheen onder andere de Belgische kust en de Westerscheldmonding. Ook turbulentie is gekenmerkt door een gradiënt: hoog dicht tegen de kust en afnemend naar offshore toe. Dit komt overeen met een toename in waterdiepte naar offshore toe. Bij geringere waterdieptes is de turbulentie hoger, de verticale menging dus sneller en dus de tijd met lage SPM concentratie korter. Naar offshore toe zal de lichthoeveelheid in de waterkolom dus toenemen in de oppervlaktelaag omdat de diepte toeneemt. Vanaf een bepaalde diepte bereikt het SPM niet meer de oppervlakte tijdens verticale menging. De afname in SPM concentratie is dus mogelijks een afspiegeling van de gradiënten in diepte en turbulentie. Dit proces werd aangetoond in andere delen van de Noordzee (Duitse Bocht), maar nog niet in de Belgische kustzone.

Het onderzoek zal gericht zijn op het verzamelen van in situ meetdata van TEP, SPM en Chl concentratie op een drietal locaties gelegen op verschillende afstanden van de kust; het varen van ADCP transects dwars op de kust; en het analyseren van de data. TEP en Chl zijn een onderdeel van het SPM, die een significante invloed heeft op de seizoenaliteit van de SPM dynamica.

Taak 3.4: Alternatieve Stortstrategie Nieuwpoort

Er zal ondersteuning gegeven worden aan afdeling kust in verband met het opzetten van een wetenschappelijke terreinproef om de impact van het verpompen van baggerspecie uit de haven van Nieuwpoort op een stortzone te evalueren. Details hiervan zullen op een vergadering van de technische werkgroep besproken worden.

1.4. Gerapporteerde en/of uitgevoerde taken

Periode Januari 2017 – Juni 2017

Taak 1.1: De meetreeks te MOW1 werd verdergezet.

Taak 1.2: Calibratie van sensoren werd uitgevoerd tijdens campagne 2017/20 (21-23/06/2017).

Taak 2.1 De bodemschuifspanning gemodelleerd met het hydrodynamisch model werd gevalideerd met in situ data te MOW1. Dit is een eerste stap bij de validatie van een slibtransportmodel voor het BCP gebaseerd op Coherens V2, zie Appendix 2 van activiteitsrapport MOMO/8/MF/201707/NL/AR/1.

Taak 2.2: Simulaties met de nieuwe versie van het COHERENS V3 model voor de Belgische kustzone werden uitgevoerd ter ondersteuning van de MER studie voor een alternatieve stortlocatie, zie Hoofdstuk 2 in activiteitsrapport MOMO/8/MF/201707/NL/AR/1

Taak 3.2 Waterstalen voor de bepaling van TEP concentratie werden 1-2 wekelijks genomen te Oostende.
Een 1 klasse flocculatiemodel werd aangepast om biologisch flocculatie te simuleren. De resultaten werden gevalideerd met metingen te MOW1, zie Hoofdstuk 3 in activiteitsrapport MOMO/8/MF/201707/NL/AR/1.

Periode Juli 2017 – December 2017

Taak 1.1: De meetreeks te MOW1 werd verdergezet. Het factual data rapport voor 2016 werd opgesteld.

Taak 1.2: Calibratie van sensoren werd uitgevoerd tijdens campagne 2017/24 (16-18/08/2017), 2017/34 (21-22/11/2017), 2017/38 (18-21/12/2017).

Taak 1.3 Een uitgebreide onzekerheidsanalyse van de optische en akoestische sensoren gebruikt bij langdurige metingen is in uitvoering. Resultaten werden op de INTERCOH conferentie getoond, zie Appendix 1 van activiteitsrapport MOMO/8/MF/201801/NL/AR/2

Taak 3.2 Waterstalen voor de bepaling van TEP concentratie werden 1-2 wekelijks genomen te Oostende. TEP werd tijdens de 13 uursmeting als standaard parameter opgenomen.

Taak 3.3: De stalen en data genomen tijdens 13 uursmetingen (vanaf 2003 t.e.m. nu) in de kustzone en offshore werden geanalyseerd om de geografische verschillen in SPM eigenschappen tussen het kustgebonden turbiditeitsmaximum en het offshore gebied met lage turbiditeit te beschrijven, zie Hoofdstuk 2 in activiteitsrapport MOMO/8/MF/201801/NL/AR/2.

1.5. Publicaties (januari 2017 – december 2018)

Hieronder wordt een overzicht gegeven van publicatie met directe betrokkenheid van het KBIN waar resultaten en data uit het MOMO project in werden gebruikt.

Activiteits-, Meet- en Syntheserapporten

Fettweis M, Baeye M, Francken F, Van den Eynde D. 2018. MOMO activiteitsrapport (1 juli – 31 december 2017). BMM-rapport MOMO/8/MF/201801/NL/AR/2, 27pp + app.

Backers J, Hindryckx K, Vanhaverbeke W. 2017. Rapport van de RV Belgica Meetcampagnes en Verankering van Meetsystemen MOMO - 2016. BMM rapport ODNatuur-MDO/2017-04/MOMO/2016, 103pp + CD.

Fettweis M, Baeye M, Francken F, Van den Eynde D, Chen P, Yu J. 2017. MOMO activiteitsrapport (1 januari – 30 juni 2017). BMM-rapport MOMO/8/MF/201707/NL/AR/1, 32pp + app.

Conferenties/Workshops

Adriaens R, Zeelmakers E, Fettweis M, Vanlierde E, Vanlede J, Stassen P, Elsen J, Środoń J, Vandenberghe N. 2017. Quantitative clay mineralogy as provenance indicator for the recent muds located in the southern North Sea. INTERCOH, 13-17 November, Montevideo (Uruguay).

Fettweis M, Riethmüller R, Verney R, Becker M, Backers J, Baeye M, Chapalain M, Claeys S, Claus J, Cox T, Deloffre J, Depreiter D, Druine F, Flöser G, Grünler S, Jourdin F, Lafite R, Nauw J, Nechad B, Röttgers R, Sotollichio A, Vanhaverbeke W, Van Hoestenberghe T, Vereecken H. On best practice for in situ high-frequency long-term observations of suspended particulate matter concentration using optical and acoustic systems. INTERCOH, 13-17 November, Montevideo (Uruguay).

Shen X, Toorman E, Fettweis M. 2017. A tri-modal flocculation model coupled with TELEMAC for suspended cohesive sediments in the Belgian coastal zone. INTERCOH, 13-17 November, Montevideo (Uruguay).

Vanlede J, Dujardin A, Fettweis M. 2017. Mud dynamics in the harbor of Zeebrugge. INTERCOH, 13-17 November, Montevideo (Uruguay).

Adriaens R, Zeelmakers E, Fettweis M, Vanlierde E, Vanlede J, Stassen P, Elsen J, Środoń J, Vandenberghe N. 2017. Quantitative clay mineralogy as provenance indicator for the recent muds located at the marine limit of influence of the Scheldt estuary. Schelde-Ems workshop, 16-17 February, Antwerp (Belgium).

Publicaties (tijdschriften, hoofdstuk in boeken)

Adriaens R, Zeelmaekers E, Fettweis M, Vanlierde E, Vanlede J, Stassen P, Elsen J, Środoń J, Vandenberghe N. 2018. Quantitative clay mineralogy as provenance indicator for recent muds in the southern North Sea. *Marine Geology* (accepted).

Chen P, Yu JCS, Fettweis M. 2018. Modelling storm-influenced SPM flocculation using a tide–wave-combined biomineral model. *Water Environment Research, 90.* doi:10.2175/WERD1600107

Fettweis M, Lee BJ. 2017. Spatial and seasonal variation of biomineral suspended particulate matter properties in high-turbid nearshore and low-turbid offshore zones. *Water*, 9, 694. doi:10.3390/w9090694.

2. Geografische en seizoensgebonden variaties van het bio-minerale suspensiemateriaal in de zuidelijke Noordzee

Suspended particulate matter (SPM), produced by biological and geophysical actions on the Earth's crust, enters into marine and coastal waters and is dispersed by flow-driven transportation, such as advection and dispersion (Ouillon et al. 2004; Winterwerp & van Kesteren 2004; Perianez 2005). The SPM concentration is an important parameter to understand the marine ecosystem as it controls the water turbidity and mediates many physical and biochemical processes (Chen et al. 2005; Lee et al. 2011, 2012).

SPM consists of a wide variety of biomineral clay to sand sized particles, comprising living (microbes, phyto- and zooplankton) and non-living organic matter (fecal and pseudofecal pellets, detritus and its decomposed products from microbial activity such as mucus, exopolymers), and minerals from physico-chemical (e.g. clay minerals, quartz, feldspar) and biogenic origin (e.g. calcite, aragonite, opal), which are practically grouped into organic biomass and inorganic sediments (Droppo 2001). It is important to note that when clays or other charged particles and polymers are in suspension they become attached to each other (flocculation) and form fragile structures or flocs with compositions, sizes, densities, and structural complexities that vary as a function of turbulence and biochemical composition (Eisma 1986; Winterwerp & van Kesteren 2004; Droppo et al. 2005; Jago et al. 2007; Tan et al. 2012). Flocculation combines biomass and sediments together into large aggregates and depending on biomass composition, such aggregates are classified into mineral, biomineral, and biological aggregates (Maggi 2009, Maggi & Tang 2015). Mineral and biomineral aggregates form in the sediment-enriched environment, such as a turbidity maximum zone (TMZ) or a nearshore area (van Leussen 1994; Chen et al. 2005; Fettweis et al. 2006), while biological aggregates (i.e., marine snow) form in the mineral-depleted environment typically found in an offshore zone (OSZ) (Alldredge & Silver 1988).

Flocculation mediated by biomass-sediment interactions determines the size, density and settling velocity of aggregates (van Leussen 1994; Maggi 2009; Markussen & Andersen, 2013). For example, in a tidal cycle, low flow intensity during slack water enhances flocculation capability, building large, settleable aggregates, whereas high flow intensity at peak flow reduces flocculation capability, breaking down aggregates to small, less (or hardly) settleable aggregates or primary particles(Lee et al. 2012; 2014). Moreover, sticky biomass (e.g., extracellular polymeric substances (EPSs) or transparent extracellular polymers (TEPs)) helps build large biomineral aggregates (Droppo 2001; Passow 2002; Engel et al. 2004; Sahoo et al. 2013; Mari et al. 2017). Flocculation which can be mediated by biological factors consequently controls sedimentation, resuspension, deposition, and erosion, and determines the overall SPM dynamics in marine and coastal waters (Jouon et al. 2008; Maggi 2009).

Bio-medicated flocculation and SPM dynamics are important in science and engineering because they eventually control the sediment, carbonaceous, and nitrogenous mass balances at the regional or global scale (Tranvik et al. 2009, Gudasz et al. 2012). Despite their importance, bio-mediated flocculation and SPM dynamics are not fully understood in coastal and marine waters. Geologists and hydraulic engineers have focused more on sediments and less on biomass (van Leussen 1994; Winterwerp & van Kesteren 2004), and marine biologists vice versa (Alldredge & Silver 1988). In our opinion, the biomass-sediment interactions in coastal and marine waters have only recently been studied in a systematic and quantitative way (Burd & Jackson 2002; Droppo et al. 2005; Barkmann et

al. 2010; Maggi 2013; Maggi & Tang 2015; Tang & Maggi 2016; Chen et al. 2017), and mathematical models which can take into account the heterogeneous composition/morphology of biomineral aggregates were developed only a few years ago (Maggi 2009; 2013). These efforts should be paid more attention.

Therefore, the aim of the study was to add to our current understanding of bio-mediated flocculation and its impact on the SPM in marine and coastal waters. First, we investigated the spatial variation of SPM dynamics in a sediment-enriched TMZ and a mineral-depleted OSZ, especially concerning bio-mediated flocculation. Second, we investigated the seasonal variation of SPM dynamics in a TMZ to understand how seasonal changes in biological activity, especially algae blooms, affect bio-mediated flocculation and SPM dynamics. This paper describes and discusses bio-mediated flocculation and SPM dynamics for different locations and seasons.

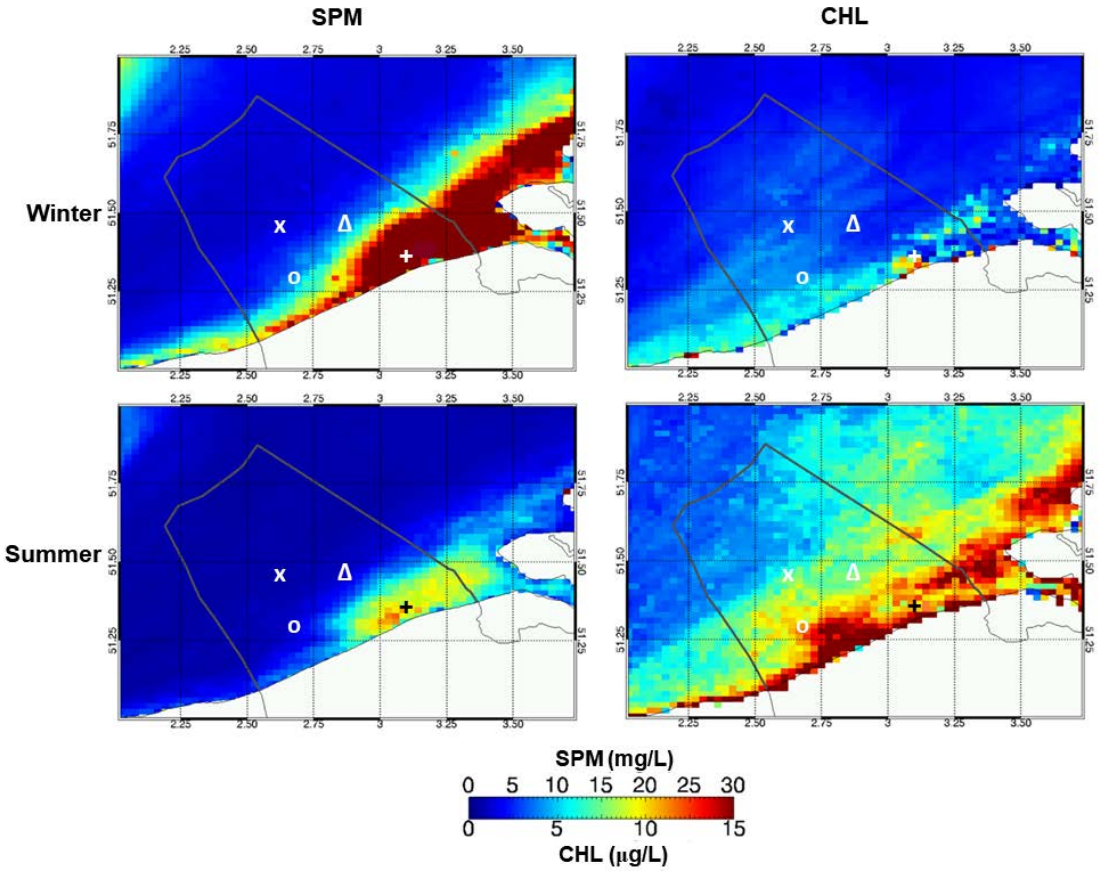

Figure 2.1: Mean surface suspended particulate matter (SPM) and chlorophyll-a (CHL) concentrations in the southern North Sea during the winter (October–March, top) and summer season (April–September, bottom) derived from MERIS satellite. The +, Δ, X, and O symbols indicate the measurement sites of MOW1, Gootebank (G-Bank), Hilnderbank (H-Bank) and Kwintebank (K-Bank), respectively.

2.1. Materials and methods

2.1.1. Site description

The study area is situated in the Southern Bight of the North Sea, specifically in the Belgian coastal zone. Measurements have indicated SPM concentrations of 20–70 mg/L in the nearshore area; reaching 100 to more than a few g/L near the bed; lower values (<10 mg/L) occur in the offshore (Fettweis et al. 2012). As shown in Figure 2.1, the MOW1 measurement site is located in the TMZ. The Gootebank (G-Bank), Hinderbank (H-Bank),

and Kwintebank (K-Bank) sites are in the OSZ, out of or at the edge of the turbidity maximum. Satellite images of surface SPM and chlorophyll-a (Chl) concentrations in the study area show clear spatial and seasonal changes. Regarding the seasonality, the annual cycle of SPM concentration in the high turbidity area off the Belgian coast is mainly caused by the seasonal biological cycle, rather than wind and waves. Wind strengths and wave heights have a seasonal signal, but these do not explain the large differences observed in SPM concentration (Fettweis et al. 2014; Fettweis & Baeye 2015). This seasonality is linked with the seasonal changes in aggregate size and thus settling velocity due to biological effects. The aggregate sizes and settling velocities are smaller in winter and larger in summer. As a result, the SPM is more concentrated in the near-bed layer, whereas in winter, the SPM is better mixed throughout the water column. This explains the inverse correlation found between the surface SPM and the Chl concentrations in Figure 1. Water depths of the measuring area vary between 5 and 35 m. The mean tidal ranges at Zeebrugge are 4.3 and 2.8 m at spring and neap tides, respectively. The tidal current ellipses are elongated in the nearshore area and become gradually more semicircular towards the offshore area. The current velocities near Zeebrugge (nearshore) vary from 0.2 to 1.5 m/s during spring tide and from 0.2 to 1.0 m/s during neap tide. Salinity varies between 28 and 34 practical salinity units (PSU) in the coastal zone, because of the wind-induced advection of water masses and river discharge (Lacroix et al. 2004; Fettweis et al. 2010). The most important sources of SPM are from the erosion and resuspension of the Holocene mud deposits outcropping in the Belgian nearshore area; the French rivers discharging into the English Channel, and the coastal erosion of the Cretaceous cliffs at Cap Gris-Nez and Cap Blanc-Nez (France) are only minor sources (Fettweis et al. 2007; Zeelmaekers 2011; Adriaens 2014; Adriaens et al. 2017).

2.1.2. Tidal measurements

Field measurements in the TMZ (MOW1) and in the OSZ (G-Bank, H-Bank, and K-Bank) were carried out about four times a year from February 2004 until 2011. During each campaign, sensor measurements (flow, SPM dynamics) and water sampling (SPM properties) were executed, while the research vessel was moored to maintain a specific measuring position for a 13-h tidal cycle. A Sea-Bird SBE09 SCTD carousel sampling system (containing twelve 10 or 5 L Niskin bottles) was kept at least 4.5 m below the surface and about 3 m above the bottom. A LISST 100X (range 2.5–500 µm) was attached directly to the carousel sampling system to measure particle size distribution (PSD) at the same location as the water sampling system (Agrawal & Pottsmith 2000). The volume concentration of each size group was estimated with an empirical volume calibration constant, which was obtained under a presumed sphericity of particles (Agrawal & Pottsmith 2000; Mikkelsen et al. 2007; Fettweis 2008). The LISST has a sampling volume which permits it to statistically sample the less numerous large aggregates, but it cannot detect aggregates larger than 500 µm or smaller than 2.5 µm. Particles smaller than the size range affect the entire PSD, with an increase in the volume concentration of the smallest two size classes, a decrease in the next size classes and, an increase in the largest size classes (Andrews et al. 2010). Similar remarks have been formulated by Graham and coworkers (2012), who observed an overestimation of one or two orders of magnitude in the number of fine particles measured by the LISST. A rising tail in the lowest size classes of the LISST occurs regularly in the data during highly turbulent conditions and is interpreted as an indication of the presence of very fine particles and thus a break-up of the aggregates. Particles exceeding the LISST size range of 500 µm also contaminate the PSD. The large out of range particles increase the volume concentration of particles in multiple size classes in the

range between 250 and 500 μm and in the smaller size classes (Mikkelsen et al. 2005; Smith & Friederichs 2011; Davies et al. 2012). The occurrence of rising tail in the largest size classes indicates the occurrence of large particles rather than an absolute value. Other uncertainties of the LISST-100X are related to the often non-spherical shape of the particles occurring in nature (Andrews et al. 2010; Davies et al. 2012; Graham et al. 2012). A hull mounted, RDI Acoustic Doppler current profiler (ADCP) type, Workhorse Mariner 300 kHz, was used to determine the velocity profiles.

2.1.3. Water samples and analysis

A Niskin bottle of the carousel sampling system was closed every 20 min, thus collecting about 40 samples during a 13 hours flood-ebb tidal cycle. The carousel was brought aboard every hour. Three sub-samples from each water sample were then filtered on board using pre-weighed filter papers (Whatman GF/C). In total, 120 filtrations were thus carried out per tidal cycle. After filtration, the filter papers were rinsed with demineralized water (± 50 mL) to remove the salt, dried at 105 °C and weighed again to determine the SPM concentrations. Every hour, a fourth sub-sample was filtered on board to determine particulate organic carbon (POC) and particulate organic nitrogen (PON) concentrations. The residues on the filter paper were carefully collected and acidified with 1 N HCl. Then, the POC and PON of the residues were quantified with a CN elemental analysis.

2.1.4. Grain size and mineralogical analysis

Primary grain size and mineralogical analyses were performed to determine the mineralogical composition of the SPM samples. Suspension samples were obtained by centrifugation of seawater collected by an ALFA Laval MMB 304S flow-through centrifuge, while the bed samples have been taken with a Van Veen grab sampler. Collected and stored samples were dried at 105 °C and chemically treated by adding HCl and H_2O_2 in order to remove the organic and carbonate fractions. The pretreated samples were rinsed with demineralised water, dried at 105 °C and added into 100 mL demineralized water with 5 mL of peptizing agent (a mixture of $NaCO_3$ and Na-oxalate). The suspension was dispersed and disaggregated using a magnetic stirrer and an ultrasonic bath. The grain size distribution and clay-silt-sand fractions of the SPM sample were analyzed with a Sedigraph 5100 for the fraction <75 μm and sieved for the coarser fraction. The mineralogical composition of the clay fraction of the samples was determined with a Seifert 3003 theta-theta X-ray diffractometer. Details of the analytical methods are documented in the earlier dissertation (Zeelmakers 2011).

2.2. Results and discussion

2.2.1. Mineralogical characteristics of TMZ and OSZ

The mineralogical composition of the bed materials in the TMZ and OSZ are shown in Table 2.1. The respective clay and quartz contents of the bed materials in the TMZ were 25.0 and 39.6 %, respectively, whereas those in the OSZ were 12.4 and 66.7 %. Thus, the bed materials in the TMZ were found to be a mud-sand mixture, while the bed materials in the OSZ were sandy. Carbonates, such as calcite, Mg-calcite, aragonite and dolomite, compose about 20 and 10 % in the TMZ and OSZ, respectively. Feldspar (i.e., K-feldspar and plagioclase) was also found to be an important content of the bed materials of the TMZ and OSZ at about 8 %. Amorphous species in the TMZ and OSZ comprised 4.2 and 1.1 %, respectively. Amorphous species are considered biogenic minerals influenced by biogeochemical actions (Kastner 1999; Zeelmaekers 2011). The clay minerals at both sites comprised about 5% Kaolinite, 10% Chlorite, and 85% 2:1 layered silicates.

In contrast to the bed materials, the SPM in the TMZ and OSZ had similar mineralogical composition. For instance, the clays and quartz contents of the SPM only differed by 5 % between the TMZ and OSZ, and the contents of carbonates, amorphous, feldspar, and others differed by less than 2.5 %. This is caused by the fact that the SPM samples do not contain coarser bed material, as the sand grains in suspension are seldom found above the near-bed layer. This also indicates that the SPM in the TMZ and OSZ have the same origin, as suggested by Zeelmaekers (2011), Adriaens (2014) and Adriaens et al. (2017). It is also important to note that the respective fractions of carbonate and amorphous species are substantial at approximately 30 and 11 % for both the TMZ and OSZ, thereby indicating a high biological activity in the measuring area.

Table 2.1: Average mineralogical fractions (%) of the bulk deposits and SPM in the turbidity maximum zone (TMZ) and offshore zone (OSZ) measuring sites.

		Clays	Quartz	Carbonates	Amorphous	Feldspar	Others
Bed Materials	**TMZ**	25.0	39.6	21.1	4.2	8.0	2.1
	OSZ	12.4	66.7	10.7	1.1	8.1	0.9
SPM	**TMZ**	36.2	14.6	29.9	12.7	4.2	2.3
	OSZ	31.3	20.6	29.7	10.1	6.4	1.8

2.2.2. Spatial Variation of SPM Dynamics in the TMZ and OSZ

During the entire measurement period (2004 to 2011), the POC/SPM ratios in the OSZ were substantially higher than those in the TMZ were (Figure 2.2a). This observation indicates that the SPM in the OSZ is composed of more biomass and less sediments, and vice versa for the SPM in the TMZ. A scatter plot with POC content and SPM concentration shows the transition from a high mineral to the low-mineral SPM, when shifting from the TMZ to the OSZ (Figure 2.3). Generally, POC content increased with a decreasing SPM concentration (i.e., mineral-depleted condition). The mineral-depleted SPM in the OSZ seemed analogous to the muddy marine snow from an Australian coastal area where minerals were binded together with planktonic and transparent exopolymer particulate matter (Bainbridge et al. 2012). However, the PON/POC ratios of the TMZ and OSZ did not show such clear difference during the entire study period, and their 95 % confidence levels overlapped (Figure 2.2b).

SPM concentrations in the TMZ are shown to be about an order magnitude higher than those in the OSZ (Figure 2.2c), similar to the satellite images of SPM concentration in Figure 2.1. This observation indicates that a substantial amount of sediments resides in the TMZ, which is transported back and forth in the flood and ebb tides. In addition, SPM concentrations in the TMZ were more vulnerable to flow intensity. High flow velocity (U) was found to increase SPM concentrations (e.g., Mar/29/2006, Feb/7/2008, Feb/10/2009, and Mar/21/2011, in Figure 2.2), because it increases sediment erosion and resuspension from the sea floor. It is also important to note that the TMZ had 2 to 3 times smaller aggregate size (D50) than the OSZ had (Figure 2.2d), see Fettweis et al. (2006). Thus, the TMZ enriched with sediments (i.e. higher SPM concentration and lower POC/SPM) had lower flocculation capability (i.e., lower D50) than the OSZ did. Maggi & Tang (2015) and Tang & Maggi (2016) reported that small, dense aggregates are formed in sediment (mineral)-enriched environments, such as the TMZ in this study, whereas large, fluffy aggregates are formed in biomass-enriched environments. The former was defined as mineral or biomineral aggregates, and the latter as biological aggregates.

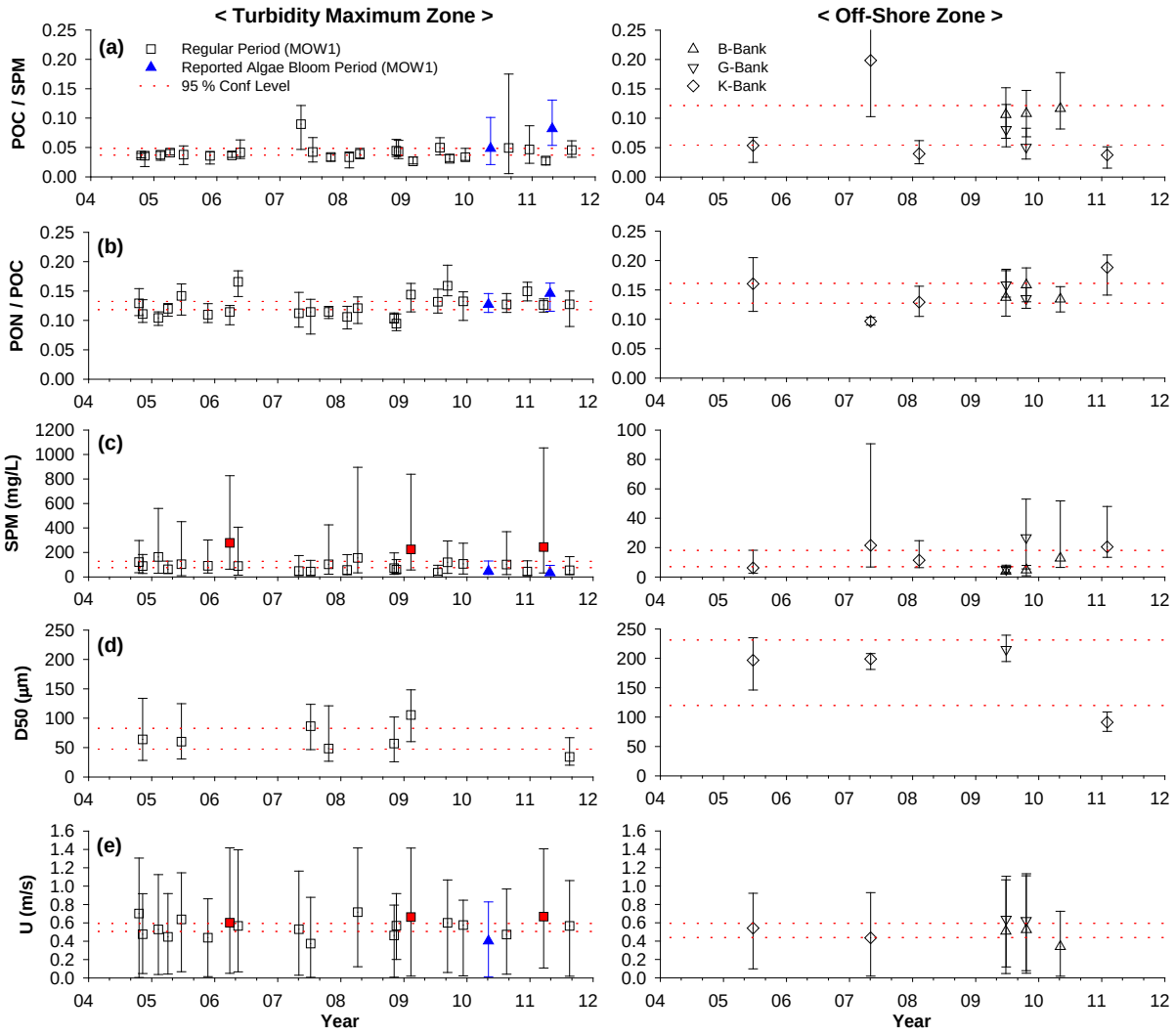

Figure 2.2: Spatial and seasonal variation of experimental indices in the measurement sites, during the entire measurement period, from 2004 to 2011. The left and right panels illustrate the data obtained from the turbidity maximum zone (TMZ) and the offshore zone (OSZ), respectively. (a) POC content in the SPM; (b) POC/PON ratio; (c) SPM concentration;(d) D50: median of the volumetric particle/aggregate size distribution; € U: flow velocity; MOW1: measurement site in the TMZ; B-Bank, G-Bank, and K-Bank: measurement sites in the OSZ.

SPM and POC concentrations and D50 in the TMZ were subject to ups and downs during the 13-hour tidal cycle (Figure 2.4a). Generally, SPM and POC concentrations increased to their maximum around the peak flows. Biomass and minerals were likely combined in large, settleable biomineral aggregates, because SPM and POC concentrations were subject to the same up-and-down movement during a tidal cycle. Such biomineral aggregates in the TMZ are vulnerable to shear-dependent flocculation, therefore changing D50 in a flow-varying tidal cycle (Lee et al. 2012; 2014). D50 increased to the maximum when approaching slack water, but decreased to a minimum around peak flow. Regarding flocculation kinetics, aggregation kinetics dominated over disaggregation kinetics for the slack water, and vice versa for the peak flow (Lee et al. 2012; 2014). In contrast, SPM and POC concentrations and D50 in the OSZ were rather constant, randomly scattered without apparent ups and downs (Figure 2.4b), showing that aggregation kinetics dominate over disaggregation kinetics for the entire period. SPM in the OSZ might be mainly composed of biomass and some mineral particles, building more shear-resistant and less settleable ma-

rine snow (Bainbridge et al. 2012). Although biological aggregates (i.e., marine snow) are usually much larger, up to several millimeters, than mineral or biomineral aggregates, they settle more slowly because of their low density and fluffy structure (Maggi 2013). The latter is confirmed by an earlier study (Fettweis 2008), where the excess density of aggregates has been calculated for some of the tidal cycles investigated here; the mean excess density was 550 kg/m³ and the mean D50 of the aggregates 65 µm (five tidal cycles) in the TMZ versus 180 kg/m³ and 115 µm (three tidal cycles) in the OSZ. Although both the TMZ and the OSZ are governed by tidal dynamics, small differences in the current regime occur between both areas (Fettweis et al. 2006), as is also shown in Figure 4.4. The TMZ is situated in the nearshore, where the current ellipses are more elongated, whereas more offshore, the ellipses tend to be more spherical. This will cause higher velocity gradients, stronger turbulence, more stress exerted on the aggregates, and a reduction of the time needed for the aggregates to reach equilibrium size in the TMZ. Considering these differences in hydrodynamics, the mineral and biomineral aggregates in the TMZ are more susceptible to the hydrodynamics than the biological aggregates in the OSZ.

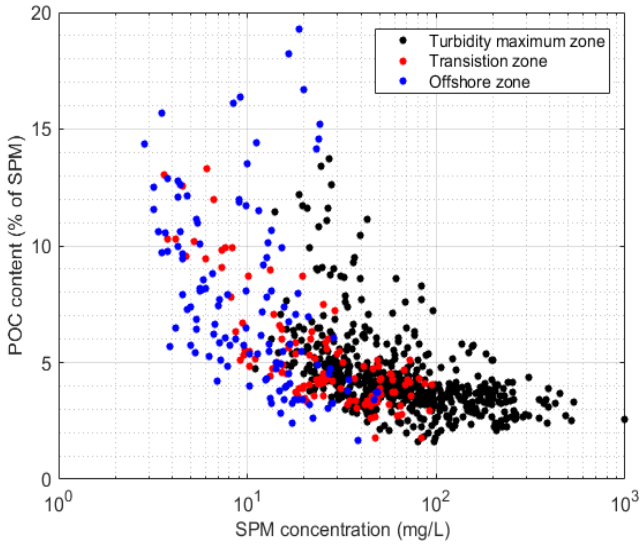

Figure 2.3: Scatter plot of POC content (% of SPM) versus SPM concentration. The coupled data sets of POC content and SPM concentration were obtained from all the 13 hours measurement campaigns.

Time series of the PSDs during the 13 hours tidal cycles are shown in Figure 2.5, for the TMZ and OSZ, respectively. PSDs in the TMZ skewed toward a smaller size around peak flow (e.g., t = 3, 4 h at location MOW1 on July/10/2007) and then to a larger size around slack water (e.g., t = 6, 7 h). Except for the PSDs in October/23/2007, the other PSDs in the TMZ showed bimodality, comprising microflocs (20–200 µm) and macroflocs (>200 µm), as reported in the earlier studies (Lee et al. 2012). The primary peak of microflocs in a PSD was prominent around the peak flow. However, while approaching the slack water, the secondary peak of macroflocs became dominant over the primary peak. Low flow/turbulence intensity might promote the aggregation of microflocs (i.e., mineral, biomineral aggregates) to macroflocs (i.e., biological aggregates) (Lee et al. 2011; 2012; 2014). On the other hand, large hardly-settleable biological aggregates which were suspended in the water column might dominate in the slack water. Maggi and Tang (2015) recently reported that larger biological aggregates can be lighter and even settle slower than smaller mineral, bio-mineral aggregates. Here, larger biological aggregates can be suspended in the slack water, while smaller mineral, bio-mineral aggregates settle and deposit, thereby developing the secondary peak of biological aggregates.

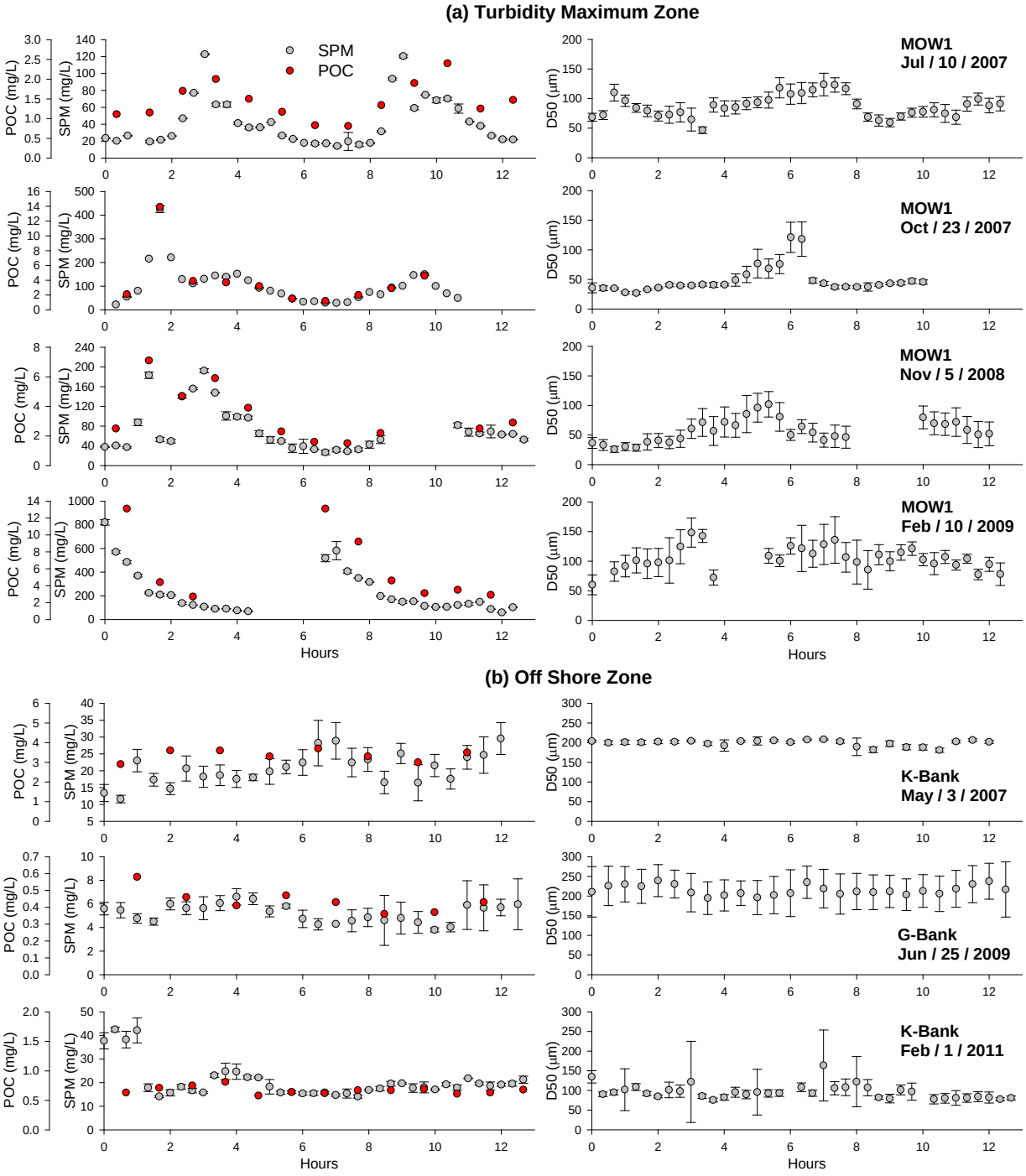

Figure 2.4: Dynamic behaviors of suspended particulate matter (SPM) and particulate organic carbon (POC) concentrations and aggregate size (D50) in 13-hour tidal cycles, in (a) the turbidity maximum zone (TMZ) and (b) the offshore zone (OSZ). Each set of the SPM/POC and D50 data was measured on a specific date of a field campaign. MOW1: measurement site in the TMZ; K-Bank and G-Bank: measurement sites in the OSZ.

a

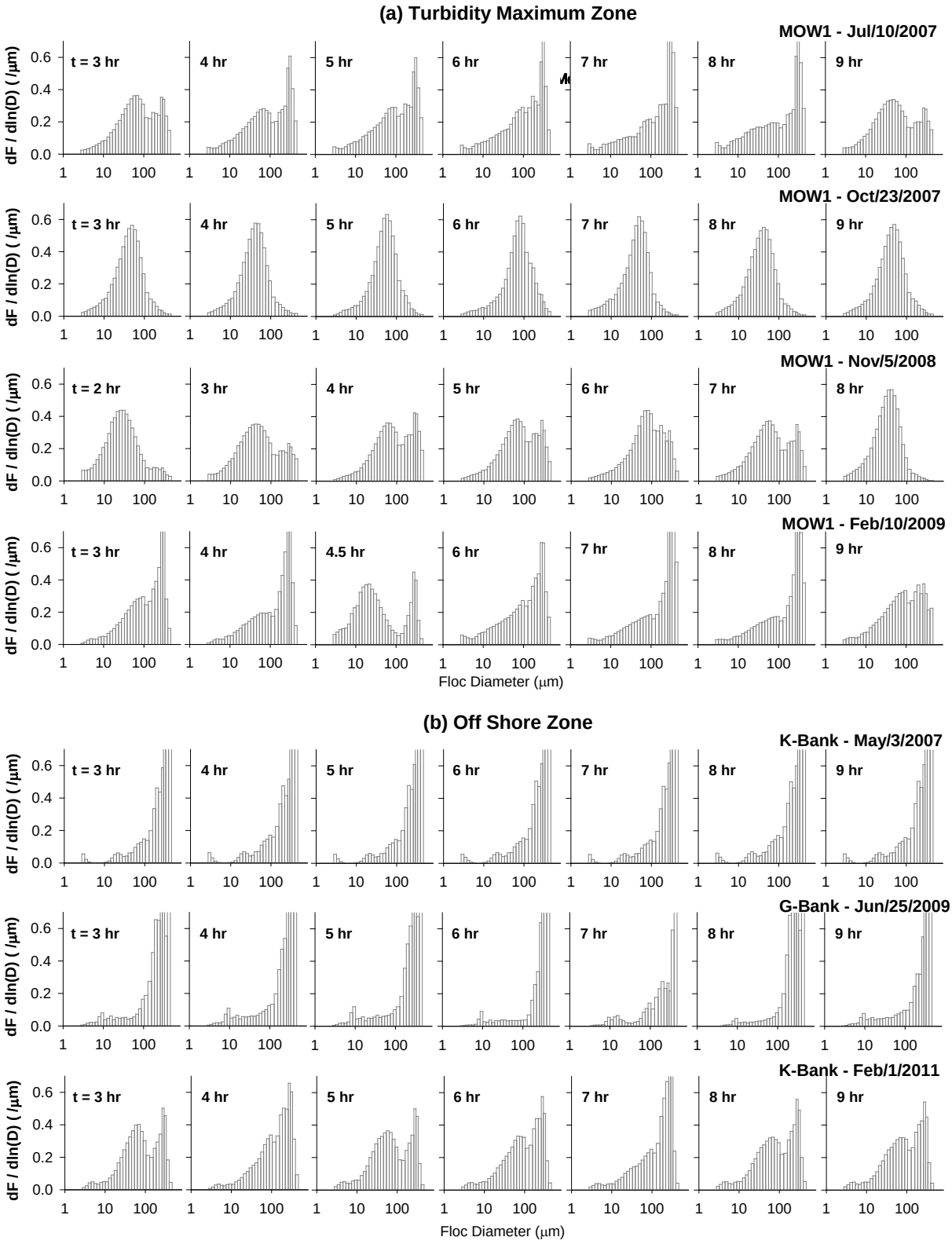

Figure 2.5: Particle size distributions (PSDs) of suspended particulate matter (SPM) in 13-hour tidal cycles, for (a) the turbidity maximum zone (TMZ) (MOW1) and (b) the offshore zone (OSZ) (K-Bank and G-Bank). Each set of the PSDs was measured on a specific date of a field campaign.Each PSD was plotted on a logarithmic scale, and the fraction of a size bin was normalized by the width of the size bin in y-axis. Thus, dF/dln (D) is the normalized volumetric fraction by the width of the size interval in the log scale, in accordance with the lognormal distribution function (Hinds 1999; Lee et al. 2012).

However, PSDs in the OSZ remained rather constant during the entire tidal cycle, consistently skewing toward a larger size (Figure 2.5b). A substantial fraction of the PSDs occupied the upper most measuring bin of the LISST-100X instrument (i.e., 500 µm). Aggregates in the OSZ, even with such a large size, apparently did not properly settle but floated in the water column (see also the previous paragraph and Figure 2.4). Thus, SPM in the OSZ is likely composed of large but light, fluffy, and hardly-settleable biological aggregates (i.e., marine snow), whereas SPM in the TMZ comprises dense, compact, and readly-setteable mineral, biomineral aggregates, as well as biological aggregates (Bainbridge et al. 2012; Maggi 2013; Maggi & Tang 2015; Tang & Maggi 2016). However, note that this argument is supported by a rather indirect measurement of SPM dynamics in this research and observations from earlier studies. Direct ways of measuring aggregate morphology might be required in the future to explain realistic structures and behaviors of mineral, biomineral, and biological aggregates.

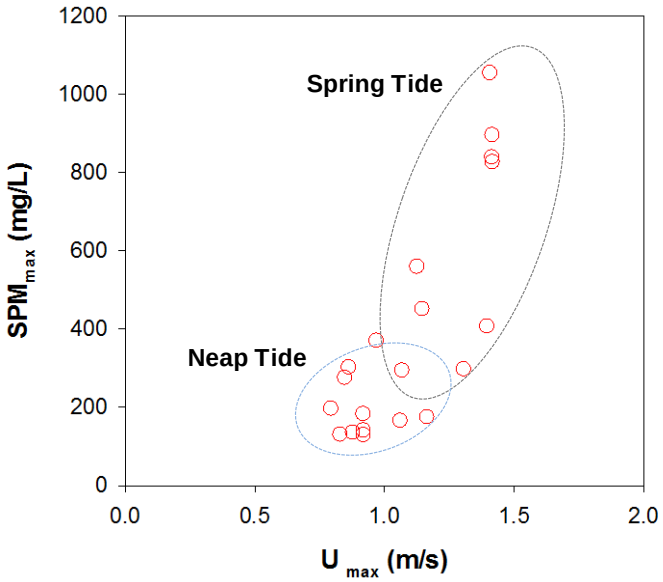

Figure 2.6: Plots of maximum suspended particulate matter concentration (SPM_{max}) versus maximum flow velocity (U_{max}). Each point represents a pair of SPM_{max} and U_{max} measured in a 13-h tidal cycle. All the data were measured in the turbidity maximum zone (TMZ) from 2004 to 2011.

2.2.3. SPM dynamics during algae bloom and normal periods in the TMZ

Flow intensity of the spring and neap tides was found to affect the SPM dynamics in the TMZ (i.e., the MOW1 site). A spring tide, associated with a strong peak flow (up to 1.5 m/s), increased SPM concentrations substantially, compared to a neap tide with a weak peak flow (up to 1.0 m/s). For example, SPM concentrations increased up to 800 mg/L during a spring tide (e.g., MOW1 - Feb/10/2009 in Figure 2.4a), whereas it remained under 120 mg/L during a neap tide (e.g., MOW1 - Jul/10/2007). When the pairs of the maximum SPM concentration (SPM_{max}) and peak flow velocity (U_{max}) in each 13 hours tidal cycle are plotted (Figure 2.6), they are shown to be proportional. A spring tide with high U_{max} resulted in high SPM_{max}, because it enhanced disaggregation, erosion and resuspension of sediment particles/flocs. However, a neap tide with low U_{max} resulted in low SPM_{max}, because it enhanced aggregation, sedimentation and deposition. Thus, SPM dynamics in the TMZ, which was governed by aggregation-disaggregation, sedimentation-resuspension and erosion-deposition, depended highly on flow intensity. However, an exception against the SPM-flow intensity relation was found during an algae bloom period.

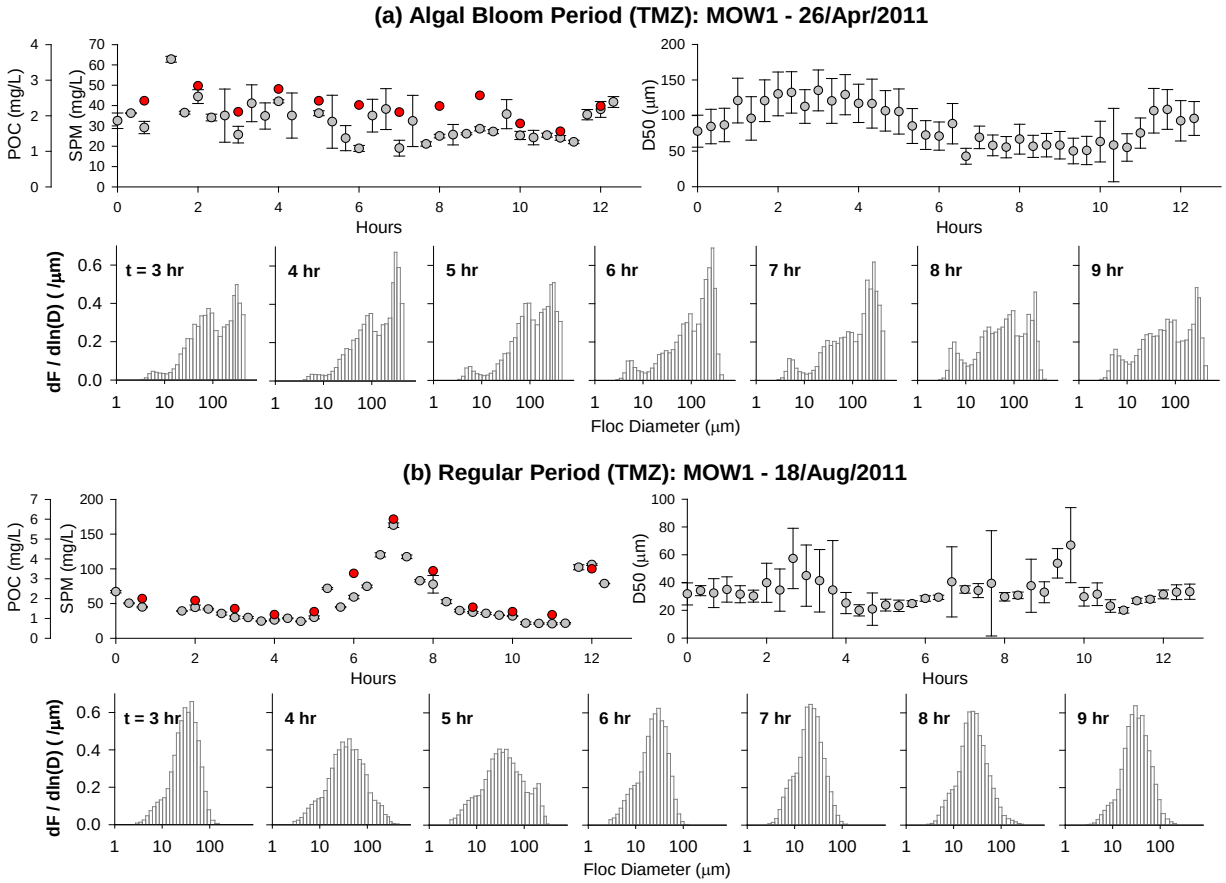

Figure 2.6: Dynamic behaviors of suspended particulate matter (SPM) and particulate organic carbon (POC) concentrations, aggregate size (D50) and particle size distribution (PSD) in a 13-hour tidal cycle. The two data sets were collected in the TMZ (i.e., the MOW1 site) on different dates in 2011, representing (a) algal bloom period and (b) regular periods.

During the reported spring algae bloom (MOW1 - Apr/26/2011 in Figure 2.7a), SPM and POC concentrations did not show a clear up-and-down trend with tide, but behaved similar to those in the OSZ. The aggregate sizes during the algae bloom period (Apr/26/2011 in Figure 2.7a) were 2 to 3 times larger than aggregates during the normal period, measured at the same site four months later (Aug/18/2011 in Figure 2.7b). Although aggregates were enlarged (>100 μm) during the algae bloom period, they did not show a clear sign of downward settling. The aggregates are thus lighter and less settleable than during a regular period, and thus more similar to the marine snow (i.e. biological aggregates) found in the OSZ (see Section 2.2.2). In the TMZ two different types of aggregates may thus occur: (1) sediment-enriched, dense, and settleable biomineral aggregates during normal periods and (2) biomass-enriched, light, and less settleable marine snow during algal bloom periods (Figure 2.7). The latter type of aggregate corresponds better to the one observed in the OSZ. The aggregates occurring during algae bloom periods or in the OSZ have lower settling velocity as a larger fraction is composed of organic matter and sticky bio-polymers organized in a fluffy structure (Alldredge & Silver 1988; Fennesey et al. 1994).

Previous studies, carried out in the same TMZ, reported that large and settleable biomineral aggregates were dominant SPM species during bio-enriched spring and summer periods (Fettweis et al. 2014; Fettweis & Baeye 2015). These large, settleable biomineral aggregates are contradictory to less settleable biological aggregates observed in this cur-

rent study. However, it is important to note that the SPM samples in this study were taken in the middle of the water column well above the near-bed layer. Dense, compacted, and settleable biomineral aggregates might be stored in the near-bed layer, causing mineral-depletion in the water column, and hence less dense, fluffy, and hardly settleable biological aggregates might formed and floated around in the water column. Enhanced primary production during an algal bloom period was reported to reduce erosion and resuspension of muddy deposits (Vos et al. 1988). A large amount of cohesive sediments are thus stored in or on the seafloor as a fluid-mud layer or a muddy deposit, and the marine snow with more biomass and less sediments is suspended in the water column (Fettweis et al. 2014). 2014; Fettweis & Baeye 2015). This SPM behavior during an algal bloom period with high primary production agrees with the satellite images of low SPM and high Chl concentrations in summer (Figure 2.1). Similar observations were made in the port of Zeebrugge. High primary production and low turbulence in summer provoked a large amount of mud deposition in the near-bed layer (or formation of a fluid mud layer) and reduction of the SPM concentration in the water column.

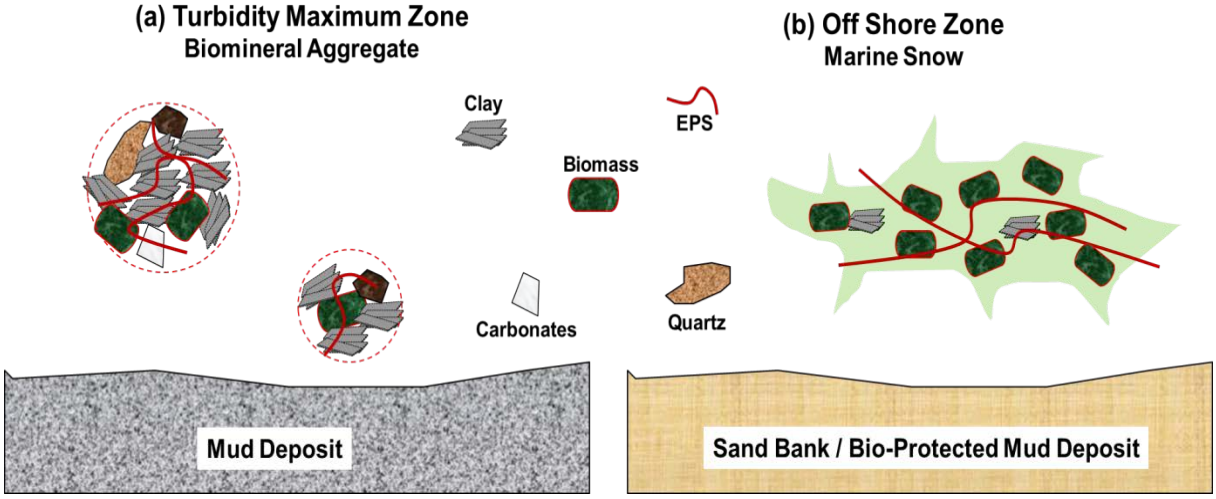

Figure 2.7: Schematic diagrams of (a) biomineral aggregates in the turbidity maximum zone (TMZ) and (b) biological marine snow in the offshore zone (OSZ). EPS: extracellular polymeric substances.

Reviewing other studies (van der Lee 2000; De Lucas Pardo et al. 2015) revealed similar SPM dynamics around an algal bloom period. Proliferation of a specific algae group could enhance flocculation and store sediments in the near-bed layer, and hence could cause large but suspended biological aggregates and a low SPM concentration in the water column. Maerz and co-workers (2016) have been looking at the whole gradient from the nearshore TMZ to the OSZ; they have found a maximum settling velocity in the transition zone between the TMZ and the OSZ where the aggregates are larger as compared to near-coast TMZ and denser as compared to the low turbid OSZ. This maximum in settling velocity is caused by similar gradients in aggregate size, POC content, density, and chlorophyll concentration than found in our data. The fact that algae are involved in these observed gradients points to seasonal influences. Another study (Van der Hout et al. 2017), however, does not confirm the leading role of the algae bloom on SPM dynamics. The reason for these different findings may be due to differences in, amongst others, hydrodynamics, wave climate, nutrient availability, and algae species at the different study sites. The importance of each of these parameters will explain to a smaller or larger part the observed seasonal variations in SPM dynamics.

Biomineral and biological aggregates are often approximated by a single parameter (e.g. a characteristic diameter) in practical applications, although they are very different in composition and mechanical property. For example, a traditional floc structure model, based on fractal theory, includes only mineral particles and disregards organic matter, which is instead assumed to be part of pore space for simplicity and ease (Khelifa et al. 2006; Maggi 2007). This approximation might not be valid for biological aggregates (i.e., marine snow) with a high content of organic matter or in environments where aggregate properties change in time (regular versus algae bloom period) or space (inside and outside harbours). Thus, in our opinion, heterogeneity of aggregates, at least the two fractions of biomass and sediments, should be considered when developing a rigorous floc structure model and predicting accurately the fate and transport of biomass and sediments in marine and coastal waters (Maggi 2013).

A higher biomass content (indicated by a higher POC/SPM ratio) was generally found to enhance flocculation, thereby increasing aggregate size. However, the quantity of biomass is not the only factor determining the flocculation capability. For example, in June 2009 at G-Bank (Figure 2.2a), aggregate size increased to over 200 µm, even with a low POC/SPM. Besides the quantity of biomass, the quality, such as stickiness, is important for controlling flocculation kinetics, as reported in previous research (van der Lee 2000; 2001). Specifically, extracellular polymeric substances (EPSs) or transparent extracellular polymers (TEPs) are sticky and increase flocculation (Passow 2000; Engel et al. 2004; Jouon et al. 2008; Mari et al. 2017). Long polymeric chain structures of EPSs and TEPs, which are produced by aquatic microorganisms (e.g., algae), can bind biomass and sediment particles to large mineral, biomineral, and biological aggregates. Even in an unfavorable chemical condition for flocculation (e.g., terrestrial water with low ionic strength), a small amount of EPSs and TEPs can cause substantial flocculation, because they can overcome the electrostatic repulsive force of negatively-charged colloidal particles and bind such particles to large aggregates (Furukawa et al. 2014; Lee et al. 2017). Therefore, qualitative measures of biomass, such as EPS and/or TEP concentration, likely need to be included to explain bio-mediated flocculation and SPM dynamics in marine and coastal waters.

2.3. Conclusions

The monitoring and analysis of SPM dynamics explained how organic biomass and inorganic sediment interact with each other to build large biomineral aggregates or marine snow in marine and coastal waters. SPM in the TMZ and OSZ had a similar mineralogical composition, but encountered different fates in association with biomass. SPM in the TMZ built sediment-enriched, dense, and settleable biomineral aggregates, whereas SPM in the OSZ was composed of biomass-enriched, light, and less settleable marine snow. Biological proliferation, such as an algae bloom, also facilitated the occurrence of marine snow in the water column, even in the TMZ. Enhanced flocculation in summer could also scavenge SPM in the water column down to the sea bed, resulting in a low SPM concentration in the water column. In short, bio-mediated flocculation and SPM dynamics were found to vary spatially and seasonally, affected by the biota. The proposed concept to combine organic and mineral particles in aggregates will help us to better understand and predict bio-mediated flocculation and SPM dynamics in marine and coastal waters.

3. Referenties

Adriaens, R., 2015. Neogene and Quaternary clay minerals in the southern North Sea. PhD thesis, KULeuven, Belgium, 280pp

Adriaens R, Zeelmaekers E, Fettweis M, Vanlierde E, Vanlede J, Stassen P, Elsen J, Środoń J, Vandenberghe N. Quantitative clay mineralogy as provenance indicator for recent muds in the southern North Sea (in revision for *Marine Geology*)

Agrawal Y, Pottsmith H. 2000. Instruments for particle size and settling velocity observations in sediment transport. *Marine Geology*, *168*, 89–114.

Alldredge A, Silver M. 1988. Characteristics, dynamics and significance of marine snow. *Progress in Oceanography*, *20*, 41–82.

Andrews S, Nover D, Schladow S. 2010. Using laser diffraction data to obtain accurate particle size distributions: The role of particle composition. *Limnoogy & Oceanography: Methods, 8*, 507–526.

Bainbridge Z, Wolanski E, Alvarez-Romero JG, Lewis SE, Brodie JE. 2012. Fine sediment and nutrient dynamics related to particle size and floc formation in a Burdekin River flood plume, Australia. *Marine Pollution Bulletin*, *65*, 236–248.

Barkmann W, Schafer-Neth C, Balzer W. 2010. Modelling aggregate formation and sedimentation of organic and mineral particles. *Journal of Marine Systems*, *82*, 81–95.

Burd A, Jackson G. 2002. Modeling steady-state particle size spectra. *Environmental Science and Technology*, *36*, 323–327.

Chen MS, Wartel S, Temmerman S. 2005. Seasonal variation of floc characteristics on tidal flats, the Scheldt estuary. *Hydrobiologia*, *540*, 181–195.

Chen P, Yu JCS, Fettweis M. 2017. Modelling storm-influenced SPM flocculation using a tide–wave-combined biomineral model. *Water Environment Research* (in press).

Davies E, Nimmo-Smith A, Agrawal Y, Souza A. 2012. LISST-100 response to large particles. *Maine Geology*, *307–311*, 117–122.

De Lucas Pardo MA, Sarpe D, Winterwerp JC. 2005. Effect of algae on flocculation of suspended bed sediments in a large shallow lake. Consequences for ecology and sediment transport processes. *Ocean Dynamics*, *65*, 889–903.

Droppo IG. 2001. Rethinking what constitutes suspended sediment. *Hydrological Processes, 15*, 1551–156

Droppo I, Leppard G, Liss S. 2005. Milligan, T. *Flocculation in natural and engineered environmental systems*; CRC Press Inc., Boca Raton, Florida, USA.

Eisma D. 1986. Flocculation and de-flocculation of suspended matter in estuaries. *Netherlands Journal of Sea Research*, *20*, 183–199.

Engel A, Thoms S, Riebesell U, Rochelle-Newall E, Zondervan I. 2004. Polysaccharide aggregation as a potential sink of marine dissolved organic carbon. *Nature, 428*, 929–932.

Fettweis M, Francken F, Pison V, Van den Eynde D. 2006. Suspended particulate matter dynamics and aggregate sizes in a high turbidity area. *Marine Geology*, *235*, 63–74.

Fettweis M, Nechad B, Van den Eynde D. 2007. An estimate of the suspended particulate matter (SPM) transport in the southern North Sea using SeaWiFS images, in situ measurements and numerical model results. *Continental Shelf Research*, *27*, 1568–1583.

Fettweis M. 2008. Uncertainty of excess density and settling velocity of mud flocs derived from in situ measurements. *Estuarine, Coastal and Shelf Science*, *78*, 426–436.

Fettweis M, Francken F, Van den Eynde D, Verwaest T, Janssens J, Van Lancker V. 2010. Storm influence on SPM concentrations in a coastal turbidity maximum area with high anthropogenic impact (southern North Sea). *Continental Shelf Research*, *30*, 1417–1427.

Fettweis M, Baeye M, Lee BJ, Chen P, Yu JCS. 2012. Hydro-meteorological influence and multimodal suspended particle size distributions in the Belgian nearshore area (southern North Sea). *Geo-Marine Letters, 32,123-137*.

Fettweis M, Baeye M, Van der Zande D, Van den Eynde D, Lee BJ. 2014. Seasonality of floc strength in the southern North Sea. *Journal of Geophysical Research: Oceans*, *119*, 1911–1926.

Fettweis M, Baeye M. 2015. Seasonal variation in concentration, size and settling velocity of muddy marine flocs in the benthic boundary layer. *Journal of Geophysical Research: Oceans*, *120*, 5648–5667.

Fennessy M, Dyer K, Huntley D. 1994. INSSEV: An instrument to measure the size and settling velocity of flocs in situ. *Marine Geology*, *117*, 107–117.

Furukawa Y, Reed AH, Zhang G. 2014. Effect of organic matter on estuarine flocculation: A laboratory study using montmorillonite, humic acid, xanthan gum, guar gum and natural estuarine flocs. *Geochemical Transactions*, *15*, 1–9.

Graham GW, Davies E, Nimmo-Smith A, Bowers DG, Braithwaite KM. 2012. Interpreting LISST-100X measurements of particles with complex shape using digital in-line holography. *Journal of Geophysical Research Oceans*, *117*, C05034, doi:10.1029/2011JC007613

Gudasz C, Bastviken D, Premke K, Steger K, Tranvik LJ. 2012. Constrained microbial processing of allochthonous organic carbon in boreal lake sediments. *Limnology and Oceanography*, *57*, 163–175.

Hinds W. 1999. Aerosol Technology: Properties, Behavior, and Measurement of Airborne Particles, 2nd ed.; John Wiley: New York, NY, USA.

Jago CF, Kennaway GM, Novarino G, Jones SE. 2007. Size and settling velocity of suspended flocs during a phaeocystis bloom in the tidally stirred Irish Sea, NW European Shelf. *Marine Ecology Progress Series*, *345*, 51–61.

Jouon A, Ouillon S, Douillet P, Lefebvre JP, Fernandez JM, Mari X, Froidefond J. 2008. Spatio-temporal variability in suspended particulate matter concentration and the role of aggregation on size distribution in a coral reef lagoon. *Maine Geology*, *256*, 36–48.

Kastner M. 1999. Oceanic minerals: Their origin, nature of their environment, and significance. *Proceedings of the National Academy of Sciences*, *96*, 3380–3387.

Khelifa A, Hills P. 2006. Models for effective density and settling velocity of flocs. *Journal of Hydraulic Research*, *44*, 390–401.

Lacroix G, Ruddick K, Ozer J, Lancelot C. 2004. Modelling the impact of the Scheldt and Rhine/Meuse plumes on the salinity distribution in Belgian waters (southern North Sea). *Journal of Sea Research*, *52*, 149–163.

Lauwaert B, Fettweis M, De Witte B, Devriese L, Van Hoei G, Timmermans S, Martens C. 2016. Synthesis report on the effects of dredged material disposal on the marine environment (licensing period 2012-2016). RBINS-ILVO-AMT-AMCS-FHR report BL/2016/09, 107pp.

Lee BJ, Toorman E, Molz FJ, Wang J. 2011. A two-class population balance equation yielding bimodal flocculation of marine or estuarine sediments. *Water Research*, *45*, 2131–2145.

Lee BJ, Fettweis M, Toorman E, Molz FJ.2012. Multimodality of a particle size distribution of cohesive suspended particulate matters in a coastal zone. *Journal of Geophysical Research: Oceans*, *117*, C03014.

Lee BJ, Toorman E, Fettweis M. 2014. Multimodal particle size distributions of fine-grained sediments: mathematical modeling and field investigation. *Ocean Dynamics*, *64*, 429–441.

Lee BJ, Hur J, Toorman E. 2017. Seasonal variation in flocculation potential of river water: Roles of the organic matter pool. *Water*, *9*, 335–34

Maerz J, Hofmeister R, van der Lee EM, Grawe U, Riethmuller R, Wirtz KW. 2016. Maximum sinking velocities of suspended particulate matter in a coastal transition zone. *Biogeosciences*, *13*, 4863–4876.

Maggi F. 2007. Variable fractal dimension: A major control for floc structure and flocculation kinematics of suspended cohesive sediment. *Journal of Geophysical Research: Oceans*, *112*, C07012.

Maggi F. 2009. Biological flocculation of suspended particles in nutrient-rich aqueous ecosystems. *Jounal of Hydrology*, *376*, 116–125.

Maggi F.2013. The settling velocity of mineral, biomineral, and biological particles and aggregates in water. *Journal of Geophysical Research: Oceans*, *118*, 2118–2132.

Maggi F, Tang FHM. 2015. Analysis of the effect of organic matter content on the architec-

ture and sinking of sediment aggregates. *Marine Geology*, *363*, 102–111.
Mari X, Passow U, Migon C, Burd A, Legendre L. 2017. Transparent Exopolymer Particles: Effects on carbon cycling in the ocean. *Progress in Oceanography*, *151*, 13–37.
Markussen TN, Andersen TJ. 2013. A simple method for calculating in situ floc settling velocities based on effective density functions. *Marine Geology*, *344*, 10–18.
Mikkelsen OA, Hill PS, Milligan T, Chant RJ. 2005. In situ particle size distributions and volume concentrations from a LISST-100 laser particle sizer and a digital floc camera. *Continental Shelf Research*, *25*, 1959–1978
Mikkelsen O, Curran K, Hill P, Milligan T. 2007. Entropy analysis of in situ particle size spectra. *Estuarine, Coastal and Shelf Science*, *72*, 615–625.
Ouillon S, Douillet P, Andrefouet S. 2004. Coupling satellite data with in situ measurements and numerical modeling to study fine suspended-sediment transport: a study for the lagoon of New Caledonia. *Coral Reefs*, *23*, 109–122.
Passow U. 2002. Transparent exopolymer particles (TEP) in aquatic environments. *Progress in Oceanography*, *55*, 287–333.
Perianez R. 2005. Modelling the transport of suspended particulate matter by the Rhone River plume (France). Implications for pollutant dispersion. *Environmental Pollution*, *133*, 351–364.
Sahoo GB, Nover D, Schladow SG, Reuter JE, Jassby D. 2013. Development of updated algorithms to define particle dynamics in Lake Tahoe (CA-NV) USA for total maximum daily load. *Water Resources Research*, *49*, 7627–7643
Smith SJ, Friedrichs CT. 2011. Size and settling velocities of cohesive flocs and suspended sediment aggregates in a trailing suction hopper dredge plume. *Continental Shelf Research*, *31*, 50–63.
Tan XL, Zhang GP, Yin H, Reed A, Furukawa Y. 2012. Characterization of particle size and settling velocity of cohesive sediments affected by a neutral exopolymer. *International Journal of Sediment Research*, *27*, 473–485.
Tang FHM, Maggi F. 2016. A mesocosm experiment of suspended particulate matter dynamics in nutrient-and biomass-affected waters. *Water Research*, *89*, 76–86.
Tranvik LJ, Downing JA, Cotner JB, Loiselle SA, Striegl RG, Ballarore TJ, Dillon P, Finlay K, Fortino K, Knoll LB, Kortelainen PL, Kutser T, Larsen S, Laurion I, Leech DM, McCallister SL, McKnight DM, Melack JM, Overholt E, Porter JA, Sobek S, Tremblay A, Vanni MJ, Verschoor AM, von Wachenfeldt E, Weyhenmeyer GA. 2009. Lakes and reservoirs as regulators of carbon cycling and climate. *Limnology and Oceanography*, *54*, 2298–1314.
Van der Hout CM, Wittbaard R, Bergman MJM, Duineveld GCA, Rozemeijer MJC. 2017. The dynamics of suspended particulate matter (SPM) and chlorophyll-a from intratidal to annual time scales in a coastal turbidity maximum. *Journal of Sea Research*, doi: 10.1016/j.seares.2017.04.011.
Van der Lee WTB. 2000. Temporal variation of floc size and settling velocity in the Dollard estuary. *Continental Shelf Research*, *20*, 1495–1511.
Van der Lee WTB. 2001. Parameters affecting mud floc size on a seasonal time scale: The impact of a phytoplankton bloom in the Dollard estuary, The Netherlands. In *Coastal and estuarine fine sediment transport processes, (Eds. McAnally W.H., Mehta A.J.),* Proceedings in Marine Science, 3, Elsevier, pp. 403–421.
van Leussen, W. 1994. *Estuarine macroflocs: Their role in fine grained sediment transport*; PhD Dissertation.; Utrecht University: Utrecht, Netherlands.
Vos P, De Boer P, Misdorp R. 1998. Sediment stabilization by benthic diatoms in intertidal sandy shoals: Qualitative and quantitative observations. In *Tide-Influenced Sedimentary Environments and Facies*; D. Reidel Publishing: Dordrecht, the Netherlands, pp. 511–526.
Winterwerp J, van Kesteren W. 2004. *Introduction to the physics of cohesive sediment in the marine environment,* Elsevier, The Netherlands.
Zeelmaekers E. 2011. Computerized qualitative and quantitative clay minerology: Introduction and application to known geological cases. PhD thesis, KULeuven, Leuven, Belgium.

COLOPHON

Dit rapport werd voorbereid door de BMM in januari 2018
Zijn referentiecode is .MOMO/8/MF/201801/NL/AR/2

De scheepstijd met de RV Belgica werd voorzien door BELSPO en KBIN-OD Natuur

Indien u vragen hebt of bijkomende copies van dit document wenst te verkrijgen, gelieve een e-mail te zenden naar mfettweis@naturalsciences.be, met vermelding van de referentie, of te schrijven naar:

Koninklijk Belgisch Instituut voor Natuurwetenschappen
OD Natuur – BMM
t.a.v. Michael Fettweis
Gulledelle 100
B–1200 Brussel
België
Tel: +32 2 773 2132

BEHEERSEENHEID VAN HET
MATHEMATISCH MODEL VAN DE NOORDZEE

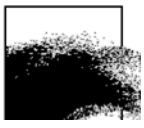

APPENDIX 1

Bijdragen INTERCOH 13-17 november, Montevideo (Uruguay)

Adriaens R, Zeelmakers E, Fettweis M, Vanlierde E, Vanlede J, Stassen P, Elsen J, Środoń J, Vandenberghe N. 2017. Quantitative clay mineralogy as provenance indicator for the recent muds located in the southern North Sea. (abstract & poster)

Fettweis M, Riethmüller R, Verney R, Becker M, Backers J, Baeye M, Chapalain M, Claeys S, Claus J, Cox T, Deloffre J, Depreiter D, Druine F, Flöser G, Grünler S, Jourdin F, Lafite R, Nauw J, Nechad B, Röttgers R, Sotollichio A, Vanhaverbeke W, Van Hoestenberghe T, Vereecken H. On best practice for in situ high-frequency long-term observations of suspended particulate matter concentration using optical and acoustic systems. (abstract)

Shen X, Toorman E, Fettweis M. 2017. A tri-modal flocculation model coupled with TELEMAC for suspended cohesive sediments in the Belgian coastal zone. (abstract)

Vanlede J, Dujardin A, Fettweis M. 2017. Mud dynamics in the harbor of Zeebrugge. (abstract)

Quantitative clay mineralogy as provenance indicator for the recent muds in the southern North

Adriaens Rieko[1], Edwin Zeelmakers[1], Michael Fettweis[2], Elin Vanlierde[3], Joris Vanlede[3], Peter Stassen[1], Jan Elsen[1], Jan Srodon[4], Noël Vandenberghe[1]

[1] Department of Earth and Environmental Sciences, KU Leuven, Celestijnenlaan 200E, 3001 Heverlee, Belgium
[2] Royal Belgian Institute of Natural Sciences, OD Nature, Gulledelle 100, 1200 Brussels, Belgium E-mail: mfettweis@naturalsciences.be
[3] Flanders Hydraulics Research, Berchemlei 115, 2140 Antwerp, Belgium
[4] Institute of Geological Sciences, Polish Academy of Sciences, Research Centre in Kraków, ul. Senacka 1, PL-31002 Kraków, Poland

Introduction

In order to assess the present state of a marine sedimentary environment and to predict changes induced by natural variability, human activities or climate change, qualitative understanding and quantitative estimates of sediment fluxes and budgets are needed. Although sediment fluxes and budgets are a key element to assess the fine-grained sediment dynamics on a regional scale, data are often not available to qualitatively understand the fluxes on a time-scale longer than the duration of in-situ measurement campaigns. One of the difficulties lays in the fact that regional fine-grained sediment dynamics is the sum of all the local sources and sinks, such as rivers, coastal erosion and accretion, deposition in inter- or subtidal areas and erosion of the geological substratum that are often not well known and that reflects the recent geological history of the area. This is also the case for the fine-grained sediment transport, the coastal turbidity maximum and the cohesive sediment deposits in the French-Belgian-Dutch nearshore area and in the Scheldt estuary, where the provenance is still under debate. The existing hypotheses for the mud provenance are based on the residual flow patterns and general sedimentological considerations (e.g. Prandle et al. 1996; Fettweis et al. 2007). The aim of the current study is to make a new contribution towards qualitative and quantitative fine-grained sediment budgets and dynamics in the southern North Sea by identifying how the provenance of the fine-grained bottom and suspended sediments is related to regional and local fine-grained sediment sources.

Method

As provenance indicator clay minerals have been used. The advantage of clay minerals is the obvious abundance of these minerals in the mud deposits and in the SPM and their stability or very minor changes if any during transport between provenance and deposition areas. Clay minerals can be considered as representative tracers as the transport of fine-grained sediment occurs either in flocs or as suspended particulate matter (e.g. Irion and Zöllmer 1999). The clay minerals have been determined using the robust quantitative analyses of Środoń & McCarthy (2009) and Hubert et al. (2009, 2012).

An extensive sampling campaign was set up in different phases to characterize the clay mineral composition of the mud deposits off the Belgian nearshore (further referred to as BCS), the SPM in the English Channel and the southern North Sea, and its possible source areas. These comprise both present-day sources, which were sampled by collecting bottom mud and/or suspension water samples, outcrop material and older, geological sources, which were sampled from borehole core material. For each source area, the clay mineral composition <2µm, referred to as the clay fraction, was quantified and compared with the mud composition from the BCS.

Results

The clay mineral compositional field for each analyzed source area is shown in Figure 1 with reference to the BCS muds and SPM compositional field. This figure demonstrates that English Channel waters, outcropping Paleogene sea floor bottom and Rhine-Meuse river water and deposits have to be excluded as an important clay mineral source of the BCS muds. The BCS muds and SPM clay mineral composition is also found in the SPM occurring in the Dutch coastal waters. This demonstrates that the clay minerals in the Dutch coastal waters do not originate from the Rhine-Meuse River but have as major source the turbidity maximum overlying the BCS muds. The turbidity maximum in the Belgian nearshore area is thus formed by erosion of the BCS mud.

The close relationship between the mud from the Scheldt estuary and the BCS mud raised the question whether the estuary effectively discharges the mud to the BCS where it is deposited or whether the inverse happens and BCS mud is imported into the estuary by tidal currents. As demonstrated in Figure 1, this combined fluvial discharge clay mineral composition plots very close

to the Scheldt estuary and BCS mud composition. It can be concluded that the BCS mud composition can only be produced by Scheldt river system.

The current tidal regime of the Scheldt estuary is, however, marine-dominated with only small amounts of fluvial mud being discharged into the North Sea (Verlaan, 2000). Presently, marine SPM dominates the estuary. This apparent contradiction with the results of the clay mineral provenance analysis can only be satisfactorily solved if the short period of hydrodynamic and sediment flux measurements in the estuary since the start of the measurements represents an unusual situation compared to the much longer period before when larger amounts of fluvial mud was exported from the river basin to the sea. The geological history suggest that the mud deposition with the BCS clay mineral composition has started since a few 100.000 years in contrast to the present hydrodynamics in the estuary and the coastal zone that exhibits a fine-grained sediment flux from out of the estuary towards inside. A consequence of this analysis is that the modern mud is derived from the erosion and resuspension of previously deposited mud. Resuspended muds contribute to a large part to the coastal turbidity maximum and represent a significant source of material in the estuary itself.

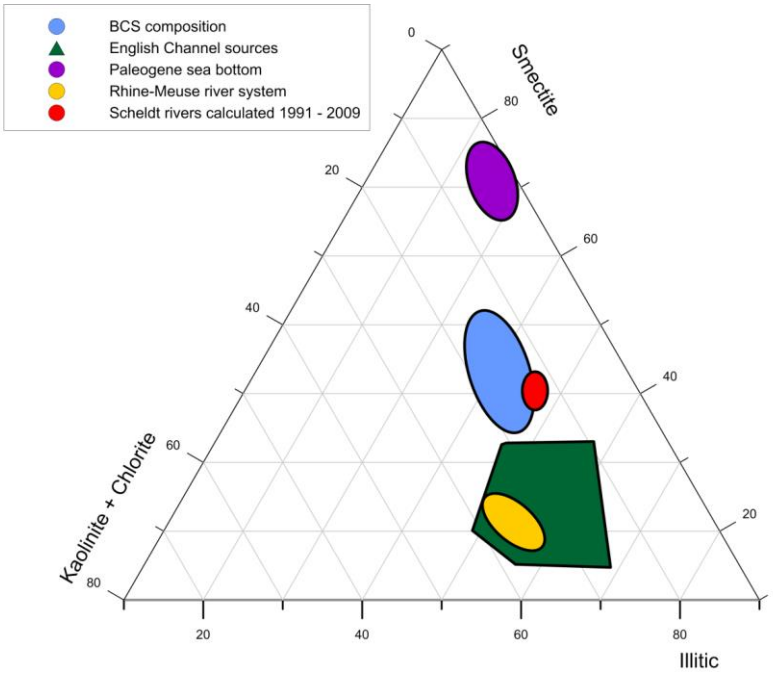

Fig. 1: Triangular diagram of the quantitative clay composition <2µm of the different analyzed regional sources and comparison with the compositional domain of the Belgian nearshore area (BCS).

References

Fettweis M, Nechad B, Van den Eynde D. (2007). An estimate of the suspended particulate matter (SPM) transport in the southern North Sea using SeaWiFS images, in-situ measurements and numerical model results. Continental Shelf Research, 27, 1568–1583.

Hubert F, Caner L, Meunier A, Lanson B. (2009). Advances in characterization of the soil clay mineralogy using X-ray diffraction: from decomposition to profile fitting. European Journal of Soil Science, 60, 1093-1105.

Hubert F, Caner L, Meunier A, Ferrage E. (2012). Unraveling complex <2µm clay mineralogy from soils using X-ray diffraction profile modeling on particle-size sub-fractions: Implications for soil pedogenesis and reactivity. American Mineralogist, 97, 384-398.

Irion G, Zöllmer V. (1999). Clay mineral associations in fine-grained surface sediments of the North Sea. Journal of Sea Research, 41, 119-12.

Prandle D, Ballard G, Flatt D, Harrison AJ, Jones SE, Knight PJ, Loch SG, McManus JP, Player R, Tappin A. (1996). Combining modelling and monitoring to determine fluxes of water, dissolved and particulate metals through the Dover Strait. Continental Shelf Research, 16, 237–257.

Srodon J, McCarty DK. (2009). Surface area and layer charge of smectite from CEC and EGME/H_2O-retention measurements. Clays and Clay Minerals, 56, 155–174.

Verlaan PAJ. (2000). Marine vs Fluvial Bottom Mud in the Scheldt Estuary. Estuarine, Coastal and Shelf Science 50, 627–638.

Quantitative clay mineralogy as provenance indicator for the recent muds in the southern North

R. Adriaens[1], E. Zeelmaekers[1,5], M. Fettweis[2], E. Vanlierde[3], J. Vanlede[3], P. Stassen[1], J. Elsen[1], J. Srodon[4], N. Vandenberghe[1]

[1]Department of Earth Science, KULeuven, Leuven, Belgium; [2]Royal Belgian Institute of Natural Sciences, Brussels, Belgium; [3]Flanders Hydraulics Research, Antwerp, Belgium; [4]Institute of Geological Sciences, Polish Academy of Sciences, Kraków, Poland; [5]present adres: Shell Exploration & Production Company, Houston, USA;

Introduction

The origin of the recent mud deposits as well as the coastal turbidity maximum in the French-Belgian-Dutch nearshore area of the southern North Sea is still under debate.
The mud provenance hypotheses (e.g. Fettweis et al. 2007) are based on an understanding of residual flow patterns in the Dover Strait and the southern North Sea and on geological and sedimentological considerations. So far no systematic sediment composition analyses have been carried in support.
Quantitative clay mineral composition was used as provenance indicator by comparing the clay mineral composition of the mud deposits and the SPM from the coastal turbidity maximum with those from samples collected at all possible local and remote sources such as the present day marine environment, estuaries and rivers, coastal erosion areas and the geological substratum.

Objective

Investigate the origin of recent mud and SPM by using clay mineral composition obtained by modern quantitative clay mineral analysis as provenance indicators.
Recommendations for sediment transport modelling

Sampling stations

Samples have been collected at sea, at land and from geological repositories in order to characterize the clay mineral composition of the sediments on the Belgian Continental Shelf (BCS), and in the different possible source areas (Paleogene clay outcrops, Pleistocene and Holocene mud outcrops, English Channel, Atlantic Ocean, Scheldt, Rhine & Meuse river basins).

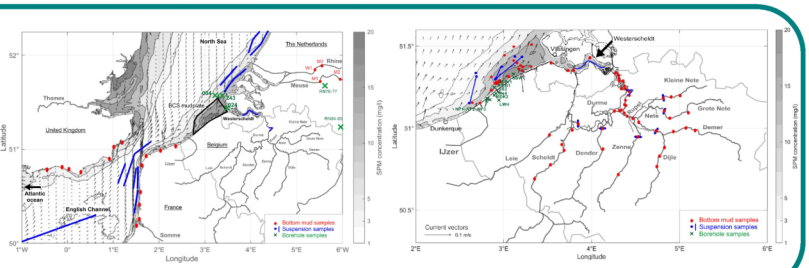

Figure 1: Samples taken in the North Sea and English Channel (left) and in the Belgian nearshore and Scheldt basin (right) showing the mudplate (black polygone) as well as of the averaged surface SPM concentration derived from MODIS satellite and the sampled locations. Arrows indicate the residual water transport.

Method

Samples of recent bottom mud and suspension water samples, representing present-day transported mud, outcrop material subject to erosion and also older strata. For each potential source area, the clay mineral composition of the <2µm fraction was quantified and compared with the BCS clay fraction composition. The clay minerals have been determined using the robust quantitative analyses (Środoń et al., 2001; Zeelmaekers et al., 2015).

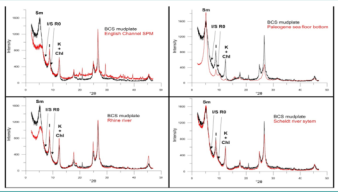

Figure 2: Examples of diffraction patterns of ethylene glycolated clay fractions <2µm from potential source areas and compared with the BCS muds.. Sm: Smectite; I/S R0: Randomly interstratified Illite-Smectite; I: Illite; K: Kaolinite; Chl: Chlorite.

Results

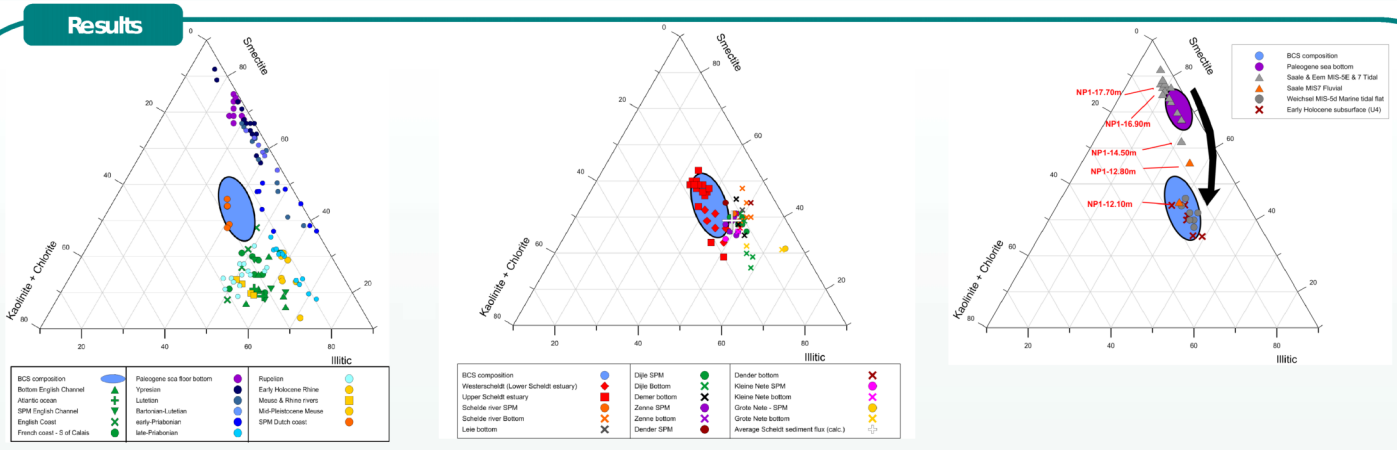

Figure 3: Ternary diagram of the quantitative clay composition <2µm of the samples from:

- **Left** English Channel, Paleogene clay samples offshore and onshore and the present-day and Pleistocene Meuse-Rhine. They all plot outside the BCS mudplate compositional domain. SPM samples from the Dutch nearshore and the Early-Holocene subsurface of the BCS mudplate plot entirely inside the BCS mudplate compositional domain.
- **Middle:** Scheldt river system, the Westerscheldt estuary (lower estuary), the upper estuary and the brackish to fresh intertidal flats as compared with the compositional domain of the BCS mudplate.
- **Right** Pleistocene samples of the Belgian coastal plain and comparison with the compositional domain of the BCS mudplate. Whereas marine samples from MIS 7-5E age systematically have a smectite-rich composition, which resembles that of the Paleogene sea bottom, the clay composition gradually evolves towards the BCS mudplate composition with the change of facies from marine towards fluvial depositional environment.

Conclusions

- Most provenance areas proposed in the literature for the muds found in the Belgian-Dutch nearshore area can be excluded whereas the Scheldt river and estuary system remained as source.
- The Scheldt estuary and river system is currently not exporting significant amounts of mud to the sea. Therefore the present-day SPM in the southern North Sea originates from the erosion and resuspension of the BCS mudplate.
- The SPM concentrations in the English Channel are low. Therefore resuspension of the local BCS muds is providing the SPM to the coastal turbidity maximim. The further advection of the SPM towards the northeastern part of the North Sea is governed by the actual hydrodynamic regime.
- It is crucial to incorporate the recent geological history to understand actual sediment transport patterns in which not only the present-day, but also the paleogeographic situation should be considered.
- SPM numerical models of the southern North Sea should incorporate bed boundary conditions (erosion) rather than specifying SPM concentration along open boundaries.

Acknowledgements
The results of this study have been obtained in the doctoral theses of E. Zeelmaekers and R. Adriaens with supervision by N. Vandenberghe, J. Środoń and J. Elsen. This study was partly funded by the Belgian Science Policy projects MOCHA (EV35), and by the Maritime Access Division of the Flemish Ministry of Mobility and Public Works (MOMO project).

References
Fettweis M., Nechad B, Van den Eynde D. 2007. An estimate of the suspended particulate matter (SPM) transport in the southern North Sea using SeaWiFS images, in-situ measurements and numerical model results. Continental Shelf Research, 27, 1568–1583
Środoń J., Drits VA., McCarty DK., Hsieh J.CC., Eberl DD. 2001. Quantitative XRD analysis of clay-rich rocks from random preparations. Clays & Clay Minerals, 49, 514-528.
Zeelmaekers E., Honty M., Derkowski A., Środoń J., De Craen M., Vandenberghe N., Adriaens R., Ufer K., Wouters L. 2015. Qualitative and quantitative mineralogical composition of the Rupelian Boom clay in Belgium. Clay Minerals, 50, 249-272.

On best practice for in situ high-frequency long-term observations of suspended particulate matter concentration using optical and acoustic systems

Fettweis Michael[1], Rolf Riethmüller[2], Romaric Verney[3], Marius Becker[4], Joan Backers[1], Matthias Baeye[1], Marion Chapalain[3], Stijn Claeys[5], Jan Claus[6], Tom Cox[7], Julien Deloffre[8] Davy Depreiter[6], Flavie Druine[8], Götz Flöser[2], Steffen Grünler[9], Frederic Jourdin[10], Robert Lafite[8], Janine Nauw[11], Bouchra Nechad[1], Rüdiger Röttgers[2], Aldo Sottolichio[12], Wim Vanhaverbeke[1], Thomas Van Hoestenberghe[13], Hans Vereecken[5]

[1] Royal Belgian Institute of Natural Sciences, OD Nature, Gulledelle 100, 1200 Brussels, Belgium E-mail: mfettweis@naturalsciences.be

[2] Helmholtz-Zentrum Geesthacht, Institute for Coastal Research, Max-Planck-Str. 1, 21502 Geesthacht, Germany

[3] IFREMER, Hydrodynamics and Sediment Dynamics Laboratory (DYNECO/PHYSED), BP 70, 29280 Plouzané, France

[4] MARUM, Centre for Marine Environmental Sciences, University of Bremen, Leobener Str. 8, 28359 Bremen, Germany

[5] Flanders Hydraulics Research, Berchemlei 115, 2140 Antwerp, Belgium

[6] IMDC, Van Immerseelstraat 66, 2018 Antwerp, Belgium

[7] University of Antwerp, Ecosystem Management Research group, Universiteitsplein 1C -C.0.32, 2610 Wilrijk, Belgium

[8] Normandie University Rouen, UMR CNRS 6143 M2C, 76821 Mont Saint Aignan, France

[9] Bundesanstalt für Wasserbau, Wedeler Landstr. 157, 22559 Hamburg, Germany

[10] Service Hydrographique et Océanographique de la Marine (SHOM), 13 rue du Chatellier, 29228 Brest, France

[11] Royal Netherlands Institute for Sea Research, PO Box 59, 1790 AB Den Burg, The Netherlands

[12] University of Bordeaux, EPOC, UMR5805, 33600, Pessac, France

[13] Fluves, Waterkluiskaai 5, 9040 Gent, Belgium

Abstract

Water clarity or turbidity is an important parameter to understand the marine ecosystem and is mainly controlled by suspended particulate matter concentration (SPMC). Measurements of SPMC spanning long time and large spatial scales have therefore became a matter of growing importance in the last decades. On many places worldwide observation platforms were installed to capture the temporal and spatial SPMC variability on scales ranging from turbulent fluctuations to entire basins. The infrastructure on which the sensors are attached is as diverse as the time scale of the processes studied, and includes fixed and moving platforms or a combination of both. The same holds for SPMC itself that may cover the range from very low to hyper-turbid conditions and concerning its composition from organic to mineral and from non-cohesive to cohesive properties.

Long-term in-situ measurements of SPMC involve in general one or several optical and acoustical sensors of similar or different technical specifications and, as the ground truth reference, gravimetric measurements of filtered water samples. The combination of indirect and reference measurements require two main calibration steps (sensor and model parameter calibration) at different moments during the workflow in order to extract reliable and homogeneous SPMC. These calibration steps are essential to be able to relate possible changes in calibration constants (sensor and model parameter) to sensor degradation or to natural variability in SPM inherent properties. The SPMC in long-term measurements is thus a surrogate of the real SPMC. A variety of parameters, particle (floc) size and composition have an impact on the optical and acoustical inherent properties of the SPM and thus on the sensor output. In case of long-term measurements, where multiple methods are often used in parallel, different sensor SPM concentration are obtained that represents surrogates or proxies that are not necessarily the same

The estimation of SPMC by optical and acoustical surrogates generally results from the combination of a number of technically independent calibration measurements and regression or inverse models. This includes all aspects of the measuring strategy, from the planning of the measurements to the

measurements itself and the post processing of the data (Figure 1). As long as measurements are carried out during a cruise with staff and laboratories ready to control the proper functioning of sensors and to react on changes in the actual field conditions, uncertainties in the separate steps can be minimized and errors quantified to some degree or even avoided. The situation is different for autonomous, long-term implementations or large-scale observation networks. The parallel or consecutive operation of numerous sensors requires additional (inter-)calibration effort to assure data homogeneity. Variabilities in the state of the studied system change the inherent particle properties which may require repeated field surveys for water sampling; electronic drift, mechanical threats or growing coverage of sensor transmitter/receiver windows by living (biofouling) or non-living matter (fouling) requires regular maintenance and sensor cleansing with sensor monitoring against well-defined references.

Direct or indirect measurements of SPMC are thus inherently associated with a number of uncertainties along the whole operational chain from planning over laboratory work, to system problems during mostly unsupervised deployment and to converting the observed continuous proxy values of optical and acoustical signals to SPMC. The aim of the study is to present and discuss potentials and limitations related with the use of optical and acoustical backscatter sensors, to describe challenges and yet unsolved problems with long-term observations of SPMC and to formulate recommendations as a basis to acquire quality-assured SPMC data sets. On the basis of examples the main sources of errors as well as means to quantify and reduce the uncertainties associated with SPMC measurements are illustrated.

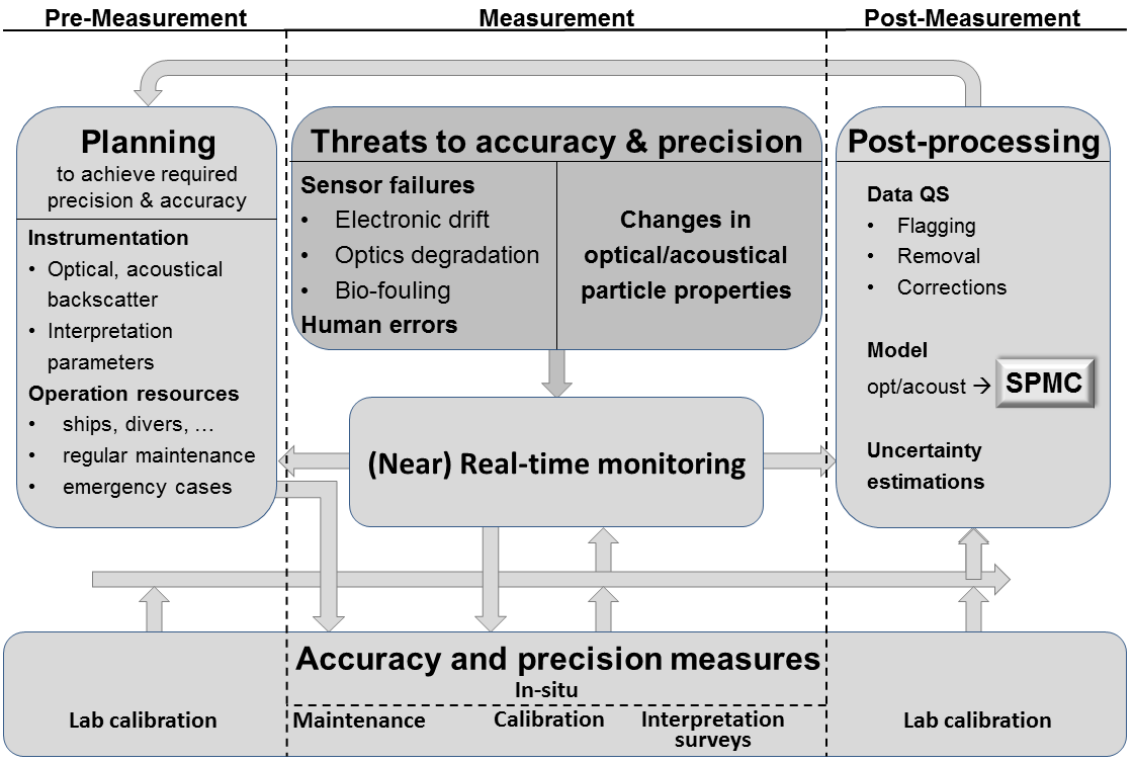

Fig. 1. Workflow of activities and tasks to be performed in long-term SPMC measurements. The arrows indicate the flow of information between the tasks and activities over the measurement phases. The measurement phases are plotted in serial order, but may overlap in the course of long-term installations.

A tri-modal flocculation model coupled with TELEMAC for suspended cohesive sediments in the Belgian coastal zone

Xiaoteng Shen[1,*], Erik Toorman[1] and Michael Fettweis[2]

[1] Hydraulics Laboratory, Department of Civil Engineering
KU Leuven, Kasteelpark Arenberg 40, B-3001 Leuven, Belgium
E-mail: xiaoteng.shen@kuleuven.be

[2] Operational Directorate Natural Environment, Royal Belgian Institute of Natural Sciences
Gulledelle 100, B-1200 Brussels, Belgium

Introduction

Estuarine and coastal regions are often characterized by a high variability of suspended sediment concentrations (SSC). The Belgian coastal zone is one of those areas where dredging works are conducted to maintain harbours and navigation channels (Fettweis et al., 2016). To investigate the SSC dynamics it is essential to understand the flocculation processes of estuarine mud, since it alters the sediment settling flux by aggregating individual clay particles into larger flocs. Previous curve fitting analysis of measured floc size distributions (FSDs) in the Belgium coastal zones showed that the multimodal FSDs can be decomposed into four log-normal FSDs to identify groups of primary particles, microflocs, macroflocs, and megaflocs, respectively (Lee et al., 2012). A two-class population balance model (PBM2C) was firstly developed using size-fixed class 1 particles (primary particles + microflocs) and size-varying class 2 particles (macroflocs + megaflocs) to describe the aggregation and breakage process of cohesive sediments. This simple model was validated by settling column test (Lee et al., 2011) and some field data collected in Zeebrugge (Lee et al., 2014), and later was coupled in the open source TELEMAC system and validated by using the same data set (Ernst, 2016). However, this two class assumption may be oversimplified as it does not address the large megaflocs that form after the peak of algae bloom periods. Moreover, the maximum errors for estimating the settling flux may largely decrease by tracking three size classes instead of two (Lee et al., 2012). For these reasons, a three-class population balance model (PBM3C) was developed in this study, also coupled with the open source TELEMAC modelling suite for the hydrodynamic and turbulence sections, to simulate the characteristic sizes of three size classes, i.e., microflocs (including primary particles), macroflocs, and megaflocs, respectively. A more recent data set from the WZBuoy in the Belgian coastal zone is used to validate the newly developed PBM3C. The objective of this study is to develop the PBM3C and implement it in TELEMAC to mimic flocculation processes of cohesive sediments, especially to reasonably address the population of megaflocs that previous PBM2C simply ignored.

Numerical modelling

Hydrodynamic model

The general open source software TELEMAC developed by the LNHE (Laboratoire National d'Hydraulique et Environnement) of EDF (Electricité De France) is used to solve the Navier-Stokes equations for variable water depth and velocity components, and to solve the tracer transport equation for various active and passive tracers. The transport of tracers is of major importance in the implementation of a flocculation model in TELEMAC3D.

Flocculation model

The PBM3C is developed to describe the flocculation processes, as an improvement of the previous PBM2C. As shown in Fig. 1, a system of equations are set up to track (1) the number of microflocs, macroflocs and megaflocs per unit volume, with symbol N_P, N_{F1}, and N_{F2}, respectively, (2) the total number of microflocs in all macroflocs (but not in megaflocs) per unit volume N_{T1}, and (3) the total number of microflocs in all megaflocs (but not in macroflocs) per unit volume N_{T2}. Take a one-dimensional vertical case as an example, the governing equation can be written as:

$$\frac{\partial N_i}{\partial t} + (w - \omega_{s,i})\frac{\partial N_i}{\partial z} = \frac{\partial}{\partial z}\left(\nu_t \frac{\partial N_i}{\partial z}\right) + (A_i + B_i) \qquad i = P, F1, F2, T1, T2 \qquad (1)$$

where N_i is number concentration (in unit of m^{-3}), w is the vertical velocity of fluid, ω_s is the settling velocity, and ν_t is the eddy viscosity. A_i & B_i are source and sink terms, which include (1) the aggregation of two microflocs, or two macroflocs, or two megaflocs, (2) the aggregation of a microfloc and a macrofloc, or a microfloc and a megafloc, or a macrofloc and a megafloc, and (3) the breakage of a macrofloc, or a megafloc. The average number of microflocs in one macrofloc per unit volume is $N_{C1} = N_{T1} / N_{F1}$, and the average number of microflocs in one megafloc per unit volume is $N_{C2} = N_{T2} / N_{F2}$. Thus, the sizes of macroflocs and megaflocs can be determined as $D_{Fi} =$

$D_p.N_{Ci}^{1/nf}$ (i = 1, 2), where D_P, D_{F1}, and D_{F2} are the characteristic sizes of microflocs, macroflocs, and megaflocs, respectively, and nf is the fractal dimension. The five parameters, i.e., N_P, N_{F1}, N_{F2}, N_{T1}, and N_{T2}, are defined as tracers in TELEMAC as long as flocculation is toggled on (e.g., a predefined logical variable PBM3C is set to true). This PBM3C flocculation model can be included in the TELEMAC software with appropriate modification of the subroutines VITCHU, WCHIND, CLSEDI, SOULSBYFLOC3D, FONVAS, etc. in TELEMAC.

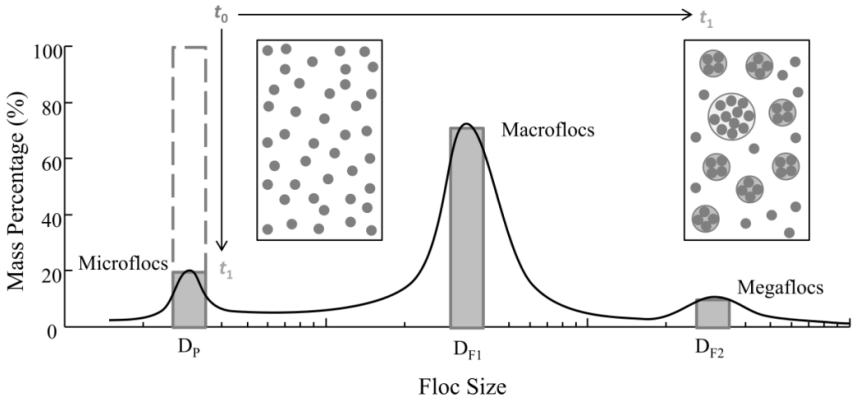

Fig. 1. Conceptual diagram for three-class population balance model (PBM3C).

Field measurements

The station WZBuoy is located about 2km outside the entrance of Zeebrugge harbour which is situated in the coastal turbidity maximum area along the southern North Sea near the Belgian coast (Fettweis et al., 2016). Although measurements were conducted with tripods for several years, only the data for several selected tidal cycles around Julian Day 322 in the year 2013 were used to validate the model. Velocity profiles and water surface elevation were recorded by an upward looking ADCP (Acoustic Doppler Current Profiler) which was mounted together with the tripod. The time series of FSDs were collected by the LISST (Laser In-Situ Scattering and Transmissometry), and temperature, salinity, and SSCs were measured or derived from the ADCP backscatter strength. Time series of water depth and the average temperature and salinity are treated as inputs to drive the model, while the velocity profiles, SSC profiles, and FSDs are used to validate the model outputs.

Results and conclusions

The PBM3C enabled TELEMAC software is validated by the flow, sediment and floc size distribution data from the WZBuoy station in the Belgian coastal zone within an intra-tidal time scale. More complicated processes such as the effect of biofilms and interaction with microplastic particles will be included in this system in a later stage.

Acknowledgements

This research was funded by the BelSPO (Belgian Science Policy Office) in the framework of the BRAIN-be (Belgian Research Action through Interdisciplinary Networks) INDI67 project, and by the JPI Oceans (Joint Programming Initiative Healthy and Productive Seas and Oceans) in the framework of the WEATHER-MIC (Microplastic Weathering) project.

References

Fettweis M., Baeye M., Cardoso C., Dujardin A., Lauwaert B., Van den Eynde D., Van Hoestenberghe T., Vanlede J., Van Poucke L., Velez C., Martens C. (2016) The impact of disposal of fine-grained sediments from maintenance dredging works on SPM concentration and fluid mud in and outside the harbor of Zeebrugge. Ocean Dynamics, 66: 1497-1516.

Lee B.J., Toorman E., Molz F.J., Wang J. (2011) A two-class population balance equation yielding bimodal flocculation of marine or estuarine sediments. Water Research, 45: 2131-2145.

Lee B.J., Fettweis M., Toorman E., Molz F.J. (2012) Multimodality of a particle size distribution of cohesive suspended particulate matters in a coastal zone. Journal of Geophysical Research, 117:C03014.

Lee B.J., Toorman E., Fettweis M. (2014) Multimodal particle size distributions of fine-grained sediments: mathematical modelling and field investigation. Ocean Dynamics, 64: 429-441.

Ernst S. (2016). Implementation of a flocculation model in TELEMAC-3D. MSc thesis, Dept. of Civil Engineering, KU Leuven. xvi+151p.

Mud dynamics in the harbor of Zeebrugge

Joris Vanlede[1,2], Arvid Dujardin[3,1] and Michael Fettweis[4]

[1] Department of Mobility and Public Works, Flanders Hydraulics Research, Berchemlei 115, B-2140 Antwerp, Belgium
E-mail: joris.vanlede@mow.vlaanderen.be

[2] Faculty of Civil Engineering and Geosciences, Delft University of Technology, Delft, The Netherlands

[3] Antea Group, Buchtenstraat 9, B-9051 Gent, Belgium

[4] Royal Belgian Institute of Natural Sciences, Operational Directorate Natural Environment, Gulledelle 100, B-1200 Brussels, Belgium

Abstract
One year of SPM concentration (SPMC) and Velocity data are analyzed to gain insight in the mud dynamics in the harbor of Zeebrugge. Seasonal dynamics are inferred from satellite images, depth soundings and SPMC data.

Study Site
The harbor of Zeebrugge is situated in the coastal turbidity maximum area along the Belgian coast (southern North Sea). About 5,3 million tons (dry matter) of mainly fine-grained sediments is dredged annually in the port (15.000 TDS/day). The fluid mud inside the port has a mean layer thickness of up to 3m in front of the entrance of the Albert 2 dock (see Figure 4).

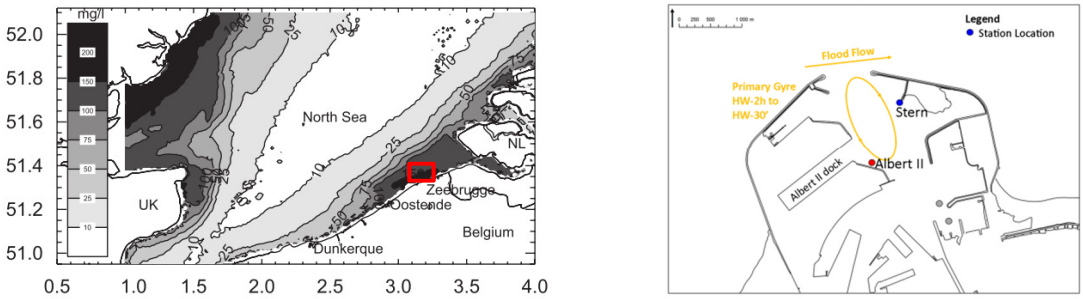

Figure 1 - Depth averaged SPM in Southern North Sea (left, Fettweis, 2007) and harbor of Zeebrugge (right)

Measurements at fixed locations inside the harbor
SPM concentration and current velocity were measured at four locations inside the harbor (see Figure 1) at two depths in the water column. Each measuring point was equipped with a point velocimeter (Aquadopp), an OBS3+ and a CT-probe (Valeport 620). The data were collected every 10 minutes for a measurement campaign lasting 400 days (March 2013 to April 2014).
The time series of SPM concentration are split-up into individual tidal cycles, and grouped according to neap, average and spring tide conditions in an ensemble analysis to study tidal dynamics.

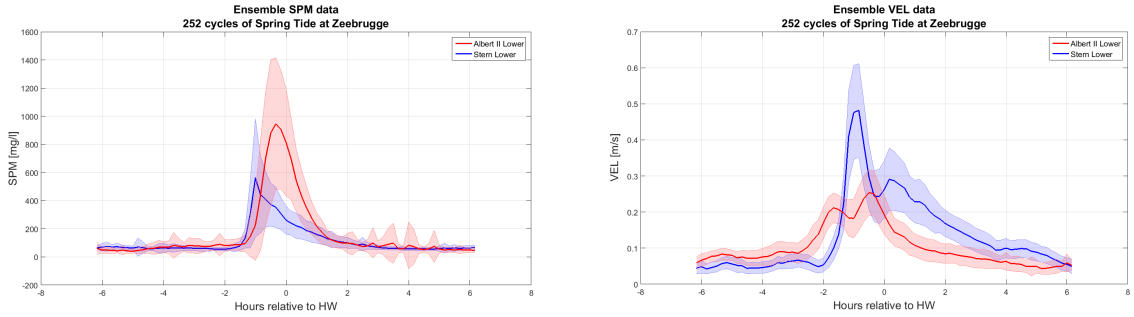

Figure 2 - Ensemble analysis of SPMC (left) and velocity data (right) for the lower set of sensors at locations Stern (in blue) and Albert II (in red) during spring tide conditions

Natural Evolution of the Top of the Mud Layer

The top of the mud layer is measured by the 210 kHz echo sounder reflector. A simple volume balance is set up to decompose the measured depth change Δh^m in the effect of dredging Δh^d and the natural evolution Δh^n.

$$\Delta h^m = \Delta h^n + \Delta h^d$$

$$\Delta h^d = -\frac{m^d(\rho_g - \rho_w)}{A\,\rho_g(\rho_b - \rho_w)}$$

The natural evolution Δh^n of the top of the mud layer corresponds to the cumulative effect of resuspension and consolidation (negative sign) and deposition (positive sign) and is calculated from daily depth soundings in Albert II dock (Figure 3).

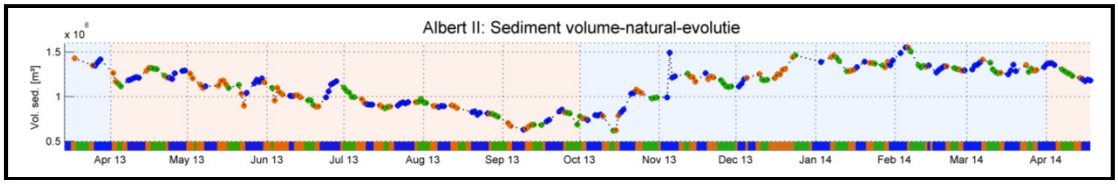

Figure 3 - Natural evolution of the mud volume in Albert II-dock during summer (red background) and winter (green background). Colored dots and (baseline) show tidal conditions: neap tide (green), average tide (orange) and spring tide (blue).

Results and Discussion

Intra-tidal variation

Both SPMC and velocity peaks at location Albert II are 50 minutes delayed to location Stern (Figure 2). The peak concentration at Albert II is higher than at Stern, even though the velocity is lower. This is explained by sediment being advected in the harbor and transported in a primary gyre, and settling out between locations Stern and Albert II. This is consistent with the analysis of Vanlede et al. (2014), who showed that horizontal transport is the most important component of the gross sediment exchange at the harbor mouth of Zeebrugge, and that most horizontal sediment exchange happens from 2h before high water to high water.

Spring-neap variation

Sediment import into the harbor during spring tide is 3 (2 to 4) times higher than during neap tide. This is consistent with the spring-neap variation of SPMC observed at a nearby station in the North Sea and with the spring-neap variation of peak SPMC observed inside the harbor.

Seasonal Variation

The mud volume in the Albert II dock is largest in winter, and reaches a minimum at the beginning of autumn (Figure 3). Density profiles also show that the sediment layers are less consolidated in winter than in summer. Figure 4 shows a striking seasonal pattern in the shape of the mud layer in the Albert II dock. Where the top of the mud layer is flat in winter, it shows a height difference of 1m (max. slope 1/400) in summer. The seasonal variations are believed to be linked to seasonal variations in the floc properties of the SPM (Fettweis & Baeye, 2015) that might influence consolidation and strength properties of the bed.

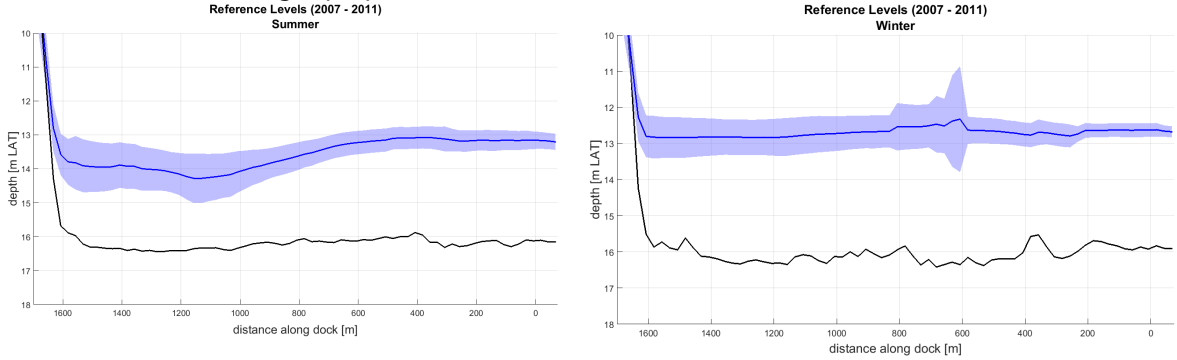

Figure 4 - Seasonal variation of levels in Albert II dock. 210 kHz level (and 1σ) in blue for summer (left) and winter (right). 33 kHz in black.

References

Fettweis, M., Baeye, M., 2015. Seasonal variation in concentration, size and settling velocity of muddy marine flocs in the benthic boundary layer. *J. Geophys. Res.* 120, 5648–5667. doi: 10.1002/2014JC010644

Vanlede, J., & Dujardin, A. (2014). A geometric method to study water and sediment exchange in tidal harbors. Ocean Dynamics, (11), 1631–1641. doi:10.1007/s10236-014-0767-9

APPENDIX 2

Chen P, Yu JCS, Fettweis M. 2018. Modelling storm-influenced SPM flocculation using a tide–wave-combined biomineral model. *Water Environment Research,* doi:10.2175/WERD1600107

Modeling Storm-Influenced Suspended Particulate Matter Flocculation Using a Tide-Wave-Combined Biomineral Model

Peihung Chen[1], Jason C. S. Yu[1*], Michael Fettweis[2]

ABSTRACT: Flocculation of suspended particulate matter (SPM) in marine and estuarine environments is a complex process that is influenced by physical, biological, and chemical mechanisms. The flocculation model of Maggi (2009) was adapted to simulate flocculation under various weather conditions and during different seasons. The adaptation incorporated the effect of tide-wave-combined turbulence on floc dynamics. The model was validated using in situ measurements of floc size and SPM concentration from the southern North Sea during both calm and storm conditions. The results show that tide-wave-combined turbulence needs to be incorporated when simulating flocculation in a tide-wave-dominated environment. The observed seasonal variations in floc size (Fettweis et al., 2014) were reproduced using varying values for various floc strengths in different seasons. The results revealed that the biological effect on floc strength, which enhances aggregation, is stronger during summer, indicating that floc strength in the model should be varied seasonally. *Water Environ. Res.*, 90 (2017).

KEYWORDS: suspended particulate matter, biomineral flocculation, tide-wave-induced velocity, floc strength, particle size distribution.

doi:10.2175/WERD1600107

Introduction

Suspended particulate matter (SPM) is a mixture of organic and inorganic particles that has specific physicochemical properties (Berlamont et al., 1993; Maggi, 2009). The SPM, which consists of inorganic and organic particles, interacts with the surrounding environment through physical, biological, and chemical mechanisms (flocculation) (Manning et al., 2006). In marine and estuarine environments, flocculation influences sediment transport and may influence coastal eutrophication, algae blooms, fate of pollutants, ephemeral sealing of the sea floor by fluffy layers, benthic and pelagic ecosystems, and siltation of navigation channels and harbors (Kirby, 2011; Lancelot et al., 1987; Lee and Wiberg, 2002). Flocculation occurs in turbulent flow fields and is caused by factors such as tides and combines aggregation, where the suspended particles form larger sized clusters or flocs, and breakage, where the larger flocs are broken into smaller particles. The conceptual relationship between floc diameter, SPM concentration and shear stress proposed by Dyer (1989) indicates that turbulent flow enhances particle aggregation and increases the size and settling velocity of the flocs. Suspended particulate matter (SPM) dynamics are further influenced by waves, particularly during storms (Mehta and Maa, 1985). In nearshore areas, waves may induce high turbulent shear, which potentially enhance floc fragmentation or breakup. Additionally, wave induced erosion may lead to the resuspension of coarser-grained sediment particles with unimodal particle size distributions (PSDs) (Li and Mehta, 2000; van Kessel and Kranenburg, 1998), or to the formation of high concentrated mud suspensions (HCMSs), or mixed suspensions that combine coarser grains and flocs that usually have a multimodal PSD (Baeye et al., 2011; Fettweis et al., 2010). The effects of wave-driven resuspensions and floc breakup may thus yield complex floc dynamics.

Several flocculation models have been developed to simulate flocculation behavior in marine and estuarine environments; they can be categorized into four types: (1) concentration dependent empirical-equation based models (van Leussen, 1994), (2) models applying a single characteristic diameter as a time-dependent variable (Maggi, 2009; Winterwerp, 1998, 2002), (3) distribution based models that consider the average floc size of a continuous floc size distribution function (Maerz and Wirtz, 2009), and (4) size-class based models which assume that floc

[1] National Sun Yat-Sen University, Department of Marine Environment and Engineering, Lien-Hai Road 70, 80424 Kaohsiung, Taiwan; e-mail: jasonyu@mail.nsysu.edu.tw

[2] Royal Belgian Institute of Natural Science, Operational Directorate Natural Environment, Gulledelle 100, 1200 Brussels, Belgium

[*] National Sun Yat-Sen University, Department of Marine Environment and Engineering, Lien-Hai Road 70, 80424 Kaohsiung, Taiwan; e-mail: jasonyu@mail.nsysu.edu.tw

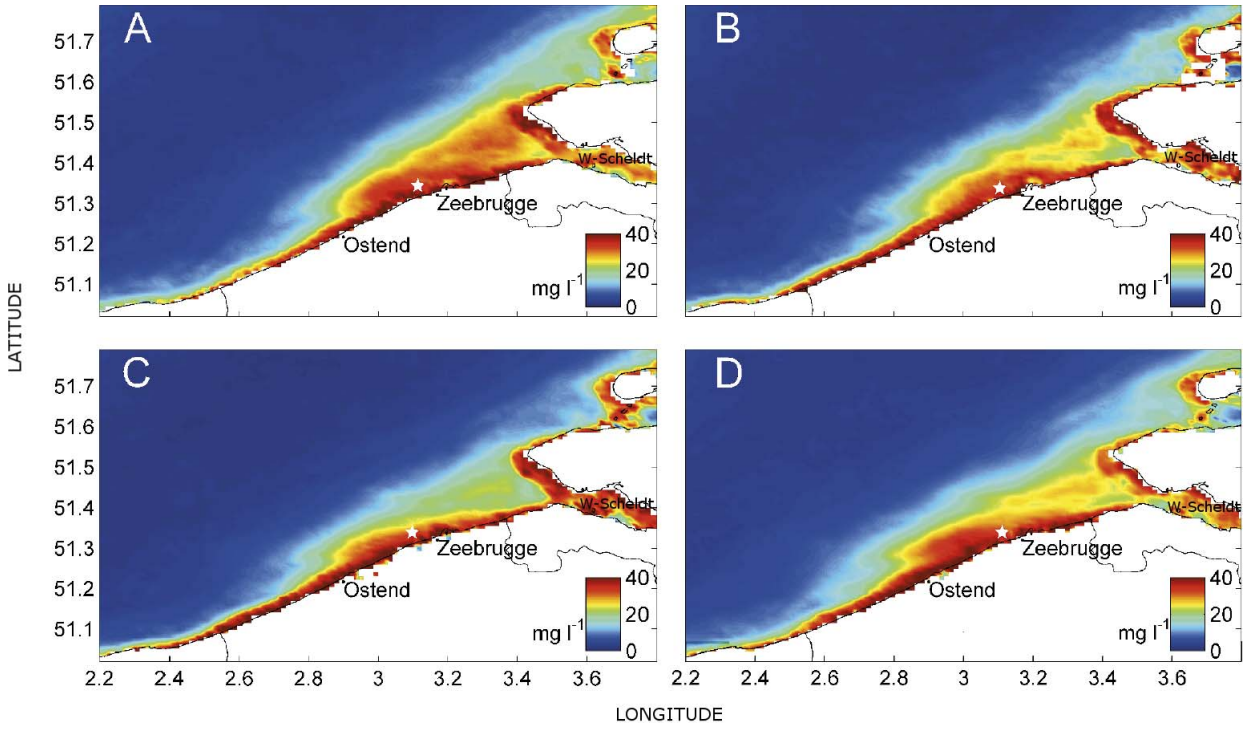

Figure 1—Mean surface SPM concentration (mg/L) in the southern North Sea, obtained from moderate resolution imaging spectroradiometer images (2002–2009) for different wind directions: (a) southwest winds; (b) northeast winds; (c) northwest winds; and (d) southeast winds (adapted from Baeye et al., 2011). The star indicates the in situ measuring station Blankenberge.

distributions are composed of discrete size classes (Lee et al., 2011; Verney et al., 2010). Most of these models focus on tide induced dynamics (e.g., Lee et al., 2011; Maerz and Wirtz, 2009; Maggi, 2009; Verney et al., 2010; Winterwerp, 2002), however, waves can also critically influence cohesive sediment transport on continental shelves (Green et al., 1995; Traykovski et al., 2007). Wright et al. (2006) included both tidal and wave velocity in their model to represent the effects of tide and wave supported sediment flows on shelf deposition and morphology in wave dominated environments. Such transport is a primary cause of across-shelf transport and emplacement of flood deposits on muddy shelves.

The present study focuses on the southern North Sea, which is characterized by high turbid nearshore areas and intense seasonal algal blooms (Fettweis et al., 2014). Suspended particulate matter (SPM) dynamics in this area are controlled by tidal forces on calm days and by a combination of tides and waves during storms (Howarth et al., 1993). Additionally, human activities supply excess nutrients to coastal zones, resulting in intense algal blooms, especially during spring and early summer (Borges and Gypens, 2010), making the area a relevant site to investigate links between biomass, SPM concentration, and tide-wave effects. Algae release abundant sticky, gel-like organic colloids (e.g., extracellular polymeric substances (EPS) and transparent extracellular particles (TEP)) that enhance the binding strength of floc aggregations (Alldredge et al., 1993; Fettweis et al., 2014). Maggi (2009) proposed a biomineral flocculation model and validated it by using field data to study the floc behaviors in this area. However, the data were collected during calm days, and the model only considered tide-driven floc processes.

The present study investigates wave-influenced SPM flocculation in the highly productive southern North Sea during the storm season. The model (Maggi, 2009), which represents a single characteristic particle considering the biological effect on floc dynamics, was adapted to incorporate the combined effects of tides and waves. Suspended particulate matter, (SPM) particle size (D50), measured in situ in the southern North Sea (Fettweis et al., 2012; Lee et al., 2012) was used to validate the model simulations. The simulation considered both tide and tide-wave-combined forcings and the biological effects on floc strength and flocculation.

Methodology

Field Measurements. *Study Area.* The measurement station Blankenberge (BLA, Figure 1) is situated approximately 5 km southwest of the port of Zeebrugge, Belgium. It is positioned in a turbidity maximum zone, where the water depth varies between 6 and 10 m, and the maximum tidal current can increase to more than 1 m/s (Lee et al., 2012). Zeebrugge has a semidiurnal tidal regime and a mean tidal range of 4.3 and 2.8 m during spring and neap tides, respectively. The winds predom-

Allen Press, Inc. ■ 30 November 2017 ■ 11:16 am ■ Customer MS#WER-D-16-00107
//titan/production/w/waer/live_jobs/waer-90/waer-90-03/waer-90-03-07/layouts/waer-90-03-07.3d

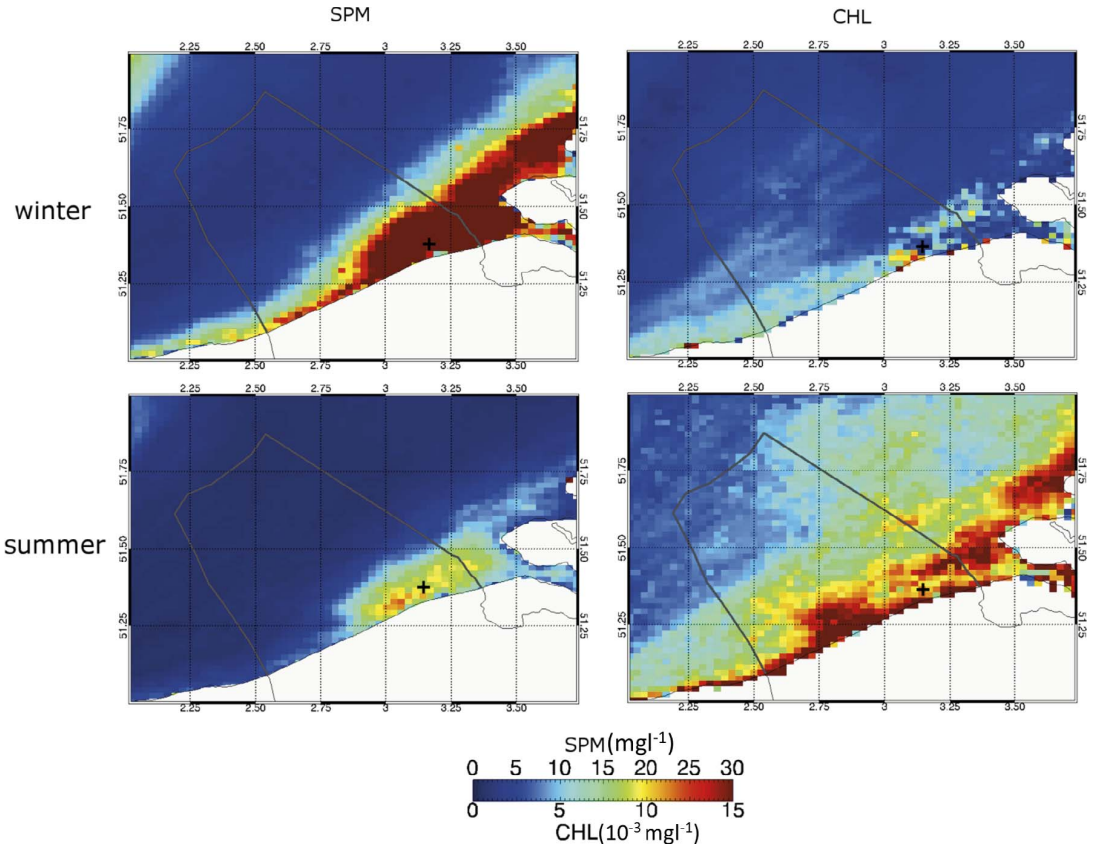

Figure 2—Mean surface SPM (mg/L, left) and chlorophyll (CHL, 10^{-3} mg/L, right) concentrations in the southern North Sea during winter (October–March, top) and summer season (April–September, bottom). Data were obtained from a MERIS satellite (adapted from Fettweis et al., 2014). The cross indicates the in situ measuring station Blankenberge.

inantly blow in from the southwest for 33% of the year; northeast winds are the second most predominant. The maximum wind speed coincides with the southwest winds, however, the highest waves occur during northwest winds (Fettweis et al., 2010). Suspended particulate matter (SPM) concentration ranges between 20 and 100 mg l^{-1} at the surface and between 100 and more than 3000 mg l^{-1} near the bed; lower values (<100 mg l^{-1}) occur offshore (Baeye et al., 2011; Fettweis et al., 2010). Suspended particulate matter (SPM) concentrations decrease during southwest winds but increase during northeast winds because the outflow from the Westerschelde estuary is more turbid than that from the English Channel (Baeye et al., 2011) (Figure 1). The SPM concentration in the high turbidity zones of the southern North Sea are inversely correlated with chlorophyll concentration (Fettweis et al., 2014). During the winter season (October–March) SPM concentration is high and chlorophyll concentration is low; these conditions are reversed during the summer season (April–September) (Figure 2). Fettweis et al. (2014) noted that the strength of floc aggregations is controlled by the sticky organic substances associated with enhanced primary production (high chlorophyll concentration) during the summer season.

Instruments. Data were collected using a multisensory benthic lander (tripod) to measure floc size, SPM concentration, and tidal currents. The tripod measuring system included a Sequoia Scientific laser in situ scattering and transmissometer 100C (LISST-100C), 3-MHz SonTek Acoustic Doppler Profiler (ADP), and two D&A optical backscatter point sensors (OBSs) (Fettweis et al., 2012; Lee et al., 2012). The LISST was mounted 2 m above the bed (mab), which was subsequently analyzed for particle size information (e.g., D50 and PSDs). The OBSs were installed at 0.2 and 2 mab, and their voltage was converted into SPM concentration by calibration against filtered water samples during several field campaigns (Fettweis et al., 2006). A linear regression between all OBS signals and SPM concentrations from filtration was assumed (factor = 1.78). The ADP profiler was attached at 2.3 mab to measure tidal current in the lowest 2 m of the water column.

Experimental Data. Measurements were taken in early 2008; the weather was stormy from February to March and calm throughout April. The environmental characteristics of storm and calm events used for the periods that have been modeled are listed in Table 1 (Fettweis et al., 2012; Lee et al., 2012). The first storm (February 1 and 2) occurred during a neap tide and caused

Allen Press, Inc. ■ 30 November 2017 ■ 11:16 am ■ Customer MS#WER-D-16-00107
//titan/production/w/waer/live_jobs/waer-90/waer-90-03/waer-90-03-07/layouts/waer-90-03-07.3d

Table 1—Environmental characteristics of storm events for model simulation.

Month	February		March		April	
Date	1–2	5–7	10–13	16–19	21–25	26–30
Storm	SW	SW	SW	NE	NE	***
Wind Speed (m/s)	9.2	7.4	10.8	6.1	6.9	4.2
Wind direction	northeast	northeast	northeast	southwest	southwest	southwest
Tidal type	neap	spring	spring	neap-spring	spring	spring-neap
Max. H_s (m)	2.8	1.5	2.5	2.0	3.0	0.42
D50 (μm)	45.55	67.37	56.21	47.97	26.44	98.33
PSD	Unimodal	Unimodal	Unimodal	Multimodal	Multimodal	Multimodal

Note: *** indicates calm weather; PSD = particle size distribution; SW = southwest; NE = northeast; Hs = significant wave height.

significant wave heights of up to 2.8 m. By contrast, the significant wave height during the second storm (February 5–7) reached 1.5 m (Figure 3a). The winds blowing from the west-southwest during both of these storms produced a positive (northward) subtidal alongshore flow; all storms with these characteristics were named southwestward storms (southwest storms) in this study.

In March, three storm events occurred (Figure 3b). The first event was took place between March 10 and 13, producing a significant wave height of 2.5 m, and was also classified as a southwest storm. The storm events of March 16 to 19 and March 21 to 25 were mainly generated by northerly winds resulting in negative (southward) subtidal alongshore flows directed toward the southwest; all storms with these characteristics were named northeastward storms (northeast storms) in this study. The maximum significant wave height of the two northeast storms reached 2.0 and 3.0 m, respectively.

Overall, the measurements indicated that a unimodal PSD of granular particles (mean value of approximately 50 μm) occurred during the southwest storms (Figures 4a–c and Table 1), and that a multimodal PSD of mixed sediments (mean value ≤ 50 μm) occurred during the northeast storms (Figure 4d,e and Table 1) (Baeye et al., 2011). For comparison, field data for a calm event, during blooms from April 26 to 30, were subsequently collected, where the significant wave height was less than 0.5 m (Figure 3c).

Model Setup and Parameterization. To investigate storm-influenced flocculation in the highly productive southern North Sea, the biomineral flocculation model of Maggi (2009) was further complemented to include both tide- and wave-induced forcing. Finally, a model parameterization procedure was applied to ensure that the simulation results aligned with the measured data.

Flocculation Model. The flocculation model (Maggi, 2009) includes mineral and biomass fractions. In particular, the biomass fraction considers the microorganism effects (e.g., EPS, TEP, organic residues, and excreta) on floc-binding strength (Kiorboe et al., 1990). The floc solid volume V is the sum of mineral volume (V_M) and biomass volume (V_B); the time derivative of floc volume is expressed as follows (see Table 2 for the description of the variables):

$$dV/dt = dV_M/dt + dV_B/dt \tag{1}$$

$$\frac{dV_M}{dt} = (1-\alpha)nf\frac{D^{nf-1}}{D_p^{nf-3}}\frac{k_a C_M G}{D^{nf-4}} - (1-\alpha)nf\frac{D^{nf-1}}{D_p^{nf-3}}\frac{k_b(1-\alpha)G^{3/2}}{(D-D_p)^{nf-3}}D^2 \tag{2}$$

$$\frac{dV_B}{dt} = \alpha nf\frac{D^{nf-1}}{D_p^{nf-3}}\frac{k_a C_B G}{D^{nf-4}} - \alpha nf\frac{D^{nf-1}}{D_p^{nf-3}}\frac{k_b \alpha G^{3/2}}{(D-D_p)^{nf-3}}D^2 + \eta V_B\left(1-\frac{V_B}{K}\right) \tag{3}$$

Variations in both mineral volume (dV_M/dt) and biomass volume (dV_B/dt) depend on floc aggregation and breakage of floc particles (eqs 2 and 3). The change in aggregation volume ($dV_{aggregation}$) and breakage volume ($dV_{breakage}$) in the whole floc volume is controlled by the turbulence shear rate (G) and can be written as:

$$dV_{aggregation} = dt\left[(1-\alpha)nf\frac{D^{nf-1}}{D_p^{nf-3}}\frac{k_a C_M G}{D^{nf-4}} + \alpha nf\frac{D^{nf-1}}{D_p^{nf-3}}\frac{k_a C_B G}{D^{nf-4}}\right] \tag{4}$$

$$dV_{breakage} = dt\left[(1-\alpha)nf\frac{D^{nf-1}}{D_p^{nf-3}}\frac{k_b(1-\alpha)G^{3/2}}{(D-D_p)^{nf-3}}D^2 + \alpha nf\frac{D^{nf-1}}{D_p^{nf-3}}\frac{k_b \alpha G^{3/2}}{(D-D_p)^{nf-3}}D^2\right] \tag{5}$$

Moreover, $C_M = (1-\delta)C$ is the concentration of the SPM mineral fraction (δ = biomass fraction) and $\alpha = V_B/V$ is the floc biomass volume fraction. The aggregation rate (k_a) and breakup rate (k_b) functions are expressed as follows:

$$k_a = (1+\alpha)k_a'\frac{1}{\rho\, D_p^{3-nf}nf} \tag{6}$$

$$k_b = (1+\alpha)k_b'\frac{1}{D_p^{3-nf}nf}\left(\frac{\mu}{F_y}\right)^{1/2} \tag{7}$$

where k'_a and k'_b are dimensionless aggregations and breakup calibration parameters, μ is the dynamic viscosity of water, and F_y is the floc strength. Additionally, ρ is the average density of

Allen Press, Inc. ■ 30 November 2017 ■ 11:16 am ■ Customer MS#WER-D-16-00107
//titan/production/w/waer/live_jobs/waer-90/waer-90-03/waer-90-03-07/layouts/waer-90-03-07.3d

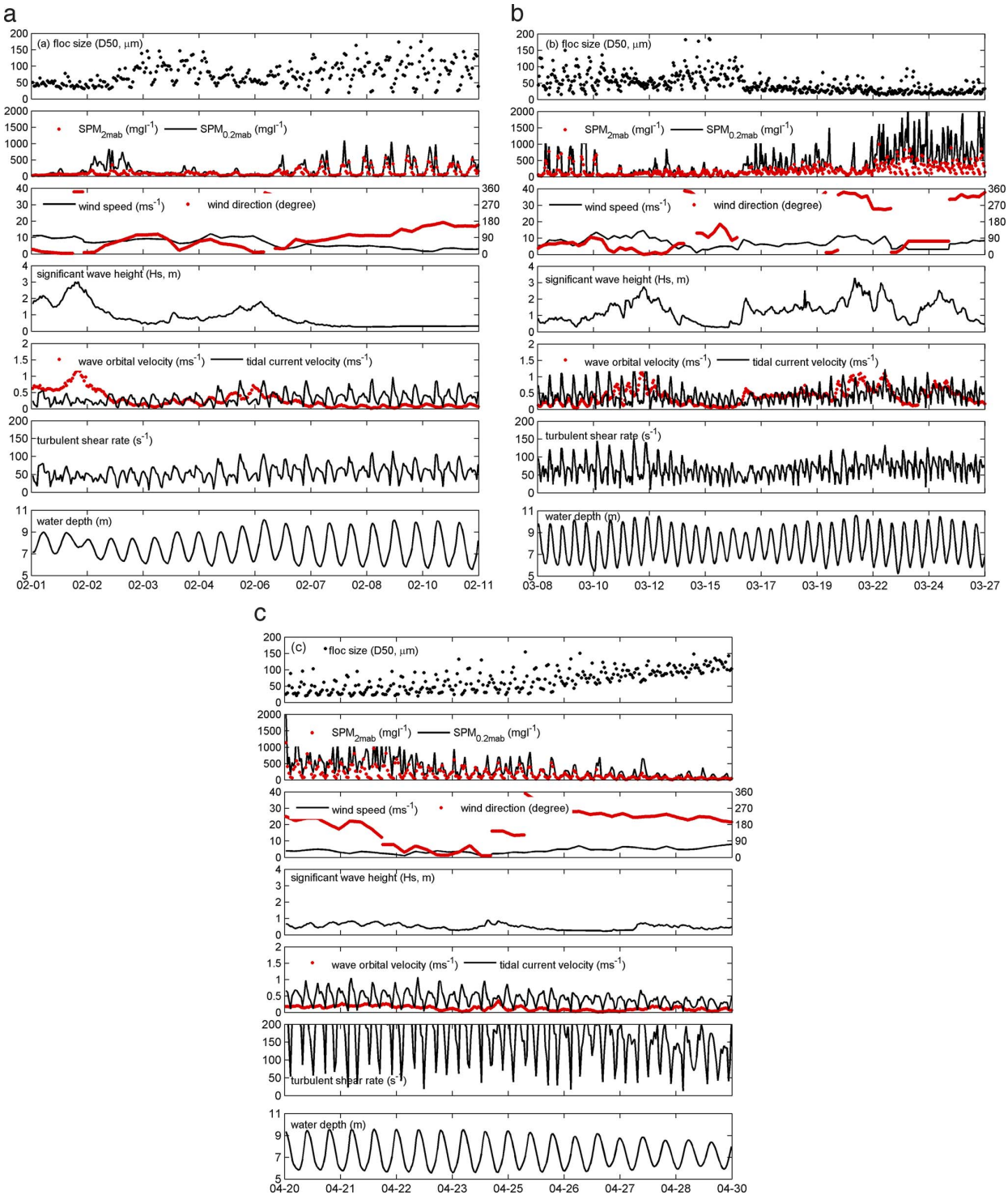

Figure 3—Time series of field data at the Blankenberge station for the period (a) February 2 to 11, (b) March 8 to 27, and (c) April 20 to 30. The figure shows (from top to bottom) floc size (D50, m), SPM concentration at 0.2 and 2 mab (mg/L), wind speed (m/s) and direction (degree), significant wave height (m), tidal and wave orbital velocities (m/s), turbulent shear rate (1/s), and water depth (m).

Allen Press, Inc. ■ 30 November 2017 ■ 11:16 am ■ Customer MS#WER-D-16-00107
//titan/production/w/waer/live_jobs/waer-90/waer-90-03/waer-90-03-07/layouts/waer-90-03-07.3d

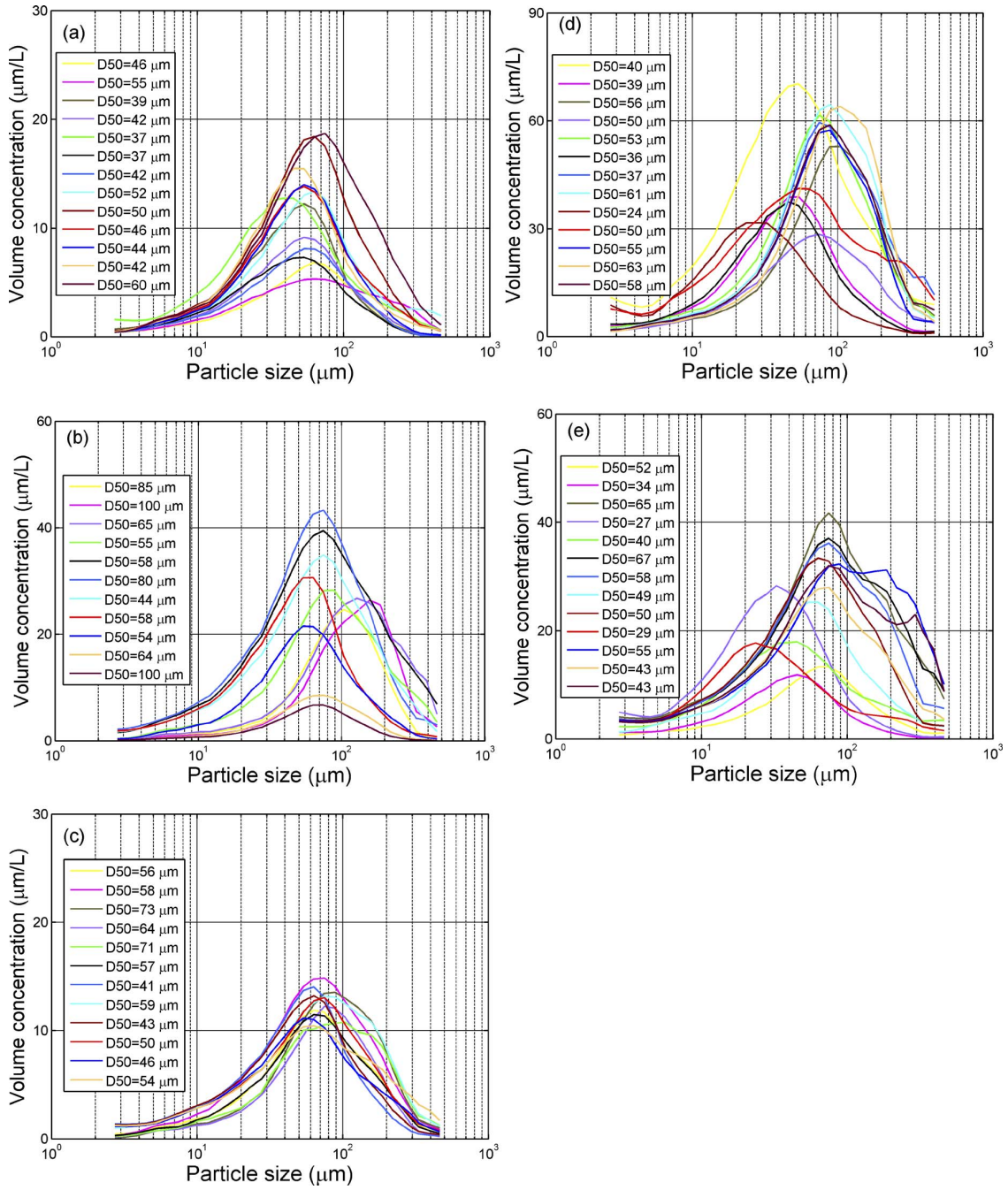

Figure 4—Hourly particle size distribution (PSD) during a tidal cycle and during different storm events: (a) February 1 to 2 (southwest storm), (b) February 5 to 7 (southwest storm), (c) March 10 to 13 (southwest storm), (d) March 16 to 19 (northeast storm), and (e) March 21 to 25 (northeast storm).

the floc solid volume, which is computed as:

$$\rho = (1-\alpha)\rho_{\mathrm{M}} + \alpha\rho_{\mathrm{B}} \tag{8}$$

where ρ_M and ρ_B are mineral and biomass densities, respectively.

Microorganism growth affected the floc volume growth; the $\eta V_B\left(1-\frac{V_B}{K}\right)$ introduced in eq 3 represents the microbial effects, where the specific growth rate $\langle\eta\rangle$ is expressed as follows:

$$\eta = \eta_{\max}\frac{\mathrm{N}}{\mathrm{N}+\mathrm{k_m}} \tag{9}$$

where η_{max} is the maximum specific growth rate, N is the nutrient concentration, and k_m is the half-saturation

Allen Press, Inc. ■ 30 November 2017 ■ 11:18 am ■ Customer MS#WER-D-16-00107
//titan/production/w/waer/live_jobs/waer-90/waer-90-03/waer-90-03-07/layouts/waer-90-03-07.3d

Table 2—Definitions of the model parameters.

Symbol	Unit	Definition	Symbol	Unit	Definition
D	[μm]	Floc size	t	[h]	Time
D_p	[μm]	Primary floc size	k'_a	[—]	Aggregation calibration parameter
nf	[—]	Fractal dimension	k'_b	[—]	Breakup calibration parameter
V	[mm^3]	Floc volume	F_y	[N]	Floc strength
V_M	[mm^3]	Floc mineral volume	η	[1/s]	Specific growth rate
V_B	[mm^3]	Floc biomass volume	η_{max}	[1/s]	Maximum specific growth rate
α	[—]	Floc biomass volume fraction	N	[mol/L]	Nutrient concentration
C	[mg/L]	Suspended particle matter concentration	k_m	[mol/L]	Half-saturation concentration
C_M	[mg/L]	Suspended mineral particulate inorganic matter concentration (PIM)	K	[mm^3]	Floc carrying capacity
C_B	[mg/L]	Suspended particulate organic matter concentration (POM)	β	[—]	Factor
δ	[—]	Suspended matter biomass fraction	G	[1/s]	Turbulent shear rate
ρ	[kg/m^3]	Floc specific weight	μ	[kg/m•s]	Water dynamic viscosity
ρ_M	[kg/m^3]	Mineral specific weight	ν	[m^2/s]	Kinematic viscosity
ρ_B	[kg/m^3]	Biomass specific weight	λ	[μm]	Kolmogorov microscale

concentration. Additionally, the floc carrying capacity to express the maximum biomass volume in the aggregate microenvironment can be calculated as:

$$\mathrm{K} = \beta \mathrm{V_p} = \beta\left(\mathrm{D}^3 - \mathrm{V}\right) \tag{10}$$

where V_p is the floc pore volume and β is the dimensionless factor.

Thus, the single characteristic floc size (D) is obtained from the time-varying rate of the mineral and biomass volumes (dV_m/dt and dV_B/dt, respectively) in this model:

$$\mathrm{D} = \left(\mathrm{V}/\mathrm{D}_\mathrm{p}^{\mathrm{nf}-3}\right)^{1/\mathrm{nf}} \tag{11}$$

where D_p is the primary particle size and nf is the fractal dimension. All of the parameters used in the SPM flocculation model are defined in Table 2.

Combined Dynamic of Tides and Waves. The effect of waves on flocculation is critical in storm-dominated environments. Wright et al. (2006) proposed that tides, waves, and gravity currents cause sediment transportation in a shelf sea, which can be calculated using the following equation:

$$\mathrm{U} = \sqrt{\mathrm{U}_\mathrm{c}^2 + \mathrm{U}_\mathrm{w}^2 + \mathrm{U}_\mathrm{g}^2} \tag{12}$$

where U_c is the tidal current velocity, U_w is the wave orbital velocity, and U_g is the gravity current velocity. The latter can be disregarded for the flat-slope Belgian nearshore zone.

The tidal current velocity (U_c) was measured using an ADP. The wave orbital velocity (U_w) was calculated based on Soulsby (1997), who suggested that U_w can be characterized by its standard deviation (U_{rms}). This can be calculated from the wave height-period-velocity curve of the Joint North Sea Wave Project (JONSWAP) spectrum. The JONSWAP spectrum was established on the basis of wave measurements from the southern North Sea.

The turbulent shear rate (G) used in eqs 2 and 3 was obtained by calculating $G = \nu/\lambda^2$, where ν is the kinematic viscosity. Notably, the Kolmogorov microscale (λ) is highly correlated with the current velocity (U) (Winterwerp, 1998). The results of λ and U in the Belgian shelf sea obtained using the 3D-COHERENS model indicated that λ was inversely proportional to U and varied with the weather conditions (eqs 13 and 14). When only tide-driven forces are considered, the Kolmogorov microscale (λ) is expressed as follows:

$$\lambda = 374.71\mathrm{U}^{-0.43} \tag{13}$$

where $U = U_c$, and $\mathrm{R}^2 = 0.86$. However, when the combined velocity of tides and waves is considered, the Kolmogorov microscale (λ) is expressed as follows:

$$\lambda = 405.24\mathrm{U}^{-0.32} \tag{14}$$

where $U = \sqrt{U_c^2 + U_w^2}$, and $\mathrm{R}^2 = 0.90$.

Model Parameterization. To determine the appropriate values of the model parameters (Table 3) for specific sites, the Monte Carlo method was used to analyze the sensitivity of the model to parameter changes (the calibrated parameters are listed between brackets in Table 3). Standard deviation was calculated considering 20% of each parameter. The results revealed that the values of the model parameters for the present study site (BLA) were consistent with those measured in Zeebrugge, as reported by Maggi (2009). Additionally, the model was based on the concept of a single characteristic particle size to describe the floc geometric characteristics (i.e., primary particle size and fractal dimension) similar to Maggi (2009). Therefore, the parameters used by Maggi (2009) were evaluated. The model parameter values used in this study are listed in Table 3.

To test the model, each dataset simulation (Table 1) was calibrated on a set of full tidal cycle (13 hour) data and validated through other measurements. The time series of simulated floc particles during different weather conditions is depicted in Figure 5, where gray blocks represent the calibration periods and white blocks represent the validation periods. Finally, basic statistical analysis (the root mean square error, RMSE) was used to evaluate the simulation results.

Allen Press, Inc. ■ 30 November 2017 ■ 11:19 am ■ Customer MS#WER-D-16-00107
//titan/production/w/waer/live_jobs/waer-90/waer-90-03/waer-90-03-07/layouts/waer-90-03-07.3d

Table 3—Summary of the model parameters.

Parameter	Unit	Value	Parameter	Unit	Value
D_p	[μm]	2.0	(k'_a)	[—]	0.189
nf	[—]	2	(k'_b)	[—]×10^{-6}	11.41
δ	[—]	0.04	(k_m)	[mol/L]×10^{-6}	1.159
$V_M(0)$	[mm^3]×10^{-8}	2.0	(η_{max})	[1/s]×10^{-4}	6.586
$V_B(0)$	[mm^3]×10^{-8}	1.0	F_y	[N]×10^{-11}	3.0
ρ_M	[kg/m^3]	2650.0	N	[mol/L]×10^{-6}	20.0
ρ_B	[kg/m^3]	1025.0	(β)	[—]	0.226
μ	[kg/m•s]×10^{-3}	1.0	v	[m^2/s]×10^{-6}	1

Note 1: The parameters in brackets were obtained by calibration whereas all others were assigned according to Maggi (2009).
Note 2: V_M (0) and V_B (0) were initial values.

Results

Two dynamic conditions were simulated using the SPM flocculation model. Tidal velocity alone (eq 13) was considered in the first condition and included both wave and tidal velocities (eq 14) in the second condition to evaluate the effect of waves on storm-influenced flocculation. Suspended particulate matter (SPM) concentration at 2 mab and tidal current velocity were used as input data in modeling.

Calm-Day Simulation. On calm days, the tidal current was the dominant hydrodynamic force, as indicated in Figure 3c, and both wave height and orbital velocity were small. The results revealed that the simulation obtained by considering tidal dynamics alone, aligned with the measured data (Figure 5a). Specifically, a RMSE of 23 ± 2 μm was obtained through the tide-only dynamic condition, and a larger RMSE (30 ± 5 μm) was obtained through the combined tide-wave dynamic condition. Thus, a tide-induced dynamic condition is most suitable for calm-day simulations.

Storm Simulations with Tide-Only Dynamics. The floc particles were smaller and the turbulent shear during the significant wave heights (>1.5 m) was stronger during storm days than during calm days (Figure 3a,b). However, the model-predicted particle sizes for the storm events obtained by considering tidal dynamics alone were larger than the measured D50 (Figure 5b–f). Overestimations mainly occurred in the simulations of fine particles (D_{field}, <50 μm; Figure 6a,b). The RMSEs of all storm simulations were higher than 44 μm, and the highest RMSE (87 ± 10 μm) occurred during the March 21 to 25 storm (Table 4).

The large Kolmogorov microscale (500–1500 μm; Figure 6e,f,i,j) indicates that a small turbulent shear occurred when considering tidal dynamics alone. These smaller hydrodynamic forces accelerated the aggregation mechanism (i.e., a higher rate of change for the aggregation volume, $dV_{aggregation}/V_{field}$; Figure 6e,f) but decreased the breakage mechanism (i.e., a lower rate of change for the breakage volume, $dV_{breakage}/V_{field}$; Figure 6i,j). Even the spring tidal force (i.e., those simulations from February 1 to 2, March 10 to 13, and March 21 to 25) was insufficient to break floc particles during storms when tidal currents were the only hydrodynamic force included in the model.

Storm Simulations with Combined Tide-Wave Dynamics. By accounting for the effect of wave orbital motion on flow velocity in the model, improved results were obtained that more accurately represented the measured floc size, compared with the purely tidal-driven modeling (Figure 5b–f and Figure 6c,d). Specifically, the smaller Kolmogorov microscale (high turbulent shear), which was governed by the combined tide-wave velocity, enhanced the fractions of the floc volume with sufficient breakage forces. In other words, the rate of change for the breakage and aggregation volume increased and decreased, respectively (Figure 6g,h,k,l).

Overall, combining the dynamic conditions in the model more accurately represented the measured data, particularly during southwest storms. The highest accuracy was obtained in the simulations from February 1 and 2, where the RMSE was 13 μm, followed by those from February 5 to 7, and from March 10 to 13 (Table 4). However, the simulations of northeast storms were less consistent with measured D50 (Figure 4e,f); in these situations, the model overestimates the measurements (Figure 5d) and the RMSE exceeded 40 μm.

The aforementioned results indicated that the turbulent shear generated by tidal currents, which dominated floc dynamics on calm days, was insufficient to force floc breakup under storm conditions. As detailed in Table 1, this can be observed from the small particles (<50 μm) in measured data. Finally, RMSEs of both dynamic conditions were compared during storm events and determined that the average RMSE value decreased from 67 μm (tide-only dynamic) to 32 μm (combined dynamic), revealing a 50% modeling improvement through a wave-induced turbulent shear.

Discussion

The model results showed that the turbulent shear generated by tidal currents dominated floc dynamics on calm days. The tide-wave-combined turbulence must be incorporated when simulating flocculation in a tide-wave-dominated environment. The results also indicated that the hydrodynamic force causes the discrepancies between the model results and observations under the storm conditions, even during the calibration period. To explore the difference in floc behaviors during the northeast and southwest storms, this section discusses the factors governing the sediment sources and the transport processes at BLA. Additionally, the variations in floc strength among the seasons were estimated to further enhance the model's accuracy.

Floc Behaviors under Different Storm Conditions. In the southern North Sea, winds dominate the subtidal alongshore

Allen Press, Inc. ■ 30 November 2017 ■ 11:19 am ■ Customer MS#WER-D-16-00107
//titan/production/w/waer/live_jobs/waer-90/waer-90-03/waer-90-03-07/layouts/waer-90-03-07.3d

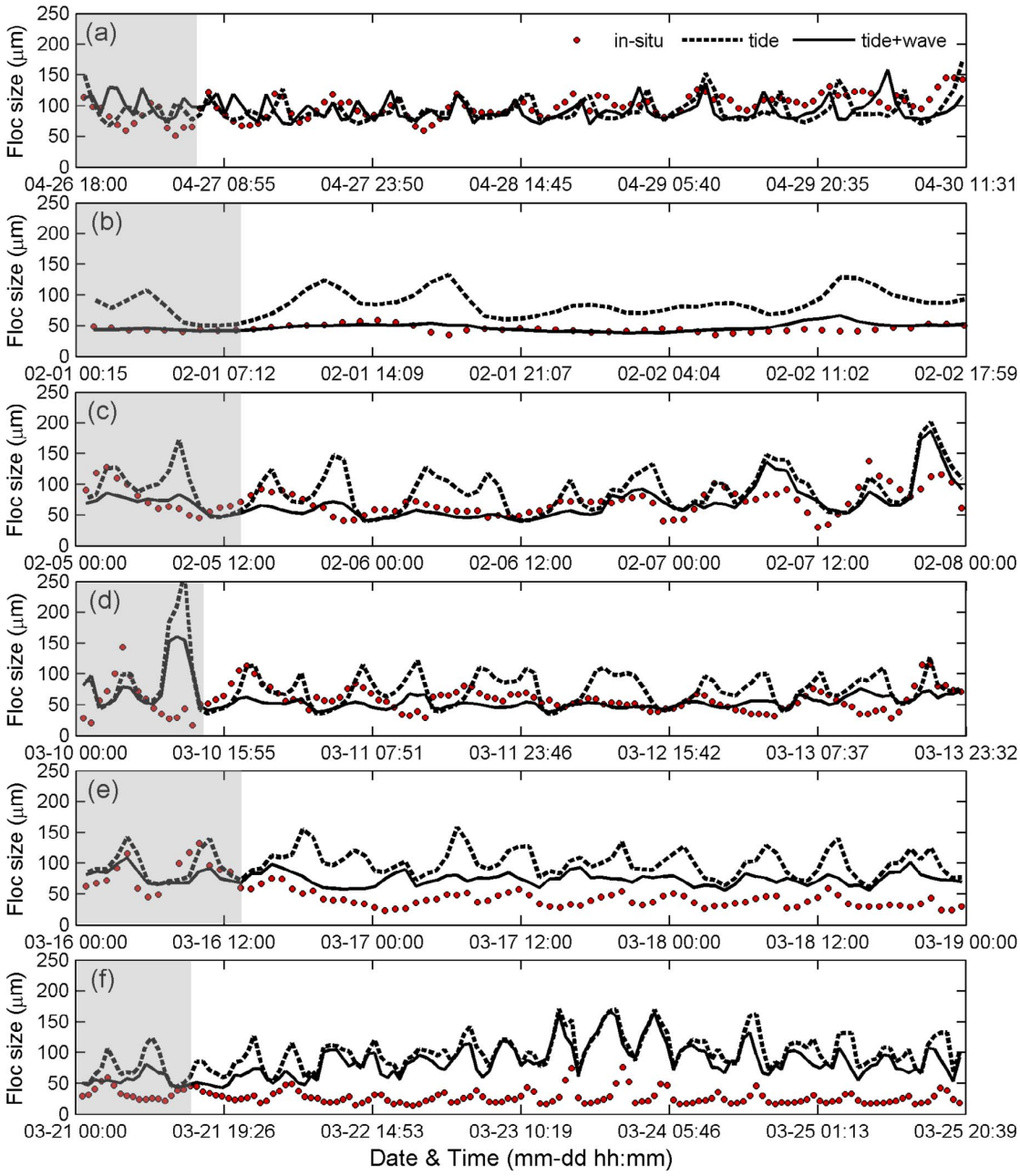

Figure 5—Measured (dots) and simulated values of floc size (m) under tide (dashed line) and combined tide–wave (solid line) forcing during (a) the calm events from April 26 to 30 and storm events in (b) February 1 to 2 (southwest storm), (c) February 5 to 7 (southwest storm), (d) March 10 to 13 (southwest storm), (e) March 16 to 19 (northeast storm), and (f) March 21 to 25 (northeast storm). The gray shaded period has been used for calibrating the model.

flow and change the flocculation mechanisms during storms (Baeye et al., 2011; Fettweis et al., 2014). Therefore, even under identical hydrodynamic conditions (e.g., tides and waves), the floc size distributions can have distinct variations depending on the storm directions. For instance, the storm events from March 10 to 13 and March 21 to 25 had similar hydrodynamic conditions (spring tide, the significant wave heights >2.5 m) but different storm directions (southwest and northeast, respectively); the D50 during these two storms was also different (Table 1). Specifically, the average D50 during the southwest storm was 56 μm (unimodal PSD; Figure 6c), whereas that of the northeast storm was only 26 μm (multimodal PSD; Figure 6e). This can be

Allen Press, Inc. ■ 30 November 2017 ■ 11:19 am ■ Customer MS#WER-D-16-00107
//titan/production/w/waer/live_jobs/waer-90/waer-90-03/waer-90-03-07/layouts/waer-90-03-07.3d

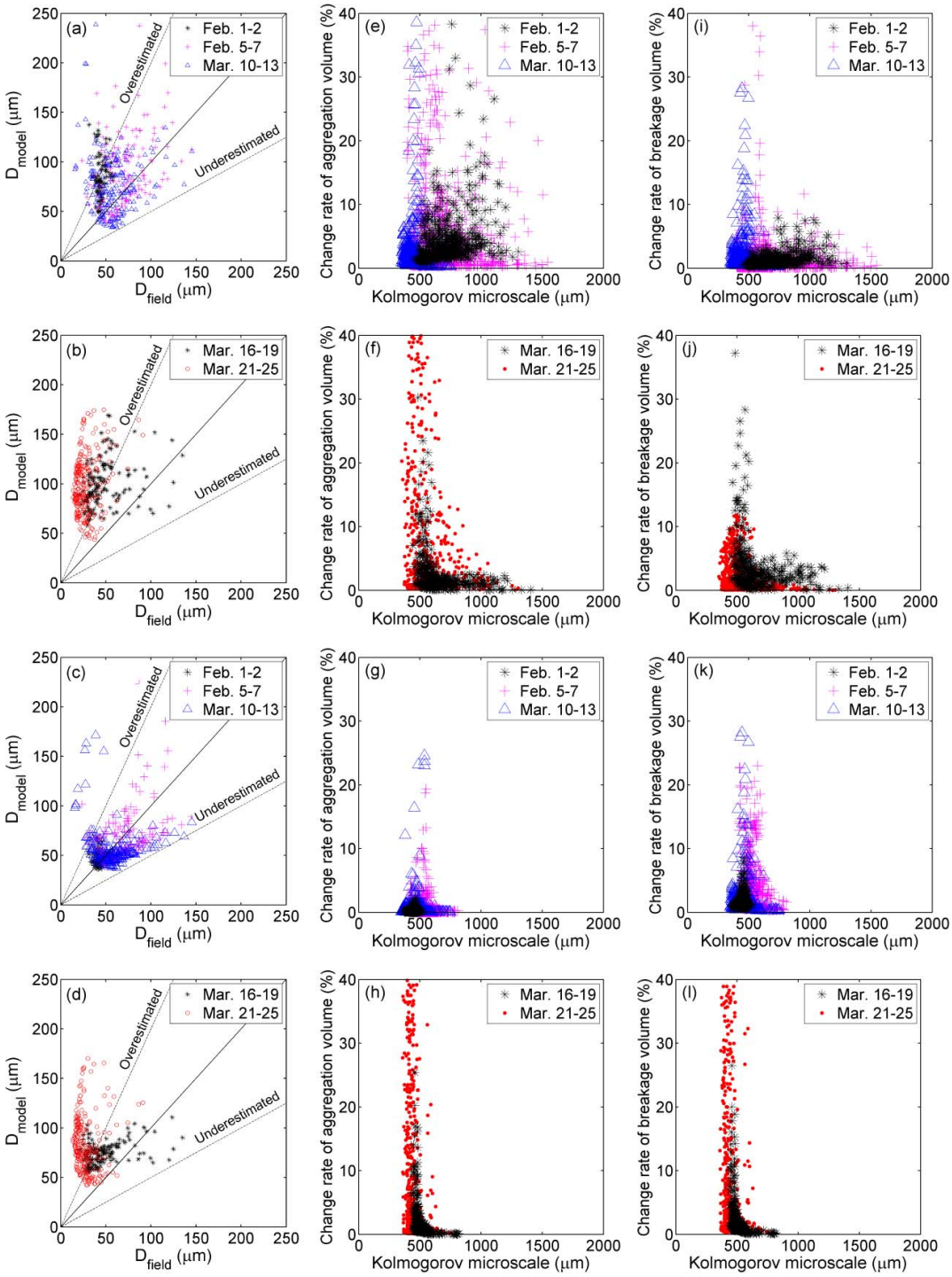

Figure 6—Comparison of modeled and measured floc size during (a) southwest storms and (b) northeast storms when only tide-induced dynamics were considered, (c) southwest storms, and (d) northeast storms when tide-wave-induced dynamics were considered. Correlation between the Kolmogorov microscale and the rate of change for the aggregation volume per measured floc volume ($dV_{aggregation}/V_{field}$) during (e) southwest storms, and (f) northeast storms when only tide-induced dynamics were considered, (g) southwest storms, and (h) northeast storms when tide–wave-induced dynamics were considered. Correlation between the Kolmogorov microscale and the rate of change for the breakage volume per field floc volume ($dV_{breakage}/V_{field}$) during (i) southwest storms, (j) northeast storms when only tide-induced dynamics were considered, (k) southwest storms, and (l) northeast storms when tide–wave-induced dynamics were considered.

Allen Press, Inc. ■ 30 November 2017 ■ 11:19 am ■ Customer MS#WER-D-16-00107
//titan/production/w/waer/live_jobs/waer-90/waer-90-03/waer-90-03-07/layouts/waer-90-03-07.3d

Table 4—Root mean square error and simulation error* on tide-induced and combined tide-wave velocity.

Month	February		March		
Date	1–2	5–7	10–13	16–19	21–25
Storm	SW	SW	SW	NE	NE
Tide-induced dynamic system (referred to the study of Maggi, 2009)					
$F_y = 0$, RMSE (μm)	>100	>100	>100	>100	>100
$F_y = 3 \times 10^{-11}$, RMSE (μm)	67.73	60.74	44.57	75.10	86.58
The combined tide-wave dynamics system					
$F_y = 3 \times 10^{-11}$, RMSE (μm)	13.36	23.47	22.28	40.18	62.46
F − M < − 10 μm (%)	28	25	24	88	99
|F − M| ⩽ 10 μm (%)	60	31	38	6	1
F − M > 10 μm (%)	12	44	38	6	0
$F_y = 0$, RMSE (μm)	>100	>100	>100	>100	>100
$F_y = 1 \times 10^{-11}$, RMSE (μm)	13.32	23.30	23.15	23.06	33.55
$F_y = 5 \times 10^{-11}$, RMSE (μm)	28.29	40.61	39.78	55.04	84.98

Note: F_y, floc strength (N); F, field data; M, model results; southwest, SW; northeast, NE.
* Simulation error refers to the difference between field and model floc size.

explained by the occurrence of granular particles (silt and sand) eroded and resuspended from the seabed by wave orbital stress during southwest storms with a northeast-directed alongshore subtidal current (Fettweis et al., 2012). Furthermore, the SPM consisted of mixed cohesive and noncohesive particles resulting in more unimodal PSDs. The model behavior coincides with this unimodal PSD during southwest storms (Figures 6a–c).

However, the subtidal alongshore flow directions during northeast storms exhibited floc characteristics entirely different from those during southwest storms. The alongshore flows during northeast storms caused the resuspension of soft mud deposits located in the navigation channels and the adjacent areas, and a stronger outflow of SPM from the Westerschelde estuary (Baeye et al., 2011; Figure 1). Fettweis et al., (2010, 2012) also noted that the direction of subtidal alongshore flow during northeast storm events results in an increase in cohesive SPM concentration, HCMS formation and the armoring of sand. These pure cohesive particles are indicated by the presence of multimodal PSDs, which contain many small sized particles (i.e., high tails of small PSDs; Figure 6d,e). Thus, because the applied model is based on a single characteristic diameter of floc dynamics, it is appropriate for simulating particles with unimodal PSDs but less accurate for particles that exhibit multimodal behaviors.

Seasonal Floc Strength. Charged particles in suspension, such as clays or exopolymers, may become attached to each other and to other particles to form flocs with compositions, sizes, densities, and structural complexities that vary as a function of turbulence and biochemical composition (e.g., Droppo, 2001; Eisma, 1986; Maggi and Tang, 2015; Mietta et al., 2009; Pavoni et al., 1972; Tan et al., 2012; Winterwerp, 1998). The algal bloom and associated biological activities have been connected to an enhancement in the production of particle-binding microbial exudates such as TEPs (Alldredge et al., 1993; Engel, 2000; Logan et al., 1995; Passow et al., 2001). Transparent extracellular particles (TEPs) may increase not only the floc size and but also the floc strength, resulting in the formation of larger amounts of macroflocs (Fettweis et al., 2014; Lee et al., 2012). The existence of macroflocs has been demonstrated for both open oceans and turbid coastal and estuarine environments (e.g., Alldredge et al., 1993; Jago et al., 2007). In turbid coastal and estuarine environments, such as the southern North Sea, phytoplankton bloom is affected by high nutrient availability and affects SPM dynamics (Lacroix et al., 2007). An experimental study reported that the average settling velocity of the larger biomass-affected flocs was nearly equal to that of the smaller biomass-free flocs because of the opposing effects of floc size and density (Tang and Maggi, 2016), however, in situ measurements suggest that flocs during spring and summer are larger and settle faster than flocs during winter (Fettweis et al., 2014). During spring and summer when TEPs are more abundant, the SPM concentration reduces, thus increasing the light conditions, which further enhances algal growth (Desmit et al., 2005). Lower SPM concentrations and higher chlorophyll concentrations in summer have been observed at the measuring size, as shown in Figure 2. By contrast, low solar radiation decelerates physical (e.g., thermal stratification, light, and temperature) and biological (e.g., primary production) processes during winter, thus reducing primary production and the release of exopolymers (Droppo et al., 2005; Fettweis et al., 2014). Because the biological effects on floc dynamics are complicated and not yet fully understood, floc strength was used to investigate their effects on seasonal floc size variations.

To investigate the seasonal signal of floc binding ability, various floc strengths were used to test and estimate the model's accuracy across seasons. Firstly, the situations were tested without floc strength (Fy equal 0 N) to understand the effect of floc strength on floc dynamic. The floc strength that has been suggested in theoretical (Matsuo and Unno, 1981) and experimental (Van Leussen, 1994) studies is approximately 10^{-11} N. Therefore, four floc strength values were applied to the model, including 0 N (without floc strength), 1×10^{-11} N, 3×10^{-11} N (Maggi, 2009), and 5×10^{-11} N (Table 4). Compared

Allen Press, Inc. ■ 30 November 2017 ■ 11:19 am ■ Customer MS#WER-D-16-00107
//titan/production/w/waer/live_jobs/waer-90/waer-90-03/waer-90-03-07/layouts/waer-90-03-07.3d

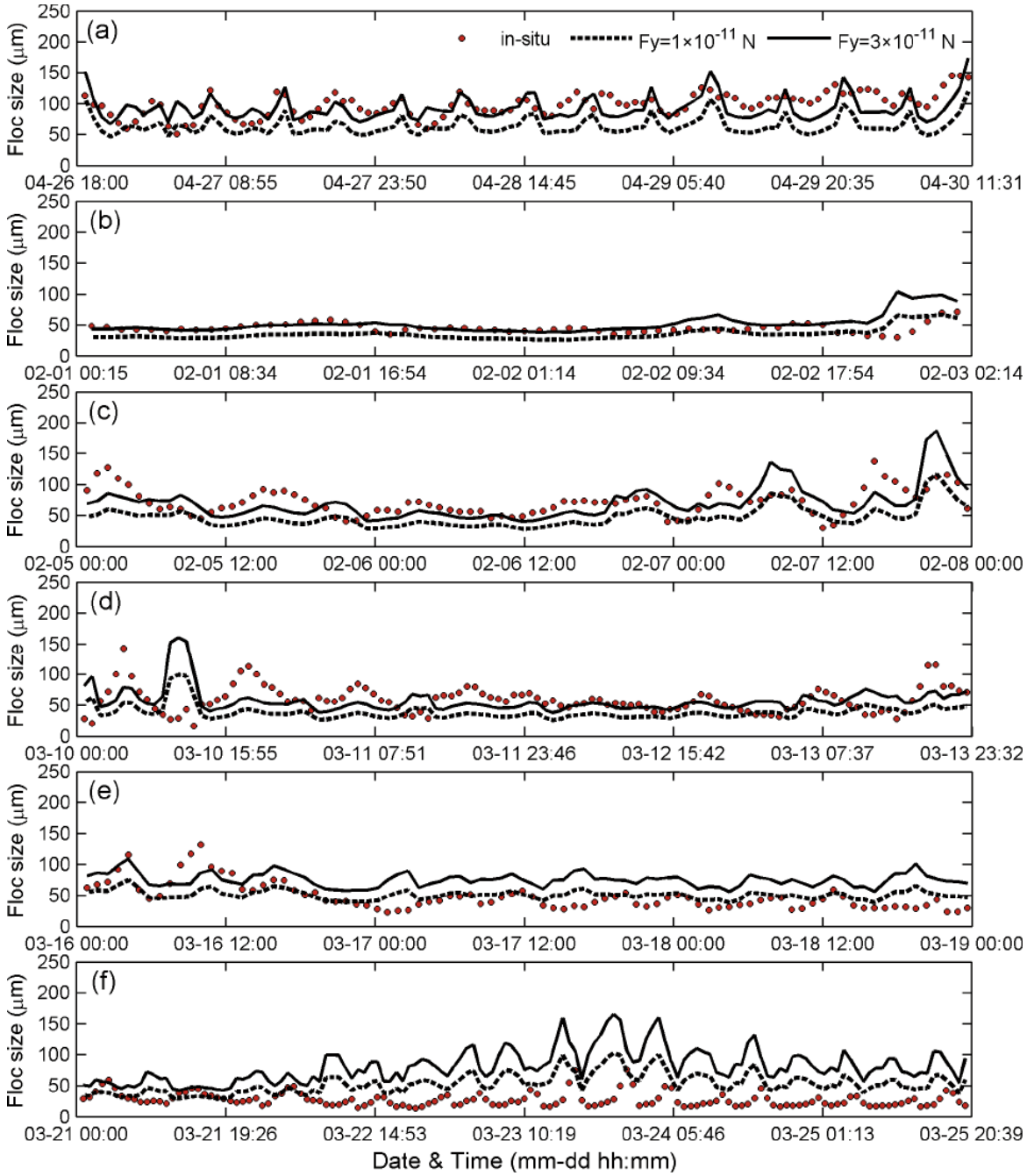

Figure 7—Floc size simulated with different values of floc strengths (*Fy*, circle: measured data, dash line: $Fy = 1 \times 10^{-11}$ N, solid line: $Fy = 3 \times 10^{-11}$ N) for (a) April 26 to 30 (calm days), (b) February 1 to 2 (southwest storm), (c) February 5 to 7 (southwest storm), (d) March 10 to 13 (southwest storm), (e) March 16 to 19 (northeast storm), and (f) March 21 to 25 (northeast storm).

with field data, the simulations without floc strength (0 N) had deviations (RMSEs large than 100 μm) whether under tidal-only or by combining dynamic systems. The results without floc strength indicated that floc strength is a key factor in determining floc particle evolution. Meanwhile, the simulations of summer conditions (April case) were obtained using 3×10^{-11} N, and were closer to the measured data than those obtained using the other two floc strength values (Table 4 and Figure 7a). The inverse relationship between floc strength and the breakage rate (eq 7) implies that the breakage rate decreases as floc strength increases. Additionally, a gradually increasing trend in D50 floc size (Figure 3c) revealed that the floc aggregation

Allen Press, Inc. ■ 30 November 2017 ■ 11:19 am ■ Customer MS#WER-D-16-00107
//titan/production/w/waer/live_jobs/waer-90/waer-90-03/waer-90-03-07/layouts/waer-90-03-07.3d

mechanism was stronger than the breakage mechanism in the summer. Therefore, a floc strength of 3×10^{-11} N is appropriate for representing summer conditions.

By contrast, using a smaller floc strength (1×10^{-11} N) significantly improved the simulation for winter conditions (February and March cases; Table 4 and Figure 7b–f) because of the small floc particles, which indicates that a weaker floc strength accelerates the floc breakage dynamics. Therefore, the floc strength used in the model must vary with season. The use of 3×10^{-11} N and 1×10^{-11} N as the floc strengths for simulating summer and winter conditions, respectively, is suggested in the southern North Sea.

Conclusions

A biomineral flocculation model was tested using a single characteristic diameter (D50) to simulate the floc variations under different weather and seasonal conditions in the southern North Sea. A conception of tide-wave-combined turbulence was proposed to investigate storm-influenced flocculation. A 50% improvement in model accuracy, compared with simulations that have only been forced by tidal velocity, demonstrates the importance of waves for SPM dynamics and transport in storm-dominated environments. Additionally, the results confirm that floc strength has a seasonal influence on floc development. A stronger floc-binding strength was observed in the summer season (April–September), during which flocculation was influenced by abundant sticky organic substances, compared with the weak-biomass (Figure 2) winter season (October–March). Therefore, applying different floc strengths is essential to successfully model seasonal variations in the southern North Sea; according to this study, the ideal floc strengths are 3×10^{-11} N during summer and 1×10^{-11} N during winter.

The present model assumes a unimodal size distribution and simulated single characteristic particles. Future studies on flocculation using multimodal PSDs are warranted. Additionally, the constant values of the floc strength used in this model are insufficient to represent seasonal characteristics. Thus, accurate understanding of the correlations between floc strength properties and physical, chemical, and biological environments (e.g., hydrometeorological conditions, sunlight intensity, microorganisms, and chlorophyll), and their seasonal effects on floc binding ability require further investigation.

Acknowledgments

The study was supported by the National Science Council, Taiwan (NSC98-2221-E110-086), the Maritime Access Division of the Flemish Ministry of Mobility and Public Works (MOMO project), and the BRAIN-be program (BELSPO, INDI67 project). The Ship time RV Belgica was provided by BELSPO and the RBINS-Operational Directorate Natural Environment. The wave and wind data are from the Agency for Maritime and Coastal Services - Coastal Division (Flemish Ministry of Mobility and Public Works). The authors thank L. Naudts and his team for assisting with all of the technical aspects of instrumentation and moorings, and Dr. Yi-Hsiang Yu for his valuable comments on the overall presentation and content of this study.

Submitted for publication , ; accepted for publication , .

References

Alldredge, A. L.; Passow, U.; Logan, B. E. (1993) The Abundance and Significance of a Class of Large, Transparent Organic Particles in the Ocean. *Deep-Sea Res.*, **Part I** (40), 1131–1140.

Baeye, M.; Fettweis, M.; Voulgaris, G.; Van Lancker, V. (2011) Sediment Mobility in Response to Tidal and Wind-Driven Flows along the Belgian Inner Shelf, Southern North Sea. *Ocean Dynam.*, **61** (5), 611–622.

Berlamont, J.; Ockenden, M.; Toorman, E.; Winterwerp, J. (1993) The Characterisation of Cohesive Sediment Properties. *Coast. Eng.*, **21** (1–3), 105–128.

Borges, A. V.; Gypens, N. (2010) Carbonate Chemistry in the Coastal Zone Responds More Strongly to Eutrophication than to Ocean Acidification. *Limnol. Oceanogr.*, **55** (1), 346–353.

Desmit, X.; Vanderborght, J. P.; Regnier, P.; Wollast, R. (2005) Control of Phytoplankton Production by Physical Forcing in a Strongly Tidal, Well-Mixed Estuary. *Biogeosci.*, **2**, 205–218.

Droppo, I. G. (2001) Rethinking What Constitutes Suspended Sediment. *Hydrol. Proc.*, **15**, 1551–1564, DOI:10.1002/hyp.228.

Droppo, I. G.; Nackaerts K.; Walling, D. E.; Williams, N. (2005) Can Flocs and Water Stable Soil Aggregates be Differentiated Within Fluvial Systems? *Catena*, **60**, 1–18.

Dyer, K. R. (1989) Sediment Processes in Estuaries: Future Research Requirements. *J. Geophys. Res.*, **94** (C10), 14327–14339.

Eisma, D. (1986) Flocculation and De-Flocculation of Suspended Matter in Estuaries. *Neth. J. Sea Res.* **20**, 183–199.

Engel, A. (2000) The Role of Transparent Exopolymer Particles (TEP) in the Increase in Apparent Particle Stickiness During the Decline of a Diatom Bloom. *J. Plankton Res.*, **22**, 485–497.

Fettweis M.; Francken F.; Pison V.; Van den Eynde, D. (2006) Suspended Particulate Matter Dynamics and Aggregate Sizes in a High Turbidity Area. *Mar. Geol.*, **235**, 63–74.

Fettweis, M.; Francken, F.; Ven den Eynde, D.; Verwaest, T.; Janssens, J.; Van Lancker, V. (2010) Storm Influence on SPM Concentrations in a Coastal Turbidity Maximum Area with High Anthropogenic Impact (Southern North Sea). *Cont. Shelf Res.*, **30** (13), 1417–1427.

Fettweis, M.; Baeye, M.; Lee, B. J.; Chen, P.; Yu, J. C. R. (2012) Hydro-Meteorological Influences and Multimodal Suspended Particle Size Distributions in the Belgian Nearshore Area (Southern North Sea). *Geo-Mar. Lett.*, **32** (2), 123–137.

Fettweis, M.; Baeye, M.; Van der Zande, D.; Van den Eynde, D.; Lee, B. J. (2014) Seasonality of Floc Strength in the Southern North Sea. *J. Geo. Res.*, **119** (3), 1911–1926.

Green, M. O.; Vincent, C. E.; McCave, I. N.; Dickson, R. R.; Rees, J. M.; Pearson, N. D. (1995) Storm Sediment Transport: Observations from the British North Sea Shelf. *Cont. Shelf. Res.*, **15** (8), 889–912.

Howarth, M. J.; Dyer, K. R.; Joint, I. R.; Hydes, D. J.; Purdie, D. A.; Edmunds, H.; Jones, J. E.; Lowry, R. K.; Moffat, T. J.; Pomroy, A. J.; Proctor, R.; Van Leussen, W. (1993) Seasonal Cycles and Their Spatial Variability. *Philos. Trans. R. Soc., A*, **343** (1669), 383–403.

Jago, C. F.; Kennaway, G. M.; Novarino, G.; Jones S. E. (2007) Size and Settling Velocity of Suspended Flocs During a Phaeocystis Bloom in the Tidally Stirred Irish Sea, NW European Shelf. *Mar. Ecol. Prog. Ser.*, **345**, 51–62.

Kirby, R. (2011) Minimising Harbour Siltation - Findings of PIANC Working Group 43. *Ocean Dynam.*, **61**, 233–244.

Kiorboe, T.; Andersen, K. P.; Dam, H. G. (1990) Coagulation Efficiency and Aggregate Formation in Marine-Phytoplankton. *Mar. Biol.*, **107** (2), 235–245.

Lacroix, G.; Ruddick, K.; Park, Y.; Gypens, N.; Lancelot, C. (2007) Validation of the 3D Biogeochemical Model MIRO&CO with Field Nutrient and Phytoplankton Data and MERIS-Derived Surface Chlorophyll a Images. *J. Mar. Syst.*, **64**, 66–88.

APPENDIX 3

Fettweis M, Lee BJ. 2017. Spatial and seasonal variation of biomineral suspended particulate matter properties in high-turbid nearshore and low-turbid offshore zones. *Water*, 9, 694. doi:10.3390/w9090694

water

MDPI

Article

Spatial and Seasonal Variation of Biomineral Suspended Particulate Matter Properties in High-Turbid Nearshore and Low-Turbid Offshore Zones

Michael Fettweis [1] and Byung Joon Lee [2,*]

[1] Operational Directorate Natural Environment, Royal Belgian Institute of Natural Sciences, Gulledelle 100, B-1200 Brussels, Belgium; mfettweis@naturalsciences.be

[2] Department of Disaster Prevention and Environmental Engineering, Kyungpook National University, 2559 Gyeongsang-daero, Sangju, Gyeongbuk 742-711, Korea

* Correspondence: bjlee@knu.ac.kr; Tel.: +82-54-530-1444

Received: 3 August 2017; Accepted: 11 September 2017; Published: 12 September 2017

Abstract: Suspended particulate matter (SPM) is abundant and essential in marine and coastal waters, and comprises a wide variety of biomineral particles, which are practically grouped into organic biomass and inorganic sediments. Such biomass and sediments interact with each other and build large biomineral aggregates via flocculation, therefore controlling the fate and transport of SPM in marine and coastal waters. Despite its importance, flocculation mediated by biomass-sediment interactions is not fully understood. Thus, the aim of this research was to explain biologically mediated flocculation and SPM dynamics in different locations and seasons in marine and coastal waters. Field measurement campaigns followed by physical and biochemical analyses had been carried out from 2004 to 2011 in the Belgian coastal area to investigate bio-mediated flocculation and SPM dynamics. Although SPM had the same mineralogical composition, it encountered different fates in the turbidity maximum zone (TMZ) and in the offshore zone (OSZ), regarding bio-mediated flocculation. SPM in the TMZ built sediment-enriched, dense, and settleable biomineral aggregates, whereas SPM in the OSZ composed biomass-enriched, less dense, and less settleable marine snow. Biological proliferation, such as an algal bloom, was also found to facilitate SPM in building biomass-enriched marine snow, even in the TMZ. In short, bio-mediated flocculation and SPM dynamics varied spatially and seasonally, owing to biomass-sediment interactions and bio-mediated flocculation.

Keywords: suspended particulate matter; aggregates; flocculation; biomass; sediment

1. Introduction

Suspended particulate matter (SPM), produced by biological and geophysical actions on the Earth's crust, enters into marine and coastal waters and is dispersed by flow-driven transportation, such as advection and dispersion [1–3]. The SPM concentration is an important parameter to understand the marine ecosystem as it controls the water turbidity and mediates many physical and biochemical processes [4–6].

SPM comprises a wide variety of biomineral clay to sand sized particles, comprising living (microbes, phyto- and zooplankton) and non-living organic matter (fecal and pseudo-fecal pellets, detritus and its decomposed products from microbial activity such as mucus, exopolymers), and minerals from a physico-chemical (e.g., clay minerals, quartz, feldspar) and biogenic origin (e.g., calcite, aragonite, opal), which are practically grouped into organic biomass and inorganic sediments [7]. It is important to note that when clays or other charged particles and polymers are in suspension, they become attached to each other and form fragile structures or flocs with compositions, sizes, densities,

and structural complexities that vary as a function of turbulence and biochemical composition [3,8–11]. Flocculation combines biomass and sediments into larger aggregates (i.e., flocs) that can be classified as either mineral, biomineral, or biological aggregates. Flocculation usually integrates aggregation and disaggregation (i.e., breakup) kinetics, depending on the hydrodynamics of a suspension. Electrostatic and colloidal chemistry is the fundamental driver for flocculation in a cohesive suspension. For example, high ionic strength reduces the electrostatic repulsion between colloidal particles, thereby increasing the aggregation of colloidal suspension. Also, regarding the heterogeneity of a natural suspension with various biomass and sediments, physical and biochemical conditions are favorable for flocculation, like low turbulence intensity, high ionic strength, and sticky polymeric substances, which help individual biomineral particles to build large aggregates. Clay mineralogy is also important for determining electrochemistry and flocculation capability. Depending on the biomass composition, such aggregates are classified into mineral, biomineral, and biological aggregates [12,13]. Mineral and biomineral aggregates form in the sediment-enriched environment, such as a turbidity maximum zone (TMZ) or a nearshore area [6,14,15], while biological aggregates (i.e., marine snow) form in the mineral-depleted environment typically found in an offshore zone (OSZ) [16].

Flocculation mediated by biological composition determines the size, density, and settling velocity of aggregates [12,14,17]. For example, in a tidal cycle, low flow intensity during slack water enhances flocculation capability, building large, settleable aggregates, whereas high flow intensity at peak flow reduces flocculation capability, breaking down aggregates to small, less (or hardly) settleable aggregates or primary particles [5,18]. Moreover, sticky biomass (e.g., extracellular polymeric substances (EPSs) or transparent extracellular polymers (TEPs)) helps build large biomineral aggregates [7,19–22]. Flocculation which can be mediated by biological factors consequently controls sedimentation, resuspension, deposition, and erosion, and determines the overall SPM dynamics in marine and coastal waters [12,23].

Bio-medicated flocculation and SPM dynamics are important in science and engineering because they eventually control the sediment, carbonaceous, and nitrogenous mass balances at the regional or global scale [24,25]. Despite their importance, bio-mediated flocculation and SPM dynamics are not fully understood in coastal and marine waters. Geologists and hydraulic engineers have focused more on sediments and less on biomass [3,14], and marine biologists vice versa [16]. In our opinion, the biomass-sediment interactions in coastal and marine waters have only recently been studied in a systematic and quantitative way [7,9,13,26–29], and mathematical models which can take into account the heterogeneous composition/morphology of biomineral aggregates were developed only a few years ago [12,30]. These efforts should be paid more attention.

Therefore, the aim of the study was to add to our current understanding of bio-mediated flocculation and its impact on the SPM in marine and coastal waters. First, we investigated the spatial variation of SPM dynamics in a sediment-enriched TMZ and a mineral-depleted OSZ, especially concerning bio-mediated flocculation. Second, we investigated the seasonal variation of SPM dynamics in a TMZ to understand how seasonal changes in biological activity, especially algae blooms, affect bio-mediated flocculation and SPM dynamics. This paper describes and discusses bio-mediated flocculation and SPM dynamics for different locations and seasons.

2. Materials and Methods

2.1. Site Description

The study area is situated in the Southern Bight of the North Sea, specifically in the Belgian coastal zone. Measurements have indicated SPM concentrations of 20–70 mg/L in the nearshore area; reaching 100 to more than a few g/L near the bed; lower values (<10 mg/L) occur in the offshore [31]. As shown in Figure 1, the MOW1 measurement site is located in the TMZ. The Gootebank (G-Bank), Hinderbank (H-Bank), and Kwintebank (K-Bank) sites are in the OSZ, out of or at the edge of the turbidity maximum. Satellite images of surface SPM and chlorophyll-a (Chl) concentrations in the

study area show clear spatial and seasonal changes. Regarding the seasonality, the annual cycle of SPM concentration in the high turbidity area off the Belgian coast is mainly caused by the seasonal biological cycle, rather than wind and waves. Wind strengths and wave heights have a seasonal signal, but these do not explain the large differences observed in SPM concentration [31,32]. This seasonality is linked with the seasonal changes in aggregate size and thus settling velocity due to biological effects. The aggregate sizes and settling velocities are smaller in winter and larger in summer. As a result, the SPM is more concentrated in the near-bed layer, whereas in winter, the SPM is better mixed throughout the water column. This explains the inverse correlation found between the surface SPM and the Chl concentrations in Figure 1. Water depths of the measuring area vary between 5 and 35 m. The mean tidal ranges at Zeebrugge are 4.3 and 2.8 m at spring and neap tides, respectively. The tidal current ellipses are elongated in the nearshore area and become gradually more semicircular towards the offshore area. The current velocities near Zeebrugge (nearshore) vary from 0.2 to 1.5 m/s during spring tide and from 0.2 to 1.0 m/s during neap tide. Salinity varies between 28 and 34 practical salinity units (PSU) in the coastal zone, because of the wind-induced advection of water masses and river discharge [33,34]. The most important sources of SPM are from the erosion and resuspension of the Holocene mud deposits outcropping in the Belgian nearshore area; the French rivers discharging into the English Channel, and the coastal erosion of the Cretaceous cliffs at Cap Gris-Nez and Cap Blanc-Nez (France) are only minor sources [35,36].

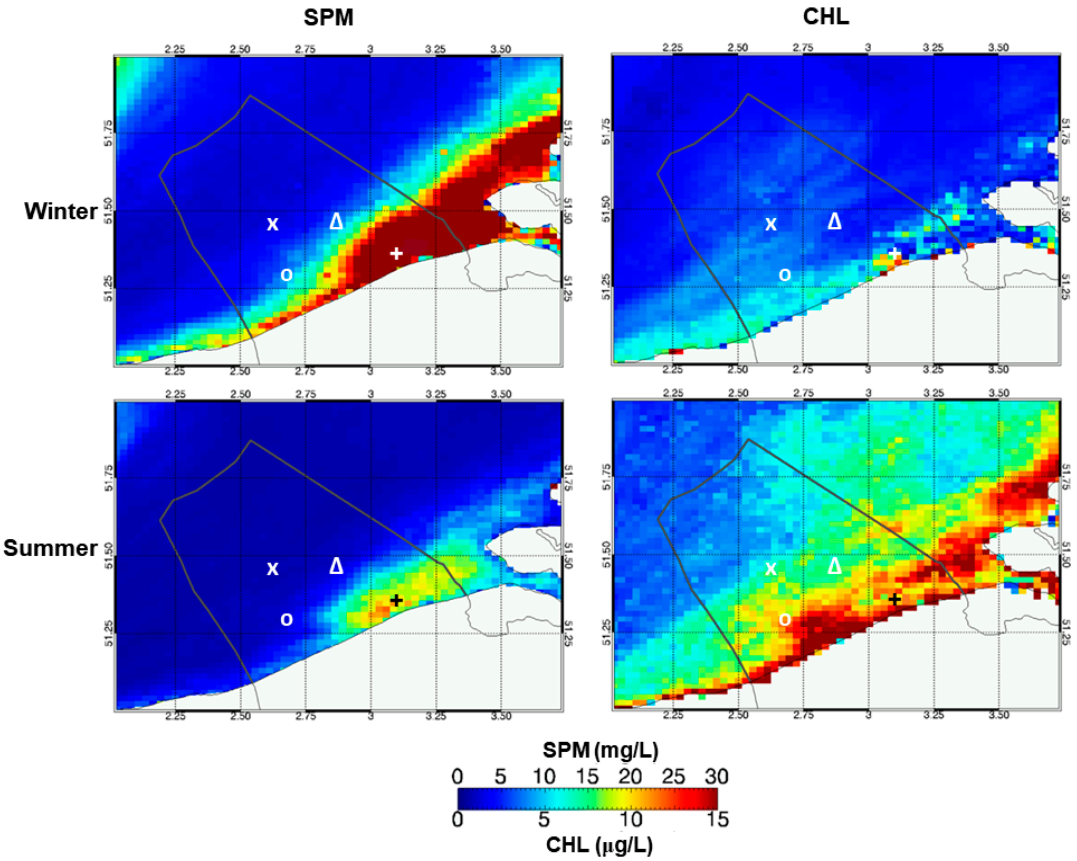

Figure 1. Mean surface suspended particulate matter (SPM) and chlorophyll-a (CHL) concentrations in the southern North Sea during the winter (October–March, top) and summer season (April–September, bottom) derived from the MERIS satellite. The +, Δ, X, and O symbols indicate the measurement sites of MOW1, Gootebank (G-Bank), Hilnderbank (H-Bank), and Kwintebank (K-Bank), respectively. Turbidity maximum zone (TMZ) has SPM concentrations above 15–20 mg/L and the offshore zone (OSZ) below 10 mg/L.

2.2. Tidal Measurements

Field measurements in the TMZ (MOW1) and in the OSZ (G-Bank, H-Bank, and K-Bank) were carried out about four times a year from February 2004 until 2011. During each campaign, sensor measurements (flow, SPM dynamics) and water sampling (SPM properties) were executed, while the research vessel was moored to maintain a specific measuring position for a 13-h tidal cycle. A Sea-Bird SBE09 SCTD carousel sampling system (containing twelve 10 L Niskin bottles) (Sea-Bird Electronics Inc., Bellevue, WA, USA) was kept at least 4.5 m below the surface and about 3 m above the bottom. A LISST 100X (Laser In-Situ Scattering and Transmissometry, range 2.5–500 µm) (Sequoia Scientific Inc., Bellevue, WA, USA) was attached directly to the carousel sampling system to measure particle size distribution (PSD) at the same location as the water sampling system [37]. The volume concentration of each size group was estimated with an empirical volume calibration constant, which was obtained under a presumed sphericity of particles [37–39]. The LISST has a sampling volume which permits it to statistically sample the less numerous large aggregates, but it cannot detect aggregates larger than 500 µm or smaller than 2.5 µm. Particles smaller than the size range affect the entire PSD, with an increase in the volume concentration of the smallest two size classes, a decrease in the next size classes and, an increase in the largest size classes [40]. Similar remarks have been formulated by Graham and coworkers [41], who observed an overestimation of one or two orders of magnitude in the number of fine particles measured by the LISST. A rising tail in the lowest size classes of the LISST occurs regularly in the data during highly turbulent conditions and is interpreted as an indication of the presence of very fine particles and thus a break-up of the aggregates. Particles exceeding the LISST size range of 500 µm also contaminate the PSD. The large out of range particles increase the volume concentration of particles in multiple size classes in the range between 250 and 500 µm and in the smaller size classes [42–44]. The occurrence of rising tail in the largest size classes indicates the occurrence of large particles rather than an absolute value. Other uncertainties of the LISST-100C are related to the often non-spherical shape of the particles occurring in nature [40,41,44]. A hull mounted, acoustic Doppler current profiler (ADCP) type, Workhorse Mariner 300 kHz (RD Instruments, Poway, CA, USA), was used to determine the velocity profiles.

2.3. Water Samples and Analysis

A Niskin bottle of the carousel sampling system was closed every 20 min, thus collecting about 40 samples during a 13 h flood-ebb tidal cycle. Note that the carousel sampling system was deployed to take water samples in the middle of the water column, at least 3 m above the bed layer. The carousel was brought aboard every hour. Three sub-samples from each water sample were then filtered on board using pre-weighed filter papers (Whatman GF/C, Sigma-Aldrich, St. Louis, MO, USA). In total, 120 filtrations were thus carried out per tidal cycle. After filtration, the filter papers were rinsed with demineralized water (±50 mL) to remove the salt, dried at 105 °C, and weighed again to determine the SPM concentrations. Every hour, a fourth sub-sample was filtered on board to determine particulate organic carbon (POC) and particulate organic nitrogen (PON) concentrations. The residues on the filter paper were carefully collected and acidified with 1 N HCl. Then, the POC and PON of the residues were quantified with a Carbon Nitrogen elemental analysis.

2.4. Grain Size and Mineralogical Analysis

Primary grain size and mineralogical analyses were performed to determine the mineralogical composition of the SPM samples. Suspension samples were obtained by the centrifugation of seawater collected by an ALFA Laval MMB 304S flow-through centrifuge (Alfa Laval Corp., Lund, Sweden), while the bed samples have been taken with a Van Veen grab sampler. Collected and stored samples were dried at 105 °C and chemically treated by adding HCl and H_2O_2 in order to remove the organic and carbonate fractions. The pretreated samples were rinsed with demineralized water, dried at 105 °C, and added to 100 mL demineralized water with 5 mL of peptizing agent (a mixture of

$NaCO_3$ and Na-oxalate). The suspension was dispersed and disaggregated using a magnetic stirrer and an ultrasonic bath. The grain size distribution and clay-silt-sand fractions of the SPM sample were analyzed with a Sedigraph 5100 (Micrometrics Instrument Corp., Norcross, GA, USA) for the fraction < 75 μm and sieved for the coarser fraction. The mineralogical composition of the clay fraction of the samples was determined with a Seifert 3003 theta-theta X-ray diffractometer (GE Measurement & Control, Billerica, MA, USA). Details of the analytical methods are documented in the earlier dissertation [36].

3. Results and Discussion

3.1. Mineralogical Characteristics of TMZ and OSZ

The mineralogical composition of the bed materials in the TMZ and OSZ are shown in Table 1. The respective clay and quartz contents of the bed materials in the TMZ were 25.0% and 39.6%, respectively, whereas those in the OSZ were 12.4% and 66.7%. Thus, the bed materials in the TMZ were found to be a mud-sand mixture, while the bed materials in the OSZ were sandy. Carbonates, such as calcite, Mg-calcite, aragonite, and dolomite, comprise about 20% and 10% of the TMZ and OSZ, respectively. Feldspar (i.e., K-feldspar and plagioclase) was also found to be an important content of the bed materials of the TMZ and OSZ, with a value of about 8%. Amorphous species in the TMZ and OSZ comprised 4.2% and 1.1%, respectively. Amorphous species are considered biogenic minerals influenced by biogeochemical actions [36,45]. The clay minerals at both sites comprised about 5% Kaolinite, 10% Chlorite, and 85% 2:1 layered silicates.

Table 1. Average mineralogical fractions (%) of the bulk deposits and suspended particulate matters (SPM) in the turbidity maximum zone (TMZ) and offshore zone (OSZ) measuring sites.

Material	Location	Clays	Quartz	Carbonates	Amorphous	Feldspar	Others
Bed Materials	TMZ	25.0	39.6	21.1	4.2	8.0	2.1
	OSZ	12.4	66.7	10.7	1.1	8.1	0.9
SPM	TMZ	36.2	14.6	29.9	12.7	4.2	2.3
	OSZ	31.3	20.6	29.7	10.1	6.4	1.8

In contrast to the bed materials, the SPM in the TMZ and OSZ had a similar mineralogical composition. For instance, the clays and quartz contents of the SPM only differed by 5% between the TMZ and OSZ, and the contents of carbonates, amorphous, feldspar, and others differed by less than 2.5%. This happened because the SPM samples do not contain coarser bed material, as the sand grains in suspension are seldom found above the near-bed layer. This also shows that the SPM in the TMZ and OSZ has the same origin, as suggested by the earlier geological survey in this area [35,36]. It is also important to note that the respective fractions of carbonate and amorphous species are large, at about 30% and 11% for both the TMZ and OSZ, thereby indicating high biological activity in the measuring area.

3.2. Spatial Variation of SPM Dynamics in the TMZ and OSZ

During the entire measurement period (2004–2011), the POC/SPM ratios in the OSZ were substantially higher than those in the TMZ (Figure 2a). This observation indicates that the SPM in the OSZ comprises more biomass and less sediments, and vice versa for the SPM in the TMZ. A scatter plot with POC content and SPM concentration shows the transition from a high mineral to the low-mineral SPM, when shifting from the TMZ to the OSZ (Figure 3). Generally, POC content increased with a decreasing SPM concentration (i.e., mineral-depleted condition). The mineral-depleted SPM in the OSZ seemed analogous to the muddy marine snow from an Australian coastal area where minerals were bound together with planktonic and transparent exopolymer particulate matter [46]. However,

the PON/POC ratios of the TMZ and OSZ did not show such a clear difference during the entire study period, and their 95% confidence levels overlapped (Figure 2b).

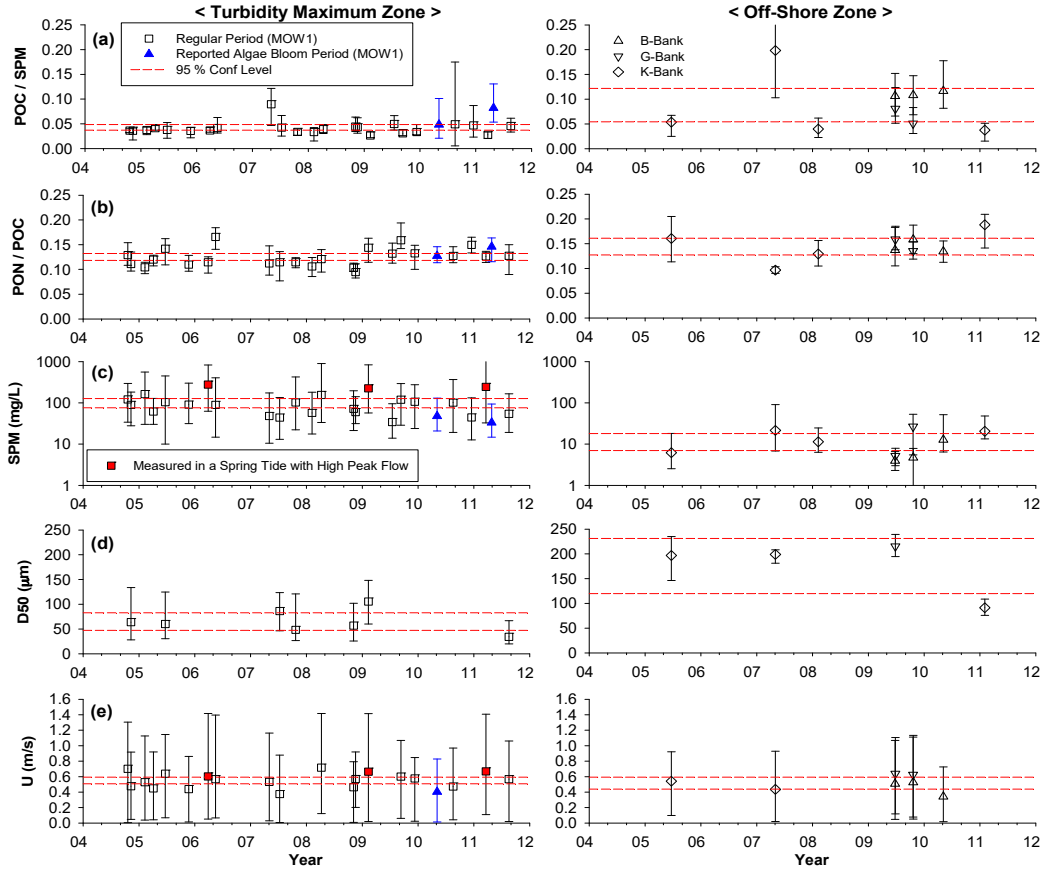

Figure 2. Spatial and seasonal variation of experimental indices in the measurement sites, during the entire measurement period, from 2004 to 2011. The left and right panels illustrate the data obtained from the turbidity maximum zone (TMZ) and the offshore zone (OSZ), respectively. (**a**) POC content in the SPM; (**b**) POC/PON ratio; (**c**) SPM concentration; (**d**) D50: median of the volumetric particle/aggregate size distribution; (**e**) U: flow velocity; MOW1: measurement site in the TMZ; B-Bank, G-Bank, and K-Bank: measurement sites in the OSZ.

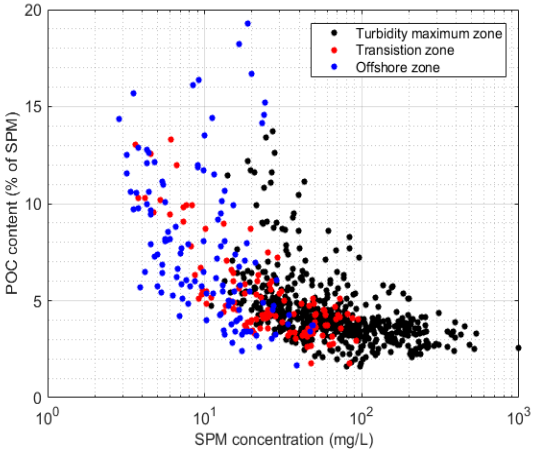

Figure 3. Scatter plot of POC content (% of SPM) versus SPM concentration. The coupled data sets of POC content and SPM concentration were obtained from all the 13 h measurement campaigns.

SPM concentrations in the TMZ are about an order magnitude higher than those in the OSZ (Figure 2c), similar to the satellite images of SPM concentration in Figure 1. This observation suggests that a substantial amount of sediment resides in the TMZ, which is transported back and forth in the flood and ebb tides. In addition, SPM concentrations in the TMZ were more vulnerable to flow intensity. High flow velocity (U) was found to increase SPM concentrations (e.g., 29 March 2006, 7 February 2008, 10 February 2009 and 21 March 2011, in Figure 2), because it increases sediment erosion and resuspension from the sea floor. It is also important to note that the TMZ had a two to three times smaller aggregate size (D50; median of the volumetric particle/aggregate size distribution) than the OSZ (Figure 2d) [15]. Thus, the TMZ enriched with sediments (i.e., higher SPM concentration and lower POC/SPM) had a lower flocculation capability (i.e., lower D50) than the OSZ. Tang and Maggi reported that small, dense aggregates are formed in sediment(mineral)-enriched environments, such as the TMZ in this study, whereas large, fluffy aggregates are formed in biomass-enriched environments [13,29]. The former was defined as mineral or biomineral aggregates, and the latter as biological aggregates.

SPM and POC concentrations and D50 in the TMZ were subject to ups and downs during the 13-h tidal cycle (Figure 4a). Generally, SPM and POC concentrations increased to their maximum around the peak flows. Biomass and minerals were likely combined in large, settleable biomineral aggregates, because SPM and POC concentrations had the same up-and-down movement during a tidal cycle. Such biomineral aggregates in the TMZ are vulnerable to aggregation and disaggregation (i.e., breakup), depending on the flow intensity (turbulence), available aggregation time to reach the equilibrium aggregate size, and organic matter content, therefore changing D50 in a flow-varying tidal cycle [5,18]. D50 increased to the maximum when approaching slack water, but decreased to a minimum around peak flow. Regarding flocculation kinetics, aggregation kinetics dominated over disaggregation kinetics for the slack water, and vice versa for the peak flow [5,18]. In contrast, SPM and POC concentrations and D50 in the OSZ were rather constant, randomly scattered without apparent ups and downs (Figure 4b), showing that aggregation kinetics dominate over disaggregation kinetics for the entire period. SPM in the OSZ might be mainly composed of biomass and some mineral particles, building more shear-resistant and less settleable marine snow [46]. Although biological aggregates (i.e., marine snow) are usually much larger, up to several millimeters, than mineral or biomineral aggregates, they settle more slowly because of their low density and fluffy structure [30]. The latter is confirmed by an earlier study [38], where the excess density of aggregates has been calculated for some of the tidal cycles investigated here; the mean excess density was 550 kg/m^3 and the mean D50 of the aggregates 65 μm (five tidal cycles) in the TMZ versus 180 kg/m^3 and 115 μm (three tidal cycles) in the OSZ. Although both the TMZ and the OSZ are governed by tidal dynamics, small differences in the current regime occur between both areas [15], as is also shown in Figure 4. The TMZ is situated in the nearshore, where the current ellipses are more elongated, whereas more offshore, the ellipses tend to be more spherical. This will cause higher velocity gradients, stronger turbulence, more stress exerted on the aggregates, and a reduction of the time needed for the aggregates to reach equilibrium size in the TMZ. Considering these differences in hydrodynamics, the mineral and biomineral aggregates in the TMZ are more susceptible to the hydrodynamics than the biological aggregates in the OSZ.

Time series of the PSDs during the 13 h tidal cycles are shown in Figure 5, for the TMZ and OSZ, respectively. PSDs in the TMZ skewed toward a smaller size around peak flow (e.g., t = 3, 4 h at location MOW1 on 10 July 2007) and then to a larger size around slack water (e.g., t = 6, 7 h). Except for the PSDs in 23 October 2007, the other PSDs in the TMZ showed bimodality, comprising microflocs (20–200 μm) and macroflocs (>200 μm), as reported in the earlier studies [5]. The primary peak of microflocs in a PSD was prominent around the peak flow. However, while approaching the slack water, the secondary peak of macroflocs became dominant over the primary peak. Low flow/turbulence intensity might promote the aggregation of microflocs (i.e., mineral, biomineral aggregates) to macroflocs (i.e., biological aggregates) [4,5,18]. On the other hand, large hardly-settleable biological aggregates

which were suspended in the water column might dominate in the slack water. Maggi and Tang recently reported that larger biological aggregates can be lighter and even settle slower than smaller mineral, bio-mineral aggregates [13]. Here, larger biological aggregates can be suspended in the slack water, while smaller mineral, bio-mineral aggregates settle and deposit, thereby developing the secondary peak of biological aggregates.

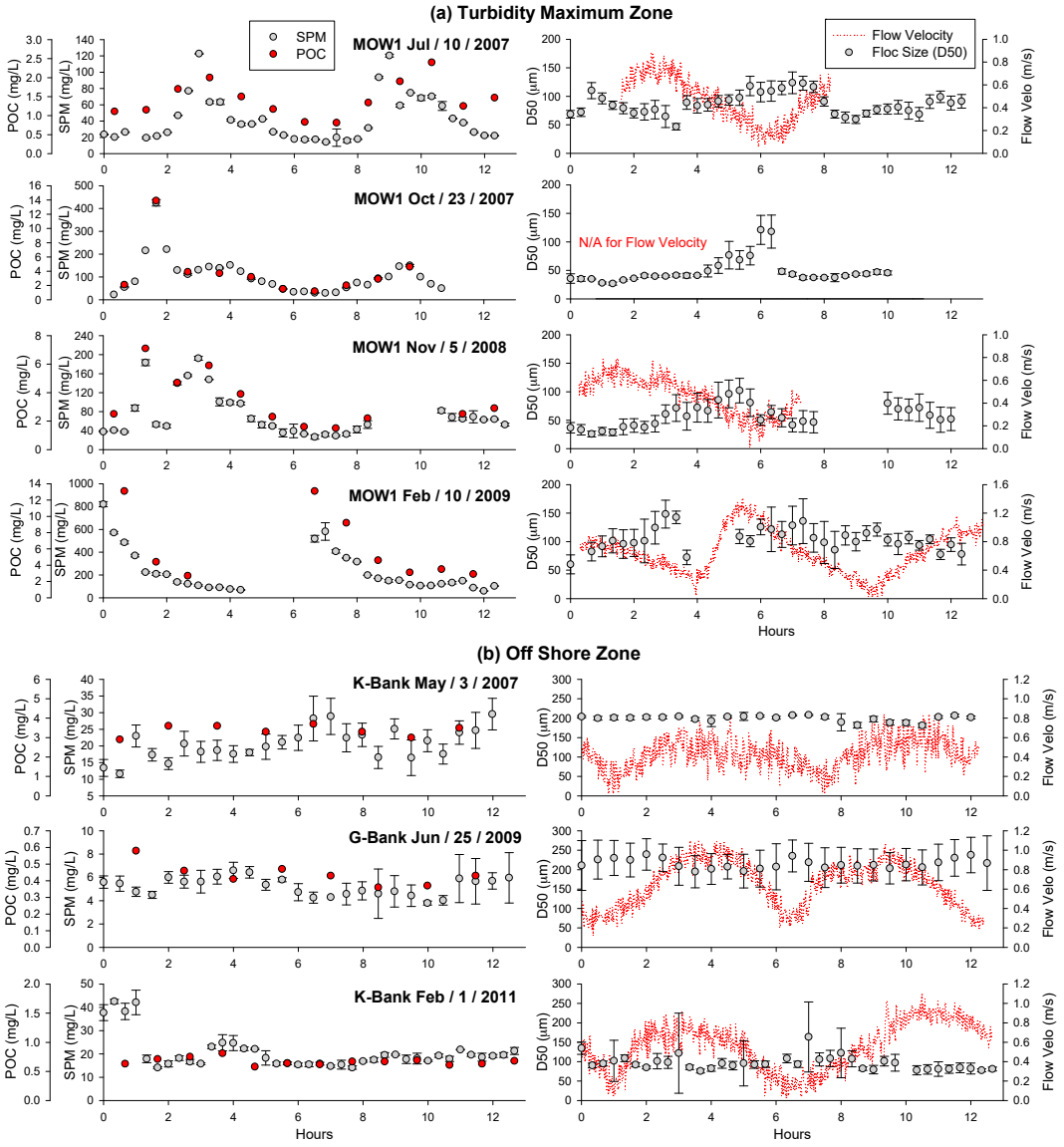

Figure 4. Dynamic behaviors of suspended particulate matter (SPM) and particulate organic carbon (POC) concentrations and aggregate size (D50) in 13-h tidal cycles, in (**a**) the turbidity maximum zone (TMZ) and (**b**) the offshore zone (OSZ). Each set of the SPM/POC and D50 data was measured on a specific date of a field campaign. MOW1: measurement site in the TMZ; K-Bank and G-Bank: measurement sites in the OSZ.

However, PSDs in the OSZ remained rather constant during the entire tidal cycle, consistently skewing toward a larger size (Figure 5b). A substantial fraction of the PSDs occupied the upper most measuring bin of the LISST-100X instrument (i.e., 500 μm). Aggregates in the OSZ, even with such a large size, apparently did not properly settle but floated in the water column (see also the previous paragraph and Figure 4). Thus, SPM in the OSZ is likely composed of large but light, fluffy, and hardly-settleable biological aggregates (i.e., marine snow), whereas SPM in the

TMZ comprises dense, compact, and readly-setteable mineral, biomineral aggregates, as well as biological aggregates [13,29,30,46]. However, note that this argument is supported by a rather indirect measurement of SPM dynamics in this research and observations from earlier studies. Direct ways of measuring aggregate morphology might be required in the future to explain realistic structures and behaviors of mineral, biomineral, and biological aggregates.

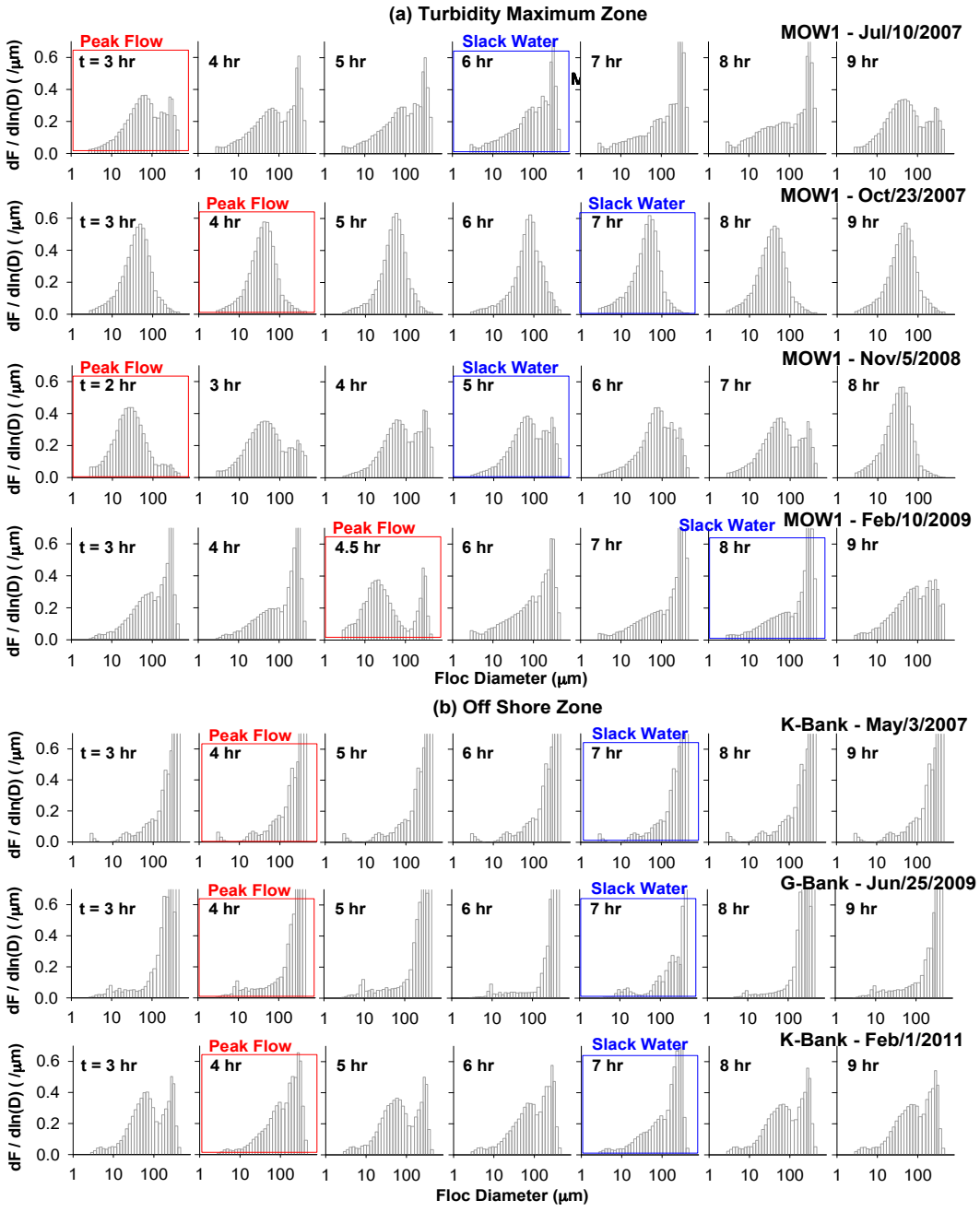

Figure 5. Particle size distributions (PSDs) of suspended particulate matter (SPM) in 13-h tidal cycles, for (**a**) the turbidity maximum zone (TMZ) (MOW1) and (**b**) the offshore zone (OSZ) (K-Bank and G-Bank). Each set of the PSDs was measured on a specific date of a field campaign. Each PSD was plotted on a logarithmic scale, and the fraction of a size bin was normalized by the width of the size bin in y-axis. Thus, dF/dln (D) is the normalized volumetric fraction by the width of the size interval in the log scale, in accordance with the lognormal distribution function [5,47].

3.3. SPM Dynamics during the Algae Bloom and Normal Periods in the TMZ

Flow intensity of the spring and neap tides was found to alter SPM properties (e.g., aggregate size and settling velocity) and SPM dynamics (e.g., flocculation, sedimentation, and deposition) in the TMZ (i.e., the MOW1 site). A spring tide, associated with a strong peak flow (up to 1.5 m/s), increased SPM concentrations substantially, compared to a neap tide with a weak peak flow (up to 1.0 m/s). For example, SPM concentrations increased up to 800 mg/L during a spring tide (e.g., MOW1—10 February 2009 in Figure 4a), whereas they remained under 120 mg/L during a neap tide (e.g., MOW1—10 July 2007). When the pairs of the maximum SPM concentration (SPM_{max}) and peak flow velocity (U_{max}) in each 13-h tidal cycle are plotted (Figure 6), they are proportional. A spring tide with high U_{max} resulted in high SPM_{max}, because it enhanced the disaggregation, erosion, and resuspension of sediment particles/aggregates. However, a neap tide with low U_{max} resulted in low SPM_{max}, because it enhanced aggregation, sedimentation, and deposition. Thus, the fate and transport of SPM in the TMZ, which was governed by aggregation-disaggregation, sedimentation-resuspension, and erosion-deposition, highly depended on flow intensity. However, an exception against the SPM-flow intensity relation was found during an algae bloom period.

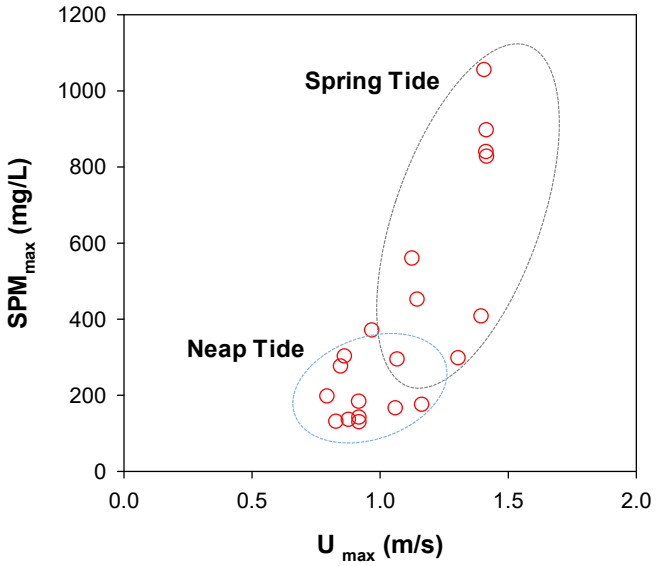

Figure 6. Plots of maximum suspended particulate matter concentration (SPMmax) versus maximum flow velocity (Umax). SPM concentration and flow velocity were measured in the middle of the water column. Each point represents a pair of SPMmax and Umax measured in a 13-h tidal cycle. All the data were measured in the turbidity maximum zone (TMZ) from 2004 to 2011.

During the reported spring algae bloom (MOW1—26 April 2011 in Figure 7a), SPM and POC concentrations did not show a clear up-and-down trend with tide, but behaved similar to those in the OSZ. The aggregate sizes during the algae bloom period (26 April 2011 in Figure 7a) were two to three times larger than aggregates during the normal period, measured at the same site four months later (18 August 2011 in Figure 7b). Although aggregates were enlarged (>100 μm) during the algae bloom period, they did not show a clear sign of downward settling. Considering that such large aggregates during the algae bloom period were subject to floatation without a clear sign of sedimentation and resuspension, they were found to be lighter and less settleable than during a regular period, and thus more similar to the marine snow (i.e., biological aggregates) found in the OSZ (see Section 3.2). In the TMZ, two different aggregates may thus occur: (1) sediment-enriched, dense, and settleable biomineral aggregates during normal periods; and (2) biomass-enriched, light, and less settleable marine snow during algal bloom periods (Figure 8). The latter type of aggregate corresponds better to the one observed in the OSZ. The aggregates occurring during algae bloom periods or in the OSZ have a lower

settling velocity as a larger fraction is composed of organic matter and sticky bio-polymers organized in a fluffy structure [16,48].

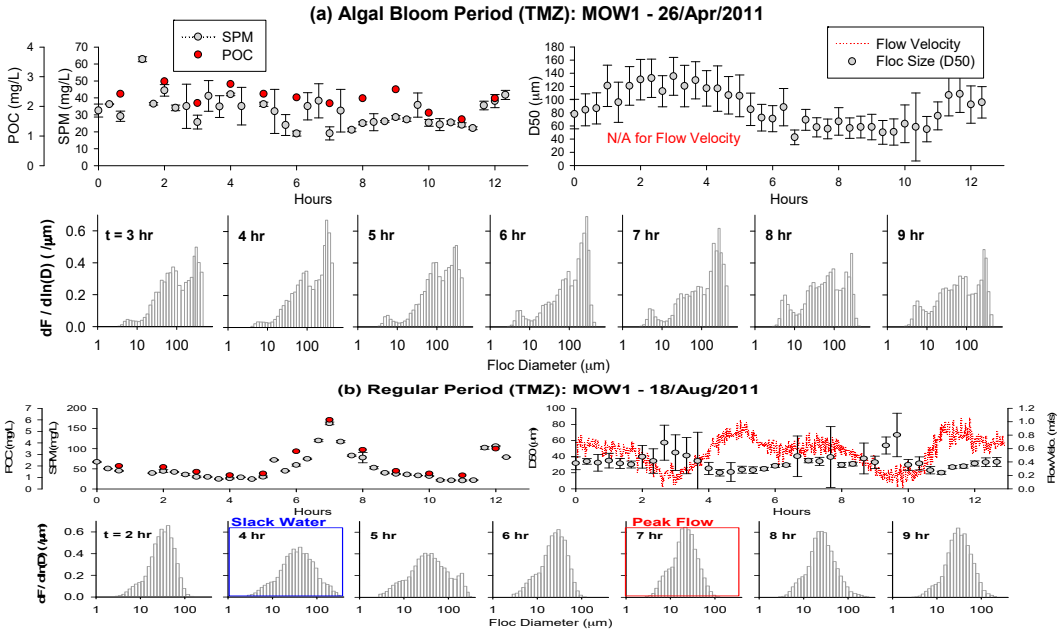

Figure 7. Dynamic behaviors of suspended particulate matter (SPM) and particulate organic carbon (POC) concentrations, aggregate size (D50), and particle size distribution (PSD) in a 13-h tidal cycle. The two data sets were collected in the TMZ (i.e., the MOW1 site) on different dates in 2011, representing (**a**) algal bloom period and (**b**) regular periods.

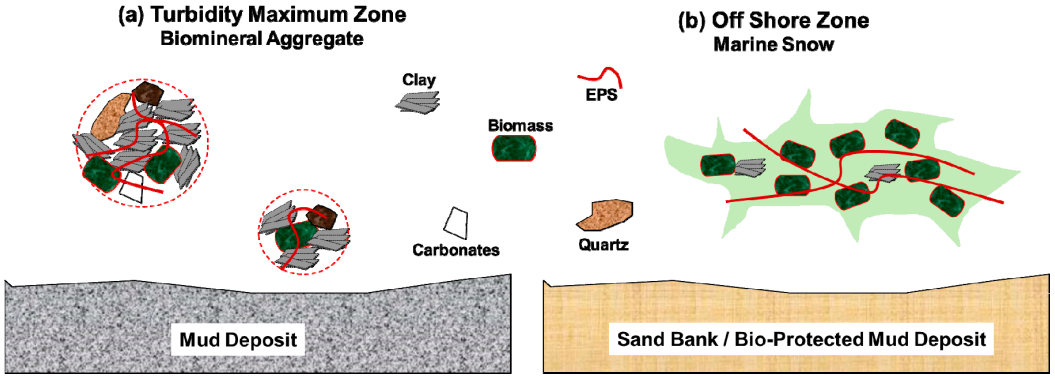

Figure 8. Schematic diagrams of (**a**) biomineral aggregates in the turbidity maximum zone (TMZ) and (**b**) biological marine snow in the offshore zone (OSZ). EPS: extracellular polymeric substances.

Previous studies, carried out in the same TMZ, reported that large and settleable biomineral aggregates were dominant SPM species during bio-enriched spring and summer periods [31,32]. These large, settleable biomineral aggregates are contrary to less settleable biological aggregates observed in this current study. However, it is important to note that the SPM samples in this study were taken in the middle of the water column, well above the near-bed layer. Dense, compacted, and settleable biomineral aggregates might be stored in the near-bed layer, causing mineral-depletion in the water column, and hence less dense, fluffy, and hardly settleable biological aggregates might be formed and float around in the water column. Enhanced primary production during an algal bloom period generates more sticky, particle-binding polymeric substances, such as EPSs and TEPs. These sticky polymeric substances can not only enhance flocculation, but also reduce the erosion and resuspension

of muddy deposits from the seabed to the water column [49]. A large amount of cohesive sediments are thus stored in or on the seafloor as a fluid-mud layer or a muddy deposit, and the marine snow with more biomass and less sediments is suspended in the water column [3]. This SPM behavior during an algal bloom period with high primary production agrees with the satellite images of low SPM and high Chl concentrations in summer (Figure 1). Similar observations were made in the port of Zeebrugge. High primary production and low turbulence in summer provoked a large amount of mud deposition in the near-bed layer (or formation of a fluid mud layer) and reduction of the SPM concentration in the water column.

Reviewing other studies [28,50] revealed similar SPM dynamics around an algal bloom period. Proliferation of a specific algae group could enhance flocculation and store sediments in the near-bed layer, and hence could cause large but suspended biological aggregates and a low SPM concentration in the water column. Maerz and co-workers [51] have been looking at the whole gradient from the nearshore TMZ to the OSZ; they have found a maximum settling velocity in the transition zone between the TMZ and the OSZ where the aggregates are larger as compared to near-coast TMZ and denser as compared to the low turbid OSZ. This maximum in settling velocity is caused by similar gradients in aggregate size, POC content, density, and chlorophyll concentration than found in our data. The fact that algae are involved in these observed gradients points to seasonal influences. Another study [52], however, does not confirm the leading role of the algae bloom on SPM dynamics. The reason for these different findings may be due to differences in, amongst others, hydrodynamics, wave climate, nutrient availability, and algae species at the different study sites. The importance of each of these parameters will explain to a smaller or larger part the observed seasonal variations in SPM dynamics.

Biomineral and biological aggregates are often approximated by a single parameter (e.g., a characteristic diameter) in practical applications, although they are very different in composition and mechanical property. For example, a traditional aggregate structure model, based on fractal theory, includes only mineral particles and disregards organic matter, which is instead assumed to be part of the pore space for simplicity and ease [53,54]. This approximation might not be valid for biological aggregates (i.e., marine snow) with a high content of organic matter or in environments where aggregate properties change in time (regular versus algae bloom period) or space (inside and outside harbours). Thus, the heterogeneity of aggregates, at least the two fractions of biomass and sediments, should be considered when developing a rigorous aggregate structure model and accurately predicting the fate and transport of biomass and sediments in marine and coastal waters [30].

A higher biomass content (indicated by a higher POC/SPM ratio) was generally found to enhance flocculation, thereby increasing aggregate size. However, the quantity of biomass is not the only factor determining the flocculation capability. For example, in June 2009 at G-Bank (Figure 2a), aggregate size increased to over 200 μm, even with a low POC/SPM. Besides the quantity of biomass, the quality, such as stickiness, is important for controlling flocculation kinetics, as reported in previous research [50,55]. Specifically, extracellular polymeric substances (EPSs) or transparent extracellular polymers (TEPs) are sticky and increase flocculation [19,20,22,23]. Long polymeric chain structures of EPSs and TEPs, which are produced by aquatic microorganisms (e.g., algae), can bind biomass and sediment particles to large mineral, biomineral, and biological aggregates. Even in an unfavorable chemical condition for flocculation (e.g., terrestrial water with low ionic strength), a small amount of EPSs and TEPs can cause substantial flocculation, because they can overcome the electrostatic repulsive force of negatively-charged colloidal particles and bind such particles to large aggregates [56,57]. Therefore, qualitative measures of biomass, such as EPS and/or TEP concentration, likely need to be included to explain bio-mediated flocculation and SPM dynamics in marine and coastal waters.

4. Conclusions

The monitoring and analysis of SPM dynamics explained how organic biomass and inorganic sediment interact with each other to build large biomineral aggregates or marine snow in marine and coastal waters. SPM in the TMZ and OSZ had a similar mineralogical composition, but encountered

different fates in association with biomass. SPM in the TMZ built sediment-enriched, dense, and settleable biomineral aggregates, whereas SPM in the OSZ was composed of biomass-enriched, light, and less settleable marine snow. Biological proliferation, such as an algae bloom, also facilitated the occurrence of marine snow in the water column, even in the TMZ. Enhanced flocculation in summer could also scavenge SPM in the water column down to the sea bed, resulting in a low SPM concentration in the water column. In short, bio-mediated flocculation and SPM dynamics were found to vary spatially and seasonally, affected by the biota. The proposed concept to combine organic and mineral particles in aggregates will help us to better understand and predict bio-mediated flocculation and SPM dynamics in marine and coastal waters.

Acknowledgments: This research was supported by the Basic Science Research Program through the National Research Foundation of Korea (NRF) funded by the Ministry of Education (No: NRF-2017R1D1A3B03035269), the Maritime Access Division of the Flemish Ministry of Mobility and Public Works (MOMO project), and the Belgian Science Policy (BELSPO) within the BRAIN-be program (INDI67 project). The ship time RV Belgica was provided by BELSPO and the RBINS–Operational Directorate Natural Environment.

Author Contributions: M.F. conceived, designed, and performed the experiments; B.J.L. analyzed the experimental data; and M.F. and B.J.L. wrote the paper.

Conflicts of Interest: The authors declare no conflict of interest.

References

1. Ouillon, S.; Douillet, P.; Andrefouet, S. Coupling satellite data with in situ measurements and numerical modeling to study fine suspended-sediment transport: A study for the lagoon of New Caledonia. *Coral Reefs* **2004**, *23*, 109–122.
2. Perianez, R. Modelling the transport of suspended particulate matter by the Rhone River plume (France). Implications for pollutant dispersion. *Environ. Pollut.* **2005**, *133*, 351–364. [CrossRef] [PubMed]
3. Winterwerp, J.; van Kesteren, W. *Introduction to the Physics of Cohesive Sediment in the Marine Environment*; Elsevier B.V.: Amsterdam, The Netherlands, 2004.
4. Lee, B.J.; Toorman, E.; Molz, F.J.; Wang, J. A two-class population balance equation yielding bimodal flocculation of marine or estuarine sediments. *Water Res.* **2011**, *45*, 2131–2145. [CrossRef] [PubMed]
5. Lee, B.J.; Fettweis, M.; Toorman, E.; Molz, F.J. Multimodality of a particle size distribution of cohesive suspended particulate matters in a coastal zone. *J. Geophys. Res. Oceans* **2012**, *117*, C03014. [CrossRef]
6. Chen, M.S.; Wartel, S.; Temmerman, S. Seasonal variation of floc characteristics on tidal flats, the Scheldt estuary. *Hydrobiologia* **2005**, *540*, 181–195. [CrossRef]
7. Droppo, I.G. Rethinking what constitutes suspended sediment. *Hydrol. Process.* **2001**, *15*, 1551–1564. [CrossRef]
8. Eisma, D. Flocculation and de-flocculation of suspended matter in estuaries. *Neth. J. Sea Res.* **1986**, *20*, 183–199. [CrossRef]
9. Droppo, I.; Leppard, G.; Liss, S.; Milligan, T. *Flocculation in Natural and Engineered Environmental Systems*; CRC Press Inc.: Boca Raton, FL, USA, 2005.
10. Jago, C.F.; Kennaway, G.M.; Novarino, G.; Jones, S.E. Size and settling velocity of suspended flocs during a phaeocystis bloom in the tidally stirred Irish Sea, NW European Shelf. *Mar. Ecol. Prog. Ser.* **2007**, *345*, 51–61. [CrossRef]
11. Tan, X.L.; Zhang, G.P.; Yi, H.; Reed, A.H.; Furukawa, Y. Characterization of particle size and settling velocity of cohesive sediments affected by a neutral exopolymer. *Int. J. Sediment Res.* **2012**, *27*, 473–485. [CrossRef]
12. Maggi, F. Biological flocculation of suspended particles in nutrient-rich aqueous ecosystems. *J. Hydrol.* **2009**, *376*, 116–125. [CrossRef]
13. Maggi, F.; Tang, F.H.M. Analysis of the effect of organic matter content on the architecture and sinking of sediment aggregates. *Mar. Geol.* **2015**, *363*, 102–111. [CrossRef]
14. Van Leussen, W. Estuarine Macroflocs: Their Role in Fine-Grained Sediment Transport. Ph.D. Thesis, Utrecht University, Utrecht, The Netherlands, February 1994.
15. Fettweis, M.; Francken, F.; Pison, V.; Van den Eynde, D. Suspended particulate matter dynamics and aggregate sizes in a high turbidity area. *Mar. Geol.* **2006**, *235*, 63–74. [CrossRef]

16. Alldredge, A.; Silver, M. Characteristics, dynamics and significance of marine snow. *Prog. Oceanogr.* **1988**, *20*, 41–82. [CrossRef]
17. Markussen, T.N.; Andersen, T.J. A simple method for calculating in situ floc settling velocities based on effective density functions. *Mar. Geol.* **2013**, *344*, 10–18. [CrossRef]
18. Lee, B.J.; Toorman, E.; Fettweis, M. Multimodal particle size distributions of fine-grained sediments: Mathematical modeling and field investigation. *Ocean Dyn.* **2014**, *64*, 429–441. [CrossRef]
19. Passow, U. Transparent exopolymer particles (TEP) in aquatic environments. *Prog. Oceanogr.* **2002**, *55*, 287–333. [CrossRef]
20. Engel, A.; Thoms, S.; Riebesell, U.; Rochelle-Newall, E.; Zondervan, I. Polysaccharide aggregation as a potential sink of marine dissolved organic carbon. *Nature* **2004**, *428*, 929–932. [CrossRef] [PubMed]
21. Sahoo, G.B.; Nover, D.; Schladow, S.G.; Reuter, J.E.; Jassby, D. Development of updated algorithms to define particle dynamics in Lake Tahoe (CA-NV) USA for total maximum daily load. *Water Resour. Res.* **2013**, *49*, 7627–7643. [CrossRef]
22. Mari, X.; Passow, U.; Migon, C.; Burd, A.; Legendre, L. Transparent Exopolymer Particles: Effects on carbon cycling in the ocean. *Prog. Oceanogr.* **2017**, *151*, 13–37. [CrossRef]
23. Jouon, A.; Ouillon, S.; Douillet, P.; Lefebvre, J.P.; Fernandez, J.M.; Mari, X.; Froidefond, J. Spatio-temporal variability in suspended particulate matter concentration and the role of aggregation on size distribution in a coral reef lagoon. *Mar. Geol.* **2008**, *256*, 36–48. [CrossRef]
24. Tranvik, L.J.; Downing, J.A.; Cotner, J.B.; Loiselle, S.A.; Striegl, R.G.; Ballarore, T.J.; Dillon, P.; Finlay, K.; Fortino, K.; Knoll, L.B.; et al. Lakes and reservoirs as regulators of carbon cycling and climate. *Limnol. Oceanogr.* **2009**, *54*, 2298–2314. [CrossRef]
25. Gudasz, C.; Bastviken, D.; Premke, K.; Steger, K.; Tranvik, L.J. Constrained microbial processing of allochthonous organic carbon in boreal lake sediments. *Limnol. Oceanogr.* **2012**, *57*, 163–175. [CrossRef]
26. Barkmann, W.; Schafer-Neth, C.; Balzer, W. Modelling aggregate formation and sedimentation of organic and mineral particles. *J. Mar. Syst.* **2010**, *82*, 81–95. [CrossRef]
27. Burd, A.; Jackson, G. Modeling steady-state particle size spectra. *Environ. Sci. Technol.* **2002**, *36*, 323–327. [CrossRef] [PubMed]
28. De Lucas Pardo, M.A.; Sarpe, D.; Winterwerp, J.C. Effect of algae on flocculation of suspended bed sediments in a large shallow lake. Consequences for ecology and sediment transport processes. *Ocean Dyn.* **2015**, *65*, 889–903. [CrossRef]
29. Tang, F.H.M.; Maggi, F. A mesocosm experiment of suspended particulate matter dynamics in nutrient- and biomass-affected waters. *Water Res.* **2016**, *89*, 76–86. [CrossRef] [PubMed]
30. Maggi, F. The settling velocity of mineral, biomineral, and biological particles and aggregates in water. *J. Geophys. Res. Oceans* **2013**, *118*, 2118–2132. [CrossRef]
31. Fettweis, M.; Baeye, M.; Van der Zande, D.; Van den Eynde, D.; Lee, B.J. Seasonality of floc strength in the southern North Sea. *J. Geophys. Res. Oceans* **2014**, *119*, 1911–1926. [CrossRef]
32. Fettweis, M.; Baeye, M. Seasonal variation in concentration, size and settling velocity of muddy marine flocs in the benthic boundary layer. *J. Geophys. Res. Oceans* **2015**, *120*, 5648–5667. [CrossRef]
33. Fettweis, M.; Francken, F.; Van den Eynde, D.; Verwaest, T.; Janssens, J.; Van Lancker, V. Storm influence on SPM concentrations in a coastal turbidity maximum area with high anthropogenic impact (southern North Sea). *Cont. Shelf Res.* **2010**, *30*, 1417–1427. [CrossRef]
34. Lacroix, G.; Ruddick, K.; Ozer, J.; Lancelot, C. Modelling the impact of the Scheldt and Rhine/Meuse plumes on the salinity distribution in Belgian waters (southern North Sea). *J. Sea Res.* **2004**, *52*, 149–163. [CrossRef]
35. Fettweis, M.; Nechad, B.; Van den Eynde, D. An estimate of the suspended particulate matter (SPM) transport in the southern North Sea using SeaWiFS images, in situ measurements and numerical model results. *Cont. Shelf Res.* **2007**, *27*, 1568–1583. [CrossRef]
36. Zeelmaekers, E. Computerized Qualitative and Quantitative Clay Minerology: Introduction and Application to Known Geological Cases. Ph.D. Thesis, Katholieke Universiteit Leuven, Leuven, Belgium, April 2011.
37. Agrawal, Y.; Pottsmith, H. Instruments for particle size and settling velocity observations in sediment transport. *Mar. Geol.* **2000**, *168*, 89–114. [CrossRef]
38. Fettweis, M. Uncertainty of excess density and settling velocity of mud flocs derived from in situ measurements. *Estuar. Coast. Shelf Sci.* **2008**, *78*, 426–436. [CrossRef]

39. Mikkelsen, O.; Curran, K.; Hill, P.; Milligan, T. Entropy analysis of in situ particle size spectra. *Estuar. Coast. Shelf Sci.* **2007**, *72*, 615–625. [CrossRef]
40. Andrews, S.; Nover, D.; Schladow, S. Using laser diffraction data to obtain accurate particle size distributions: The role of particle composition. *Limnol. Oceanogr. Methods* **2010**, *8*, 507–526. [CrossRef]
41. Graham, G.W.; Davies, E.; Nimmo-Smith, A.; Bowers, D.G.; Braithwaite, K.M. Interpreting LISST-100X measurements of particles with complex shape using digital in-line holography. *J. Geophys. Res. Oceans* **2012**, *117*, C05034. [CrossRef]
42. Mikkelsen, O.A.; Hill, P.S.; Milligan, T.; Chant, R.J. In situ particle size distributions and volume concentrations from a LISST-100 laser particle sizer and a digital floc camera. *Cont. Shelf Res.* **2005**, *25*, 1959–1978. [CrossRef]
43. Smith, S.J.; Friedrichs, C.T. Size and settling velocities of cohesive flocs and suspended sediment aggregates in a trailing suction hopper dredge plume. *Cont. Shelf Res.* **2011**, *31*, S50–S63. [CrossRef]
44. Davies, E.; Nimmo-Smith, A.; Agrawal, Y.; Souza, A. LISST-100 response to large particles. *Mar. Geol.* **2012**, *307–311*, 117–122. [CrossRef]
45. Kastner, M. Oceanic minerals: Their origin, nature of their environment, and significance. *Proc. Natl. Acad. Sci. USA* **1999**, *96*, 3380–3387. [CrossRef] [PubMed]
46. Bainbridge, Z.; Wolanski, E.; Alvarez-Romero, J.G.; Lewis, S.E.; Brodie, J.E. Fine sediment and nutrient dynamics related to particle size and floc formation in a Burdekin River flood plume, Australia. *Mar. Pollut. Bull.* **2012**, *65*, 236–248. [CrossRef] [PubMed]
47. Hinds, W. *Aerosol Technology: Properties, Behavior, and Measurement of Airborne Particles*, 2nd ed.; John Wiley: New York, NY, USA, 1999.
48. Fennessy, M.; Dyer, K.; Huntley, D. INSSEV: An instrument to measure the size and settling velocity of flocs in situ. *Mar. Geol.* **1994**, *117*, 107–117. [CrossRef]
49. Vos, P.; De Boer, P.; Misdorp, R. Sediment stabilization by benthic diatoms in intertidal sandy shoals: Qualitative and quantitative observations. In *Tide-Influenced Sedimentary Environments and Facies*; D. Reidel Publishing: Dordrecht, The Netherlands, 1988; pp. 511–526.
50. Van der Lee, W.T.B. Temporal variation of floc size and settling velocity in the Dollard estuary. *Cont. Shelf Res.* **2000**, *20*, 1495–1511. [CrossRef]
51. Maerz, J.; Hofmeister, R.; van der Lee, E.M.; Grawe, U.; Riethmuller, R.; Wirtz, K.W. Maximum sinking velocities of suspended particulate matter in a coastal transition zone. *Biogeosciences* **2016**, *13*, 4863–4876. [CrossRef]
52. Van der Hout, C.M.; Wittbaard, R.; Bergman, M.J.M.; Duineveld, G.C.A.; Rozemeijer, M.J.C. The dynamics of suspended particulate matter (SPM) and chlorophyll-a from intratidal to annual time scales in a coastal turbidity maximum. *J. Sea Res.* **2017**. [CrossRef]
53. Khelifa, A.; Hills, P.S. Models for effective density and settling velocity of flocs. *J. Hydraul. Res.* **2006**, *44*, 390–401. [CrossRef]
54. Maggi, F. Variable fractal dimension: A major control for floc structure and flocculation kinematics of suspended cohesive sediment. *J. Geophys. Res. Oceans* **2007**, *112*, C07012. [CrossRef]
55. Van der Lee, W.T.B. Parameters affecting mud floc size on a seasonal time scale: The impact of a phytoplankton bloom in the Dollard estuary, The Netherlands. In *Coastal and Estuarine Fine Sediment Transport Processes*; McAnally, W.H., Mehta, A.J., Eds.; Elsevier: Amsterdam, The Netherlands, 2001; Volume 3, pp. 403–421.
56. Furukawa, Y.; Reed, A.H.; Zhang, G. Effect of organic matter on estuarine flocculation: A laboratory study using montmorillonite, humic acid, xanthan gum, guar gum and natural estuarine flocs. *Geochem. Trans.* **2014**, *15*, 1–9. [CrossRef] [PubMed]
57. Lee, B.J.; Hur, J.; Toorman, E. Seasonal Variation in Flocculation Potential of River Water: Roles of the Organic Matter Pool. *Water* **2017**, *9*, 335. [CrossRef]